

A MULTISCALE APPROACH TO MOISTURE DIFFUSIVITY FOR DRYING PLANT-BASED FOOD MATERIALS

Zachary G. Welsh

**Bachelor of Engineering
Master of Engineering (Mechanical)**

Submitted in fulfilment of the requirements for the degree of
Doctor of Philosophy

School of Mechanical, Medical and Process Engineering

Faculty of Engineering
Queensland University of Technology

2021

Keywords

Cell rupture
Cellular microstructure
Drying
Generalised diffusivity
Heterogenous material
Homogenisation
Intracellular diffusivity
Mathematical model
Moisture diffusivity
Multiscale modelling
Plant-based food material
Spatial heterogeneity
Temporal Heterogeneity
Theoretical modelling
Upscaling

Abstract

Drying plant-based food materials is time consuming and energy intensive, making optimisation of its processes essential. Mathematical modelling is crucial in the development of optimal drying strategies. However, current mathematical models are based on condition-dependent diffusivities with limited predictive capabilities, restricting a model's performance in these optimisation scenarios. Food materials have complex heterogeneous microstructures, which dynamically changes during drying as a result of the simultaneous heat transport, mass transport and anisotropic deformation. Transitioning towards a more physics-based model, capturing the heterogeneity, will improve a model's predictive capabilities while accurately modelling the transport phenomena.

This research applies multiscale modelling to develop a moisture diffusivity considering the cellular water heterogeneity in terms of space and time for drying plant-based food materials. A multiscale model with a generalised moisture diffusivity is developed, and its predictive capabilities are thoroughly investigated. Additionally, to utilise the generalised moisture diffusivity, cell rupturing was considered through a novel rupture threshold.

It was found that the cellular water heterogeneity could be approximated by considering two subdomains: grouping the effects of the protoplast, cell membrane and cell wall within the intracellular subdomain. When significant microstructural deformation occurs, the dynamic heterogeneity can be approximated through a linear decrease in the intracellular water content. Additionally, a function was developed for the diffusivity of intracellular water in terms of sample temperature and intracellular water content. Utilising the function, a multiscale model with a generalised moisture diffusivity was constructed. The generalised diffusivity was able to distinguish between materials through considering their intracellular water content. This improved the model's predictive capabilities while accurately describing the drying kinetics at multiple drying temperatures. The multiscale approach also constructed a rupture threshold exploiting the equilibrium vapor pressure to recognise if cell rupturing had occurred. The multiscale model and generalised diffusivity will allow future

researchers to conduct large scale optimisation investigations, leading to the development of optimum drying systems with improved food quality.

This thesis is a ‘Thesis by Publication’

List of publications

Journal

- **Welsh, Z.**, Simpson, M. J., Khan, M. I. H., & Karim, M. A. (2018). Multiscale modeling for food drying: State of the art. *Comprehensive Reviews in Food Science and Food Safety*, 17(5), 1293-1308. **Q1 and Impact Factor: 8.738**
- **Welsh, Z. G.**, Khan, M. I. H., & Karim, M. A. (2021). Multiscale modeling for food drying: A homogenized diffusion approach. *Journal of Food Engineering*, 292, 110252. **Q1 and Impact Factor: 4.499**
- **Welsh, Z. G.**, Khan, M. I. H., Simpson, M. J., & Karim, M. A. (2020). A multiscale approach to estimate the cellular diffusivity during food drying. *Food Research International* (Under review).
- **Welsh, Z. G.**, Simpson, M. J., Khan, M. I. H., & Karim, M. A. (2020). Generalized moisture diffusivity for food drying through multiscale modeling. (Prepared for submission)

Contributions to other publications

- Khan, M. I. H., **Welsh, Z.**, Gu, Y., Karim, M. A., & Bhandari, B. (2020). Modelling of simultaneous heat and mass transfer considering the spatial distribution of air velocity during intermittent microwave convective drying. *International Journal of Heat and Mass Transfer*, 153, 119668. **Q1 and Impact Factor: 4.947**

Book

- Khan, M. I. H., **Welsh, Z.G.**, Karim, M. A. Multiscale Modelling for Food Drying Technology, Taylor & Francis Group, LLC. (Accepted on 28/04/2020)

Book Chapter

- Pham, D. N., Khan, M. I. H., **Welsh, Z.**, & Karim, M. A. (2020) Advances in intermittent batch drying of foods. In H-W, Xiao & Mujumdar, A.S. (Eds.) *Advanced Drying Technologies for Foods*. CRC Press, Boca Raton, FL, pp. 223-241

Table of Contents

Keywords	i
Abstract.....	ii
List of publications	iv
Table of Contents.....	v
List of Figures.....	viii
List of Tables	xi
List of Abbreviations	xii
Statement of Original Authorship	xiii
Acknowledgements.....	xiv
Chapter 1: Introduction	1
1.1 Background.....	1
1.2 Context.....	2
1.3 Aims and objectives.....	4
1.4 Significance, scope and definitions	4
1.5 Thesis outline.....	5
Chapter 2: Literature Review.....	11
2.1 Abstract.....	13
2.2 Introduction	13
2.3 Food structure	16
2.4 Current status of multiscale modeling	20
2.5 Multiscale modeling frameworks	22
2.6 Solution technique	35
2.7 Temporal coupling.....	40
2.8 Other factors for multiscale modeling	43
2.9 Challenges for multiscale modeling	44
2.10 Future directions	45
2.11 Conclusion.....	45
2.12 Acknowledgments	46
2.13 Author contributions	46
Chapter 3: Multiscale modelling for food drying: A homogenised diffusion approach	63
3.1 Abstract.....	65
3.2 Introduction	65
3.3 Model development	69

3.4	Input parameters.....	77
3.5	Simulation methodology	78
3.6	Experimental investigation.....	79
3.7	Results.....	81
3.8	Discussion	88
3.9	Conclusion	91
3.10	Acknowledgements	91
3.11	Model availability	91

Chapter 4: A multiscale temporal investigation for food material during drying 99

4.1	Abstract	101
4.2	Introduction.....	101
4.3	Model development.....	103
4.4	Inverse problem.....	108
4.5	Temporal heterogeneity investigation.....	109
4.6	Relationship development for the diffusivity of intracellular water	111
4.7	Computational methodology	111
4.8	Results.....	112
4.9	Diffusivity estimation for ICW	120
4.10	Conclusion	123

Chapter 5: Comprehensive multiscale model for drying plant-based food material 130

5.1	Abstract	132
5.2	Introduction.....	132
5.3	Model development.....	134
5.4	Evolution of intracellular water- rupturing threshold	140
5.5	Results.....	145
5.6	Discussion	156
5.7	Conclusion	158
5.8	Acknowledgements	158

Chapter 6: Conclusions..... 165

6.1	Conclusions	165
6.2	Contribution to knowledge and significance of this research	168
6.3	Research limitations and future work	169
6.4	Final Remarks	171

Appendices 173

Appendix A	173
Appendix B	175

Appendix C	177
Appendix D	178

List of Figures

Figure 2.1. Heterogeneous cellular structure of plant-based food material	17
Figure 2.2. Length scales. (a) Microscale, (b) Macroscale, (c) Industry scale.	18
Figure 2.3. Concurrent food drying modeling approach.....	32
Figure 2.4. Visual representation of patch dynamics. (a) Full microscale simulation, (b) Coarse integration, (c) Gap-tooth scheme, (d & e) Combining the gap-tooth scheme and coarse integration to create patch dynamics. From “Equation-free, coarse-grained multiscale computation: Enabling microscopic simulators to perform system-level analysis,” by I.G. Kevrekidis, C.W. Gear, J.M. Hyman, P.G. Kevrekidis, O. Runborg, and C. Theodoropoulos, 2003, Communications in Mathematical Sciences, p. 737. Copyright 2003 by International Press of Boston, Inc.....	38
Figure 2.5. A schematic summary of the gap-tooth/patch dynamics nomenclature in 1D. From “Equation-free, coarse-grained multiscale computation: Enabling microscopic simulators to perform system-level analysis,” by I.G. Kevrekidis, C.W. Gear, J.M. Hyman, P.G. Kevrekidis, O. Runborg, and C. Theodoropoulos, 2003, Communications in Mathematical Sciences, p.738. Copyright 2003 by International Press of Boston, Inc	39
Figure 2.6. Temporal coupling. (a) Fully coupled scheme, (b) Intermittent coupling strategy, (c) Multigrid and HMM approach, (d) Equation free, (e) Seamless HMM variate, (f) Continuous intermittent coupling scheme (Adapted from “Time-Step Coupling for Hybrid Simulations of Multiscale Flows,” by D. A. Lockerby, C. A. Duque-Daza, M. K. Borg, and J. M. Reese, 2012 in Journal of Computational Physics, 237, p.346. Copyright 2012 by Elsevier Inc).....	42
Figure 3.1. Schematic representation of the cellular water inside food materials considering two subdomains (intracellular spaces and intercellular spaces), (a) simplified representation of the real water distribution within food material, demonstrating where ICW and free water (denoted as blue) can be found, (b) REV approach demonstrating water is only considering as ‘free water’.....	67
Figure 3.2. Geometries (a) whole sample, (b) axisymmetric macroscale domain and (c) microscale domain.....	70
Figure 3.3. Modeling solution procedure.....	79
Figure 3.4. Moisture content curves for each diffusivity approach at different drying temperatures, a) 45°C, b) 60°C, c) 70°C	84
Figure 3.5. The axisymmetric moisture profile (kg/kg dry bases) at different drying times for the homogenized diffusivity approach for drying at 70°C	85

Figure 3.6. Average temperature for each diffusivity approach at different drying temperatures, a) 45°C, b) 60°C, c) 70°C	87
Figure 4.1. Domains (a) axisymmetric macroscale domain and (b) microscale domain.....	104
Figure 4.2. Water heterogeneity breakdown of ICW content and moisture content (kg/kg dry bases) with time.....	110
Figure 4.3. Computational Methodology	112
Figure 4.4. Average moisture content (kg/kg dry bases) for drying at 60 °C.....	114
Figure 4.5. Average temperature (°C) for drying at 60 °C.	114
Figure 4.6. Diffusivity (m^2/s) of intracellular water for approach 1 (base case). The temporal evolution of the microscale domain can be seen along the top of the figure, purple denotes ICW and green denotes FW.....	116
Figure 4.7. Diffusivity (m^2/s) of intracellular water for approach 2 (average). The temporal evolution of the microscale domain can be seen along the top of the figure, purple denotes ICW and green denotes FW.....	117
Figure 4.8. Diffusivity (m^2/s) of intracellular water for approach 3 (linear decrease). The temporal evolution of the microscale domain can be seen along the top of the figure, purple denotes ICW and green denotes FW.	118
Figure 4.9. Diffusivity (m^2/s) of intracellular water for approach 4 (diffusivity by stages). The temporal evolution of the microscale domain can be seen along the top of the figure, purple denotes ICW and green denotes FW.	119
Figure 4.10. Proposed D_{ICW} (m^2/s) function [Equation (4.19)] in terms of sample temperature (K) and intracellular water content (%).	121
Figure 5.1. Domains (a) axisymmetric macroscale domain and (b) microscale domain.....	135
Figure 5.2. Visual representation of the equilibrium vapor pressure (kPa) of (a) apple and (a) potato, Equation (5.6) and Equation (5.7) respectively.	137
Figure 5.3. Visual representation of proposed theoretical cell rupturing threshold, a) threshold is not reached and cell rupturing does not occur, b) threshold is reached and cell rupturing occurs.	142
Figure 5.4. Computational methodology.	144
Figure 5.5. Visual representation of the effective diffusivity (m^2/s) function ($D_{H,eff}$)	146
Figure 5.6. Average moisture content (kg/kg dry bases) for drying at 47 °C. Error bars represent plus-minus one standard deviation of the triplicate experimental data.	148
Figure 5.7. Average macroscale diffusivity (m^2/s) for drying at 47 °C.	148
Figure 5.8. Average Temperature (°C) for drying at 47 °C. Error bars represent plus-minus one standard deviation of the triplicate experimental data.....	149

Figure 5.9. Rupturing threshold investigation using the average equilibrium vapor pressure (kPa), (a) spatial distribution of apple at threshold and (b) spatial distribution of potato at threshold.	150
Figure 5.10. Average moisture content (kg/kg dry bases) for drying at 64 °C. Error bars represent plus-minus one standard deviation of the triplicate experimental data.	151
Figure 5.11. Average macroscale diffusivity (m ² /s) for drying at 64 °C.....	151
Figure 5.12. Average temperature (°C) for drying at 64 °C. Error bars represent plus-minus one standard deviation of the triplicate experimental data.....	152
Figure 5.13. The average equilibrium vapor pressure (kPa) and ICW content (%) of apple drying at 64 °C. Spatial distribution of the equilibrium vapor pressure at (a) 33 mins (when threshold is reached), (b) 125 mins, (c) 220 mins, (d) 280 mins and (e) 360 mins.	153
Figure 5.14. The average equilibrium vapor pressure (kPa) and ICW content (%) of potato drying at 64 °C. Spatial distribution of the equilibrium vapor pressure at (a) 92 mins (when threshold is reached), (b) 125 mins, (c) 220 mins, (d) 280 mins and (e) 360 mins.	154
Figure 5.15. Sensitivity investigation for the material density ± 10%, a) average moisture content (kg/kg dry bases), b) average temperature (°C).....	155
Figure 5.16. Sensitivity investigation for the heat transfer coefficient ± 10%, a) average moisture content (kg/kg dry bases), b) average temperature (°C).	156
Figure B.1. Residual plot of the property developed for the diffusivity of ICW....	176
Figure D.2. Boundary condition comparison utilising the heat and mass transfer drying model constructed in Chapter 5 for convective drying apple tissue at 47°C, a) average moisture content (kg/kg dry bases), b) average surface temperature (°C).	179

List of Tables

Table 1.1.Thesis outline	7
Table 3.1. Microscale domains for each drying temperature where the blue subdomain denotes ICW (ω_{ICW}) and the green subdomain denotes FW (ω_{FW}).	76
Table 3.2. Input parameters.....	77
Table 3.3. Summary of the mean absolute error (MAE) between the model predictions and experimental data	85
Table 3.4. Effective diffusivity results of different approaches.....	90
Table 4.1. Input parameters.....	107
Table 5.1. Material Properties	138
Table 5.2. Input parameters.....	143
Table A.1. Summary of heat and mass calculations	173
Table B.2. Summary of heat and mass calculations	175

List of Abbreviations

DMM	Distributed microstructure model
EDMM	Extended distributed microstructure model
FW	Free water
HMM	Heterogeneous multiscale model
ICW	Intracellular water
LBW	Loosely bound water
MAE	Mean absolute error
MRE	Mean relative error
NMR	Nuclear magnetic resonance
REV	Representative elementary volume
SBW	Strongly bound water

Statement of Original Authorship

The work contained in this thesis has not been previously submitted to meet requirements for an award at this or any other higher education institution. To the best of my knowledge and belief, the thesis contains no material previously published or written by another person except where due reference is made.

Signature: _____ [QUT Verified Signature](#)

Date: _____ 1/07/2021

Acknowledgements

Firstly, I would like to express my sincere thanks to my supervisors Associate Professor Azharul Karim and Professor Matthew J. Simpson for all their advice, support, guidance and encouragement throughout my journey, without which this dissertation would not have been possible. Thank you for all the time you have spent reading drafts and discussing issues/challenges, your feedback and help has enabled me to grow personally and academically. Also, I would especially like to thank you for your huge support through the difficult and personal challenges I faced during my journey.

Secondly, I would like to acknowledge the financial support from the Australian Government Research Training Program Scholarship. I would also like to acknowledge the research facilities and software provided by QUT.

Thirdly, thank you to Dr. Imran Khan for his helpful suggestions and discussion throughout my PhD journey, thank you to Dr. Chandan Kumar for his assistance in the early stage of my journey and thank you to my colleagues in the Energy and Drying research group for their help and encouragement.

Lastly, I would like to express my sincere gratitude to my family for their enduring love, support and patience during my journey. Additionally, I would like to thank my friends and colleagues, Amar Velic and Alka Jaggesar, for their support, friendship and coffee breaks.

Chapter 1: Introduction

This chapter first outlines the background (section 1.1), context (section 1.2) and the motivation (section 1.3) of the research. Then, section 1.4 describes the significance of this research and provides definitions of some key terms used. Finally, section 1.5 outlines the remaining chapters of the thesis.

1.1 BACKGROUND

Plant-based food materials, particularly fruits and vegetables, have high nutritional value and are an essential part of everyday life. However, due to their high perishability the wastage of food is an ongoing problem worldwide. This issue is amplified in developing countries where 30-40% of seasonal fruits and vegetables are wasted (Karim & Hawlader, 2005). Drying is a key preservation technique capable of combating this issue. Drying aims to remove moisture, preventing microbial spoilage (Kumar et al., 2015), through simultaneous heat and mass transport with anisotropic deformation (Datta, 2007; Mahiuddin et al., 2018). Drying is very time consuming and energy intensive, accounting for up to 15% of all industrial energy usage (Chua et al., 2001; Kudra, 2004). This makes optimisation of its processes, systems and configurations very important. Mathematical modelling is crucial in the development of optimal drying strategies, since a predictive model and simulation-based approach allows multiple design and control configurations to be investigated for a wide range of process conditions (Defraeye, 2014). However, drying involves many complex interacting transport phenomena, which are still not well understood. This makes mathematical modelling of its processes complex, daunting, important and necessary.

The dynamic migration of moisture is one of these complex interacting processes and is often critical in determining the final quality of a dried sample. The diffusivity of moisture is interconnected and influenced by the structure of the material. Food material is a heterogeneous porous medium with moisture distributed in its various cellular environments. In plant-based food materials, three main types of water exist, namely i) intracellular water (ICW), located within intracellular environments ii) free water (FW), found within intercellular environments, and iii) strongly bound water

(SBW), water inside cell walls (Khan & Karim, 2017). During convective drying, the migration of ICW causes dynamic modifications to the material's physical structure (uneven volume reductions), changing its heterogeneity and nutritional characteristics, effecting the product's quality (Dinçer & Zamfirescu, 2016). Additionally, convective drying is notorious for producing low quality dried foods in terms of their taste, colour and nutritional value (Maskan, 2001). These structural and quality changes depend on temperature, moisture content and the structure of the material. To compensate for these complexities, researchers have embedded condition-dependent diffusivities within mathematical models. The resulting models have limited predictive capabilities restricting a model's performance in optimisation scenarios. Moving towards a more physics-based approach to diffusivity will aid in improving a model's predictive capabilities while accurately modelling the transport which is occurring.

1.2 CONTEXT

Considering condition-dependent moisture diffusivity is very common within mathematical food drying models. Generally, when modelling moisture migration, all mass transport mechanisms are lumped and Fickian diffusion is assumed. The effective diffusivity is then solved through curve fitting techniques to obtain a constant diffusivity coefficient. The resulting property is often unable to consider any variations in material, experimental set up and/or drying conditions (Dadmohammadi & Datta, 2019). To slightly improve the diffusion coefficients predictive capabilities, the Arrhenius framework is commonly applied. This allows the property to be suitable for drying at different temperatures, however, this can also cause a drop in accuracy. The resulting property is still condition-dependent, only suitable for that particular material (i.e. apple or potato) within that drier. During food drying, diffusivity is influenced by the temperature, moisture and the anisotropic deformation. This has motivated researchers to develop new approaches, such as a modified Arrhenius approach (Lentzou et al., 2019), to consider diffusivity in terms of moisture/deformation, improving its accuracy and predictive capabilities. However, these techniques can generate a dramatic demand in physical and mechanical characterization of each sample (Perré, 2007), requiring extensive experimental investigations for very little improvement in the property's predictive capabilities. Literature has been transitioning towards more mechanistic models and generalised approaches to diffusivity.

Dadmohammadi and Datta (2019) introduced a new diffusivity function, using a more mechanistic approach. The approach treats the material as a porous media, using parameters such as relative permeability, porosity, tortuosity and constrictivity. However, the approach still only models the macroscale requiring unique phase dependent diffusivities for each material.

For most food materials the effective diffusivity should be between $10^{-11} - 10^{-9}$ m²/s (Saravacos & Maroulis, 2001). Though, reported values in literature should be treated cautiously. Published experimental moisture diffusivity data is often unreliable, varying 3-5 orders of magnitude for the same material (Dadmohammadi & Datta, 2019; Saravacos & Maroulis, 2001). Additionally, many studies have reported values larger than the self-diffusion and/or diffusion of species in the solvent with no porous structure (Lentzou, et al., 2019). Early studies excluded the effects of deformation, considering a perfect geometry causing the predictive model and experimental data to significantly deviate in the latter stages of drying (Tzempelikos et al., 2015). More modern works have incorporated adjustments for shrinkage, demonstrating the importance of considering deformation (Hassini et al., 2007). The effective diffusion coefficient could be 0.1-50% smaller than free diffusion, as food material is a porous media (Khaled & Vafai, 2003).

The porous structure and heterogeneity of plant-based food materials has largely forced the condition-dependent approaches and inconsistent literature. Food materials experience unique deformation under an external heat source, which originates at a cellular level and causes the material to deform, dynamically changing its heterogeneity (Rahman et al., 2018). These changes depend on the drying conditions and migration of ICW, which can migrate three ways: cell to cell, cell to pore or through cell membrane rupture (Khan & Karim, 2017). When cells rupture, water quickly moves from intracellular spaces to intercellular spaces, thus becoming FW which can be easily transported (Khan et al., 2017). This phenomenon occurs progressively when drying at higher temperatures, generally above 50°C for convective drying. Cell rupturing can significantly influence the transport process, associated deformation and quality of the dried product. However, cell rupturing and its associated effects are not considered in current mathematical models. Some consideration of the material heterogeneity, in terms of space and time with the

presence of cell rupturing, can help transition towards more generalised models with better predictive capabilities.

Multiscale modelling can aid in transiting towards more physics-based models, considering the material heterogeneity. A multiscale model is considered to be a series of sub-models which investigates the behaviour of a particular product, over multiple spatial scales, considering substantial physics for a reasonable computational cost (Rahman et al., 2018). Recently, researchers have shown their immense interest in multiscale food drying modelling and provided some general background into the topic (Ho et al., 2013; Rahman et al., 2018). However, multiscale modelling has not been applied to the field of food drying.

1.3 AIMS AND OBJECTIVES

This study aims to apply multiscale modelling to develop a moisture diffusivity with improved predictive capabilities for drying plant-based food materials. Specifically, the work will focus on developing a generalised moisture diffusivity through accurately capturing the heterogeneous water transport, in terms of space and time, for different food materials with different cellular deformation. To do so, the following objectives have been drawn:

1. Develop a multiscale homogenisation model capable of incorporating the spatial cellular water heterogeneity of food material during drying.
2. Utilise the constructed multiscale model to investigate the temporal water heterogeneity of food material during drying.
3. Develop a comprehensive multiscale model with a generalised moisture diffusivity to investigate its predictive capabilities for drying plant-based food materials.

1.4 SIGNIFICANCE, SCOPE AND DEFINITIONS

1.4.1 Significance and scope of the research

This research aims to develop a novel multiscale model with a generalised diffusivity for drying plant-based food material. The generalised property will be developed in terms of ICW content and sample temperature, considering the cellular water heterogeneity of the material. Considering the diffusivity in relation to the ICW

content is the key to achieving the generalisation of the property. This allows the property to be suitable for various food materials through incorporating the effects of the cellular deformation and its evolution during drying. To utilise the generalised diffusivity while drying at different temperatures, cell rupturing had to be considered. This is expected to result in the creation of a novel rupture threshold to characterise which cellular transport mechanisms were occurring for ICW. The threshold should be unique for each material. This will greatly improve the model's predictive capabilities allowing the property to be suitable for various materials and various drying conditions.

This research will aid in the development of optimum drying systems with improved food quality, facilitating in depth investigations to optimise drying processes, systems and configurations. Additionally, being able to consider cell rupturing and its associated effects is significant and has huge potential in the field. Cell rupturing has not previously been considered, even though it significantly effects the cellular deformation and final quality of the sample. These advancements will allow future in depth computational food quality optimisation investigations to be conducted.

1.4.2 Key definitions used within this dissertation

- **Intracellular water (ICW):** Water located within intracellular spaces.
- **Free water (FW):** Water located within intercellular spaces.
- **Macroscale:** The scale of the plant tissue or single sample.
- **Microscale:** The cellular heterogenous structure of food material. This structure consists of intracellular spaces (cells), intercellular spaces (pores) and cell walls.
- **Cell rupturing:** When a cell wall ruptures converting an intracellular space into intercellular space.

1.5 THESIS OUTLINE

This dissertation is completed as thesis by publication with a total of six chapter. Chapters 2 to 5 correspond to four individual publications, summarised in Table 1.1.

The chapters are introduction (Chapter 1), literature review (Chapter 2), a homogenisation model for food drying (Chapter 3), a multiscale temporal investigation for food drying (Chapter 4), an investigation of a generalised moisture diffusivity for food drying (Chapter 5) and the conclusions (Chapter 6). Chapters 3-6 each chronologically address an objective to achieve the overall aim of the research. A brief outline of each Chapter is below:

In Chapter 1, the background, context, aims and objectives, significance of the research and outline of the thesis is presented.

In Chapter 2, a comprehensive literature review on multiscale modelling for food drying is presented. The chapter presents the current status of multiscale modelling, multiscale frameworks and factors affecting multiscale modelling, solution techniques for space and time, challenges for the field and future directions for applying multiscale modelling to food drying.

In Chapter 3, a multiscale homogenisation model is presented. The chapter presents an approach to homogenise the cellular water heterogeneity (in terms of space) of food material during drying, achieving an effective moisture diffusivity during drying. Three different drying temperatures (45, 60 and 70 °C) are studied and the chapter provides new insight into how to consider the heterogeneous structure of food material utilising knowledge of the microstructural evolution.

In Chapter 4, a multiscale temporal investigation is presented. The chapter conducts an inverse analysis on the multiscale homogenisation model to estimate the temporal diffusivity of ICW. The investigation also develops a function for the diffusivity of ICW in terms of sample temperature and ICW content, opening the possibilities to be applied to various food materials.

In Chapter 5, a generalised moisture diffusivity for food material during drying is investigated. This chapter explores the ICW diffusivity function developed in Chapter 4. Two materials are investigated (apple and potato) at two different drying temperatures (47 and 64 °C). Additionally, the Chapter presents a novel concept to consider when and if cell rupturing occurs.

In Chapter 6, the major conclusions, contributions to knowledge, limitations, and future work of the research are presented.

Table 1.1.Thesis outline

Chapter	Chapter title	Publication status
1	Introduction	
2	Literature Review	Welsh, Z. , Simpson, M. J., Khan, M. I. H., & Karim, M. A. (2018). Multiscale modeling for food drying: State of the art. <i>Comprehensive Reviews in Food Science and Food Safety</i> , 17(5), 1293-1308. doi:10.1111/1541-4337.12380.
3	A multiscale homogenisation model for food drying	Welsh, Z. G. , Khan, M. I. H., & Karim, M. A. (2021). Multiscale modeling for food drying: A homogenized diffusion approach. <i>Journal of Food Engineering</i> , 292, 110252. doi:10.1016/j.jfoodeng.2020.110252.
4	A multiscale temporal investigation for food drying	Welsh, Z. G. , Khan, M. I. H., Simpson, M. J., & Karim, M. A. (2020). A multiscale approach to estimate the cellular diffusivity during food drying. <i>Food Research International</i> (Under review).
5	Comprehensive multiscale model for drying plant-based food material	Welsh, Z. G. , Simpson, M. J., Khan, M. I. H., & Karim, M. A. (2020). Generalized moisture diffusivity for food drying. (Prepared for submission)
6	Conclusions	

REFERENCES

- Chua, K. J., Mujumdar, A. S., Hawlader, M. N. A., Chou, S. K., & Ho, J. C. (2001). Convective drying of agricultural products. Effect of continuous and stepwise change in drying air temperature. *Drying Technology*, 19(8), 1949-1960. <https://doi.org/10.1081/DRT-100107282>
- Dadmohammadi, Y., & Datta, A. K. (2019). Prediction of effective moisture diffusivity in plant tissue food materials over extended moisture range. *Drying Technology*, 1-15. <https://doi.org/10.1080/07373937.2019.1690500>
- Datta, A. K. (2007). Porous media approaches to studying simultaneous heat and mass transfer in food processes. I: Problem formulations. *Journal of Food Engineering*, 80(1), 80-95. <https://doi.org/10.1016/j.jfoodeng.2006.05.013>
- Defraeye, T. (2014). Advanced computational modelling for drying processes – A review. *Applied Energy*, 131, 323-344. <https://doi.org/10.1016/j.apenergy.2014.06.027>
- Dinçer, İ., & Zamfirescu, C. (2016). *Drying phenomena: theory and applications*: John Wiley & Sons.
- Hassini, L., Azzouz, S., Peczalski, R., & Belghith, A. (2007). Estimation of potato moisture diffusivity from convective drying kinetics with correction for shrinkage. *Journal of Food Engineering*, 79(1), 47-56. <https://doi.org/10.1016/j.jfoodeng.2006.01.025>
- Ho, Q. T., Carmeliet, J., Datta, A. K., Defraeye, T., Delele, M. A., Herremans, E., . . . Nicolai, B. M. (2013). Multiscale modeling in food engineering. *Journal of Food Engineering*, 114, 279-291. <https://doi.org/10.1016/j.jfoodeng.2012.08.019>
- Karim, M. A., & Hawlader, M. N. A. (2005). Drying characteristics of banana: theoretical modelling and experimental validation. *Journal of Food Engineering*, 70(1), 35-45. <https://doi.org/https://doi.org/10.1016/j.jfoodeng.2004.09.010>
- Khaled, A. R. A., & Vafai, K. (2003). The role of porous media in modeling flow and heat transfer in biological tissues. *International Journal of Heat and Mass Transfer*

Transfer, 46(26), 4989-5003. [https://doi.org/10.1016/S0017-9310\(03\)00301-6](https://doi.org/10.1016/S0017-9310(03)00301-6)

Khan, M. I. H., & Karim, M. A. (2017). Cellular water distribution, transport, and its investigation methods for plant-based food material. *Food Research International*, 99(Part 1), 1-14. <https://doi.org/10.1016/j.foodres.2017.06.037>

Khan, M. I. H., Wellard, R. M., Nagy, S. A., Joardder, M. U. H., & Karim, M. A. (2017). Experimental investigation of bound and free water transport process during drying of hygroscopic food material. *International Journal of Thermal Sciences*, 117, 266-273. <https://doi.org/10.1016/j.ijthermalsci.2017.04.006>

Kudra, T. (2004). Energy Aspects in Drying. *Drying Technology*, 22(5), 917-932. <https://doi.org/10.1081/DRT-120038572>

Lentzou, D., Boudouvis, A. G., Karathanos, V. T., & Xanthopoulos, G. (2019). A moving boundary model for fruit isothermal drying and shrinkage: An optimization method for water diffusivity and peel resistance estimation. *Journal of Food Engineering*, 263, 299-310. <https://doi.org/10.1016/j.jfoodeng.2019.07.010>

Mahiuddin, M., Khan, M. I. H., Kumar, C., Rahman, M. M., & Karim, M. A. (2018). Shrinkage of food materials during drying: Current status and challenges. *Comprehensive Reviews in Food Science and Food Safety*, 17 (5), 1113-1126. <https://doi.org/10.1111/1541-4337.12375>

Maskan, M. (2001). Kinetics of colour change of kiwifruits during hot air and microwave drying. *Journal of Food Engineering*, 48(2), 169-175. [https://doi.org/https://doi.org/10.1016/S0260-8774\(00\)00154-0](https://doi.org/https://doi.org/10.1016/S0260-8774(00)00154-0)

Perré, P. (2007). Multiscale aspects of heat and mass transfer during drying. *Transport in Porous Media*, 66, 59-76. <https://doi.org/10.1007/s11242-006-9022-2>

Rahman, M. M., Joardder, M. U. H., & Karim, A. (2018). Non-destructive investigation of cellular level moisture distribution and morphological changes during drying of a plant-based food material. *Biosystems Engineering*, 169, 126-138. <https://doi.org/10.1016/j.biosystemseng.2018.02.007>

Rahman, M. M., Joardder, M. U. H., Khan, M. I. H., Nghia, D. P., & Karim, M. A. (2018). Multi-scale model of food drying: Current status and challenges. *Critical Reviews in Food Science and Nutrition*.
<https://doi.org/10.1080/10408398.2016.1227299>

Saravacos, G. D., & Maroulis, Z. B. (2001). *Transport properties of foods*: CRC Press.

Tzempelikos, D. A., Mitrakos, D., Vouros, A. P., Bardakas, A. V., Filios, A. E., & Margaris, D. P. (2015). Numerical modeling of heat and mass transfer during convective drying of cylindrical quince slices. *Journal of Food Engineering*, 156, 10-21. <https://doi.org/10.1016/j.jfoodeng.2015.01.017>

Chapter 2: Literature Review

This chapter is originally published in **Comprehensive Reviews in Food Science and Food Safety**.

Welsh, Z., Simpson, M. J., Khan, M. I. H., & Karim, M. A. (2018). Multiscale modeling for food drying: State of the art. *Comprehensive Reviews in Food Science and Food Safety*, 17(5), 1293-1308. doi:10.1111/1541-4337.12380



Statement of Contribution of Co-Authors for Thesis by Published Paper

The following is the suggested format for the required declaration provided at the start of any thesis chapter which includes a co-authored publication.

The authors listed below have certified that:

1. they meet the criteria for authorship and that they have participated in the conception, execution, or interpretation, of at least that part of the publication in their field of expertise;
2. they take public responsibility for their part of the publication, except for the responsible author who accepts overall responsibility for the publication;
3. there are no other authors of the publication according to these criteria;
4. potential conflicts of interest have been disclosed to (a) granting bodies, (b) the editor or publisher of journals or other publications, and (c) the head of the responsible academic unit, and
5. they agree to the use of the publication in the student's thesis and its publication on the [QUT's ePrints site](#) consistent with any limitations set by publisher requirements.

In the case of this chapter:

Welsh, Z., Simpson, M. J., Khan, M. I. H., & Karim, M. A. (2018). Multiscale modeling for food drying State of the art. *Comprehensive Reviews in Food Science and Food Safety*, 17(5), 1293-1308.

Contributor	Statement of contribution
Zachary Welsh	
QUT Verified Signature	Generation of concept, manuscript preparation, drafting and critically reviewing the literature
Date: 29/11/2020	
M. J. Simpson	Assisted in drafting, organising and critically revising the manuscript.
M. I. H. Khan	Assisted in drafting, organising and critically revising the manuscript.
QUT Verified Signature	Generation of concept, manuscript revision, manuscript editing, author for correspondence and final approval
M. A. Karim	

Principal Supervisor Confirmation

I have sighted email or other correspondence from all Co-authors confirming their certifying authorship. (If the Co-authors are not able to sign the form please forward their email or other correspondence confirming the certifying authorship to the GRC).

Name

[QUT Verified Signature](#)

Signature

Date

2.1 ABSTRACT

Plant-based food materials are mostly porous in nature and heterogeneous in structure with huge diversity in cellular orientation. Different cellular environments of plant-based food materials, such as intercellular, intracellular, and cell wall environments, hold different proportions of water with different characteristics. Due to this structural heterogeneity it is very difficult to understand the drying process and associated morphological changes during drying. Transport processes and morphological changes that take place during drying are mainly governed by the characteristics of and the changes in the cells. Therefore, to predict the actual heat and mass transfer process that occurs in the drying process and associated morphological changes, development of multiscale modeling is crucial. Multiscale modeling is a powerful approach with the ability to incorporate this cellular structural heterogeneity with microscale heat and mass transfer during drying. However, due to the huge complexity involved in developing such a model for plant-based food materials, the studies regarding this issue are very limited. Therefore, we aim in this article to develop a critical conceptual understanding of multiscale modeling frameworks for heterogeneous food materials through an extensive literature review. We present a critical review on the multiscale model formulation and solution techniques with their spatial and temporal coupling options. Food structure, scale definition, and the current status of multiscale modeling are also presented, along with other key factors that are critical to understanding and developing an accurate multiscale framework. We conclude by presenting the main challenges for developing an accurate multiscale modeling framework for food drying.

2.2 INTRODUCTION

Food drying is a rapidly expanding area of research with primary focus on understanding the fundamental physics of the transport process during drying. Scientists and researchers have directed enormous effort toward uncovering the actual heat and mass transport phenomena that occurs during food drying. Many theoretical models considering the food material as a single phase or multiphase domain have been developed (Golestani, Raisi, & Aroujalian, 2013; Gulati, Zhu, & Datta, 2016; Kumar, Joardder, Farrell, & Karim, 2017). These models classically simulate the

material using a representative elementary volume (REV) by eliminating the effects of the materials microstructure. Foods, in particular fruits and vegetables, have a heterogeneous microstructure consisting of intercellular space, intracellular space, and cell walls (Khan & Karim, 2017). Evolution of heterogeneous microstructure during thermal processing has a significant role in the water migration and must be taken into consideration in order to accurately represent the transport process. During drying, the transportation of water from cellular locations to the surrounding environments causes uneven volume reductions (anisotropic shrinkage) (Khan & Karim, 2017). This anisotropic shrinkage can have many negative consequences on food material, such as deterioration of quality, surface cracking, changes in rehydration capability and textural properties (Mulet, Garcia-Reverter, Bon, & Berna, 2000; Senadeera, Bhandari, Young, & Wijesinghe, 2005). Moreover, shrinkage significantly affects the drying rate and the drying kinetics during food drying (Mahiuddin et al., 2018). In this context, accurate prediction of shrinkage during drying of food material is very important. Although many studies have been conducted to predict the shrinkage phenomena (Mahiuddin et al., 2018), all existing models have been formulated at a macroscale level based on the tissue deformation. Therefore, these studies are unable to capture the anisotropic shrinkage because the morphological changes due to the drying process initiates at cell level (Konstankiewicz et al., 2002), and final results (deformation) appears at tissue level (Mahiuddin et al., 2018). Therefore, for predicting the accurate anisotropic shrinkage phenomena and associated structural changes, multiscale modeling is essential.

Multiscale modeling is one approach that has the potential to incorporate the effects of a material's microstructure while balancing the required computational resources. Multiscale modeling is considered to be comprised of a series of submodels which investigate a product's behavior over multiple spatial scales (Rahman, Joardder, Khan, Nghia, & Karim, 2016). This allows fewer assumptions to be made while allowing a substantial amount of physics to be included across multiple length scales. Thus, the physics can be modeled to a great depth while saving on computational resources (Weinan, Engquist, Li, Ren, & Vanden-Eijnden, 2007). Multiscale modeling has been applied to various fields over the years such as material science and soft matter and biological science. However, it is still new for food drying. Work has been published for multiscale timber drying (Perré & Rémond, 2006; Perré & Turner, 1999)

in addition to a series of works produced on the multiscale dehydration aspect of food material (Aregawi, Abera, Fanta, Verboven, & Nicolai, 2014; Fanta et al., 2014; Fanta et al., 2013). However, these are significantly different from multiscale food drying. Timber drying is vastly different in terms of the deformation which occurs and the dehydration models excluding any external heat source. Recently, some researchers have shown their immense interest in multiscale food drying modeling and provided some general background into multiscale modeling (Defraeye, 2014; Ho et al., 2013; Rahman et al., 2016). Ho et al. (2013) investigated the imagery techniques for constructing a geometry for using in multiscale modeling and discussed possible numerical techniques for multiscale food modeling. Moreover, it mainly focused on one way coupled techniques, such as homogenization, to incorporate a materials heterogeneous structure. Homogenization can only account for the materials structure and is unable to capture the actual microstructural changes during drying. Furthermore, this study also fails to investigate the concurrent multiscale approaches in depth or investigate the temporal coupling. Considering the limitations of Ho et al. (2013), previously the current authors (Rahman et al., 2016) comprehensively reviewed and discussed the current challenges and status of multiscale modeling for food drying. The study reported how to bridge the scales, while providing insight into the relative properties for multiscale shrinkage. However, this study does not provide any comprehensive review on multiscale modeling frameworks. Moreover, the paper did not cover the solution techniques or temporal coupling at all. Therefore, a comprehensive study on multiscale modeling that includes development and solution procedure of a multiscale model for food drying is essential. Considering the gaps in the literature outlined above, this study provides a comprehensive overview of the multiscale model formulation and solution for food drying with their spatial and temporal coupling options.

Due to the fact that limited literature available on multiscale food drying, this review will utilize various publications from the different applicable fields including, material science, soft matter and biological science. This paper will present the current status of multiscale modeling, multiscale frameworks, and the factors affecting multiscale modeling and will explain how the structural heterogeneities affect the transport process during drying. Finally, the review will be concluded with the

consideration of current challenges and the scope for further research in multiscale modeling of food drying.

2.3 FOOD STRUCTURE

The real structure of food has multiple length scales. The definition scales utilized in the present work are discussed below:

2.3.1 Real food structure

Plant-based food material is a heterogeneous and hygroscopic porous medium. Its complex structure is composed mainly of polymers and water, with a water content of up to 80–90% (Khan, Kumar, Joardder, & Karim, 2017). In addition, food materials contain minerals and air which heavily contribute to its complex structure (Gross & Kalra, 2002). During thermal processing (such as drying) food undergoes modifications of physical, chemical, and nutritional characteristics as a result of the large amount of moisture removed. These modifications of the food's structure span across multiple scales of length (i.e., cellular to tissue). Cells are the basic units of food material and can be found at a micro-length scale (commonly referred to as microstructure). Food microstructure consists of intercellular space, intracellular space, and cell walls, as shown in Figure 2.1 (Khan, Joardder, Kumar, & Karim, 2016). The intercellular spaces are considered to be the empty spaces in between a group of cells they are also known as pores. These typically contain a small percentage of water (free water) and other solutes. Intracellular space is defined as the space within cells consisting of the vacuole and cytoplasm. The majority of the water that resides within the microstructure can be found here (known as intracellular water). Additionally, water is also located in the cell walls and is known as cell wall water or extracellular water (Khan & Karim, 2017).

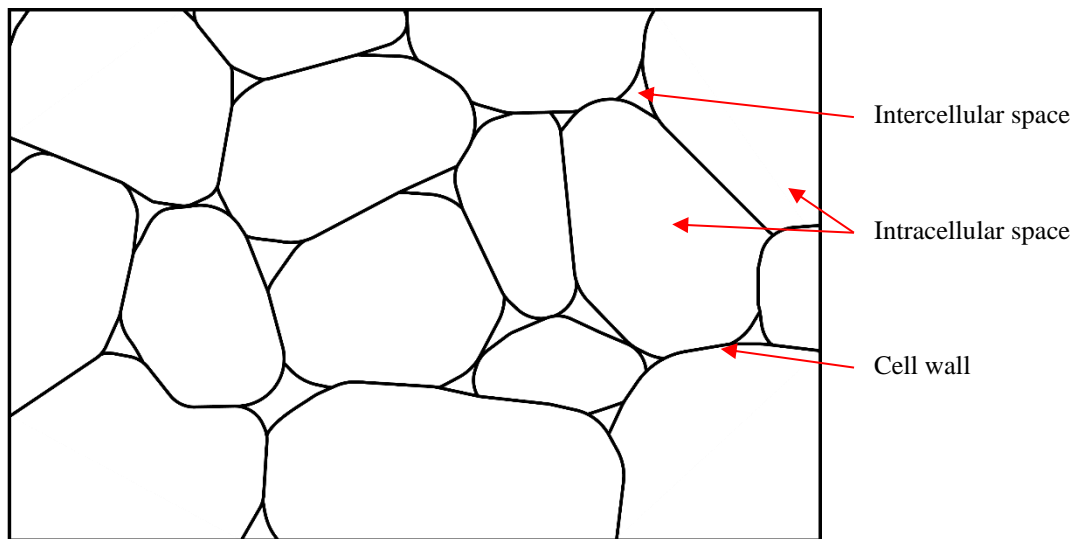


Figure 2.1. Heterogeneous cellular structure of plant-based food material.

The heat and mass transport process is significantly influenced by the microstructure of plant-based food material (Joardder, Kumar, & Karim, 2017a). Water migration is the major concern during these processes. Water within food material falls under two classifications, free water (FW) and bound water. FW is located within the pores and the capillaries. These intercellular spaces are unrestricted, which allows the FW to be effortlessly transported during drying. Bound water can be either chemically or physically bound to food material, with physically bound water being the main concern for the heat and mass transports (Khan & Karim, 2017). Physically bound water contains two subdivisions: loosely bound water (LBW) and strongly bound water (SBW); LBW is intracellular water and SBW is cell wall water (Caurie, 2011; Khan, Wellard, Nagy, Joardder, & Karim, 2017). SBW is trapped within the cell wall and is not transported during thermal processing, resulting in the FW and LBW being the major concern during drying (Khan et al., 2016). FW in the unrestricted pores can migrate to the surface and be removed due to evaporation (Srikiatden & Roberts, 2007). LBW water can migrate following three possible paths: cell to cell, cell to pore, or through cell membrane rupture. Further details can be found in the authors' previous works (Khan & Karim, 2017; Khan et al., 2018).

2.3.2 Length scales definitions

Three major scales are referred to in this work: microscale, macroscale, and industry scale, as shown in Figure 2.2. The micro-length scale considers the heterogeneous microstructure of food material, with a domain consisting of intracellular space, intercellular space, and cell walls. This scale generally has a length range of 10^{-6} to 10^{-2} m. Very few studies have been published for food drying at a microscale. Investigations have been conducted into cellular water distribution in addition to the development of a realistic microstructure domain of food (Khan et al., 2018; Rahman, Gu, & Karim, 2018). Very recently, the first microscale transport model for food drying has been published (Rahman, Kumar, Joardder, & Karim, 2018). The model investigates a heterogeneous microstructure consisting of cells and pores under convective drying. Over the years more insights have been published on soft matter for the deformation and water under dehydration (Aregawi et al., 2014; Fanta et al., 2014; Fanta et al., 2013). Also, gas transport on 2-D and 3-D microscale geometries have been investigated (Ho et al., 2014). Further research is required at a microscale to comprehensively understand what occurs during thermal processes such as drying.

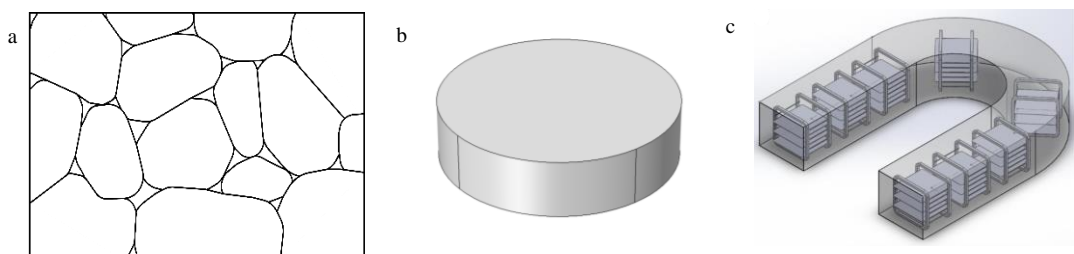


Figure 2.2. Length scales. (a) Microscale, (b) Macroscale, (c) Industry scale.

The macroscale is considered to be the plant tissue or product sample. This scale has a length range of 10^{-2} to 10 m and fails to include any information or details from finer scales. Normally the product is treated as a structureless continuum which is achieved through REV (Ho et al., 2013). REV is the volume average of the heterogeneous material properties taken over a small volume. REV utilizes a single

function approach denoting a real valued function, u , over a domain Ω . The local average form of the REV approach is considered to be

$$\langle u(x) \rangle = \int_{V(x)} u(y) dy, \quad (2.1)$$

where $V(x)$ is a small volume surrounding the point x of the size of the REV.

The macroscale approach is where the majority of food drying research has been conducted and the actual details of the microscale heterogeneity are not modeled (Ho et al., 2013). Macroscale models exist for a wide range of processes including drying. Comprehensive theoretical models for traditional drying techniques, such as convective drying, exist for both single and multiphase transports as well as deformation (Golestani, Raisi, & Aroujalian, 2013; Kaya, Aydin, & Dincer, 2008). For advanced and innovative drying technologies, such as microwave drying or hybrid techniques, theoretical models are less developed although some models on multiphase heat and mass transport for microwave drying have been reported (Chen et al., 2014; Gulati et al., 2016). Similarly, deformation model for intermittent microwave drying has been developed by Joardder et al. (2017b). Validation is also established at this scale using various techniques, such as X-ray tomography, optical methods, and magnetic resonance imaging (Cantre, Herremans, Verboven, Ampofo-Asiama, & Nicolaï, 2014; Vicent, Verboven, Ndoye, Alvarez, & Nicolaï, 2017). In addition, new methods are being published on determining heat distributions within microwave dryers utilizing a heat determination product such as low acyl gellan gel. Low acyl gellan gel can be prepared to match physical properties of foods as well as constructed with chemical markers to utilize the product for heating pattern determinations. Readers are directed to Luan, Wang, Tang, and Jain (2016) for an example where this gel is utilized, to Zhang et al. (2015) on controlling the properties, and to Morris, Nishinari, and Rinaudo (2012) for a comprehensive review of the product. It should be noted that gellan gel is currently tailored to microwave-heating validation.

The third scale referred to in this work is the industry length scale. Industry scale is considered to include the entire dryer as the domain. A predominant example of this is the inclusion of multiple products. The industry scale has a length range of 10^{-1} to 1000 m and is less common in the literature because it is usually modeled in industry. Some previous studies have focused on industry scale spray dryers or continuous dryers (Fletcher & Langrish, 2009; Huang et al., 2017). Additionally, some works have

been done for multiple products in microwaves or continuous microwave conveyor belt dryers (Chen, Lau, Chen, Wang, & Subbiah, 2017). However these can be classed as semi industrial studies. Depending on the drying technology, some results can be scaled up to a certain degree from a macroscale for industry applications such as air flow distributions, while some results cannot (i.e., electromagnetic distributions within microwave heating [Li, Wang, & Kudra, 2011; Vadivambal & Jayas, 2010]). Currently a great divide exists between what academia publishes at one scale and industry requires at another (Defraeye, 2014).

These scale definitions are arbitrary with more length scales existing and overlapping in reality. In the published literature, most of the research has been conducted on dual-scale models where a simple naming scheme is utilized to denote the different length scales: fine and coarse. These will also be used in context throughout this work as modeling across three scales is quite rare in the literature (Fish & Yu, 2001; Rohan, Turjanicová, & Lukeš, 2017).

2.4 CURRENT STATUS OF MULTISCALE MODELING

Multiscale modeling is not new, with a large number of studies existing across multiple fields such as mathematics (Carr, Turner, & Perre, 2013) and material science (Hou & Wu, 1997). Multiscale models can be classified in two types: one-way or two-way coupled models (also known as serial/sequential or concurrent) (Defraeye, 2014). These classifications are dictated by whether a model is transferring information in one direction or two. One-way coupling can be recognized where information is fed from one scale to another, such as the heat, mass, or apparent properties transferred one way from the fine to the coarse scale. These models are linked in a straightforward manner (Kohout & Stepanek, 2007; Novák, Kočí, Štěpánek, & Marek, 2011) and are commonly referred to as upscaling or downscaling. The calculations are generally kept independent of the solution. Two-way or concurrent coupling allows the subdomains to exchange data and solve simultaneously; heterogeneous multiscale modeling (HMM) and equation-free frameworks are examples of two-way coupling methods (Perré, 2007). Depending on the application, hybrid one/two-way coupled models can be constructed (Carr et al., 2013). Various multiscale models have been constructed over the years such as adaptive model refinement (Garcia, Bell, Crutchfield, & Alder,

1999) Car–Parrinello method (Car & Parrinello, 1985), multigrid (Brandt, 1977), quasi continuum method (Tadmor, Ortiz, & Phillips, 1996), HMM (Weinan & Engquist, 2003; Weinan et al., 2007), equation-free framework (Kevrekidis et al., 2003), distributed microstructure model (DMM) (Showalter, 1993), extended distributed microstructure model (EDMM) (Carr, Perré, & Turner, 2016) and computational homogenization (Geers, Kouznetsova, Matouš, & Yvonnet, 2017). However, these approaches are generally valid for specific applications. For instance, DMM is a very specific framework that is valid for a domain consisting of two sub-domains of a homogeneous material. Due to the specific nature of the DMM framework, it is not ideal for food processing. EDMM can be considered as a hybrid DMM/HMM approach, which avoids the use of traditional upscaling techniques. However, EDMM is still in its infancy with an eventual end goal of being suitable for two-scale multiphase transport. Therefore, rigorous studies are required to access the applicability of EDMM for food processing. Additionally, some techniques such as the Car–Parrinello method (Car & Parrinello, 1985) or the quasi continuum method (Tadmor, Ortiz, & Phillips, 1996) could potentially provide insight but are yet to be applied in the context of food drying (i.e. Car–Parrinello method of bridging different spatial and/or temporal couplings). The HMM and equation free framework are more generalized frameworks and therefore could be suitable for application of food drying.

Multiscale modeling is yet to be applied to food drying. However, various studies have been published over the years for both one and two-way coupled models. Mathematics is one field where multiscale heterogeneous material has been investigated. One-way coupled models for multiphase flow in porous media (Lunati & Jenny, 2006) and multiscale transport in heterogeneous porous media have been published. In addition, two-way coupled models exist on unsaturated soils (Carr & Turner, 2014) and heterogeneous heat transfer in phase transition application (Lin, Smith, Liu, & Wagner, 2017). Considerable work has been done on soft matter for one-way coupled models for deformation (Aregawi et al., 2014), pore transport (Ryan & Tartakovsky, 2011), gas transport (Ho et al., 2011; Ho, Verboven, Verlinden, & Nicolaï, 2010), general transport (Ho, Verboven, Verlinden, Herremans, & Nicolaï, 2013), and porous media (Delele et al., 2009). Material science publications provide some insight into the flow in porous sand (Szymkiewicz, Lewandowska, Angulo-Jaramillo, & Butlańska, 2008), composite/porous media (Hou & Wu, 1997), and

multiscale structure analysis (R. van der Sman & Broeze, 2014). The majority of studies published in the field of drying has been done on multiscale timber drying in two-way and hybrid coupled models (Carr et al., 2013; Perré, 2010; Perré & Rémond, 2006). In addition, work has been done on vacuum drying (Kohout & Stepanek, 2007) and rehydration of food (R. G. M. van der Sman et al., 2014). The majority of these studies cover individual aspects or phenomena for food material. Incorporating these phenomena into a multiscale model for the application of food drying will require extensive modification and adaption to achieve a concurrent coupling that comprehensively models the effect of the heterogeneous structure for all drying stages.

2.5 MULTISCALE MODELING FRAMEWORKS

Numerous multiscale frameworks exist in the literature. In this section classical techniques and modern frameworks are presented in relation to their model formulation and solution techniques. The techniques which will be focused on are homogenization extended multigrid, HMM, and the equation-free framework. Additionally, domain representation will be introduced and investigated in terms of its importance for multiscale modeling.

2.5.1 Domain representation

Constructing a theoretical model contains several key steps such as domain selection, model formulation, and solution technique regardless of the field. For multiscale modeling, the domain selection or representation is a significant process. A dual-scale model will consist of two submodels each with their own domain. These domains are required to be coupled to achieve the multiscale model. In order to achieve an accurate coupling, the fine-scale sub-domain must be represented within the coarse-scale domain. The domain representation and its associated interactions in this context are investigated.

Domain representation in each scale

One strategy that achieves a good balance between the desired results and computational resources is to represent the microscale domain within a node on a macroscale level. This allows the reconstruction/restriction of the state variables

(temperature/moisture) from microscale to macroscale to be simpler. It has also appeared in the literature as a single point at a macroscale within problems of fewer dimensions (Fachinotti, Toro, Sánchez, & Huespe, 2015; Kouznetsova, Brekelmans, & Baaijens, 2001). This simplification requires far less interpolation to achieve a consistent result across the boundary between the fine and coarse scales. In addition, it must be kept in mind that this strategy will introduce additional assumptions for the compression/interpolation portion of the coupling from macro to micro; for example, the state variables at a certain node are assumed to be constant on the microscale domain.

An alternative approach is to represent the fine-scale domain as a small region within the macroscale, connected through elements and nodes. This increases the computational resources and complexity of the coupling. This style of coupling introduces an additional step within the coupling methodology which will be required to interpolate between the scales; for example, the distribution of the state variables on the fine-scale domain will be a result of the surrounding nodal results (a similar methodology to a finite difference form of the heat equation (Zhang, Cao, Feng, & Wang, 2017)). The advantage of this approach is that the final result will be more detailed and a true representation of the actual food material.

Another strategy is to represent the domain as a periodic microscale unit cell. This is a highly effective method for certain materials, especially when a material has a naturally periodic heterogeneous structure. This strategy is often paired with the first two methods to achieve a desired model. It is quite common in multiscale mathematics and can considerably reduce the computational resources required (Carr et al., 2013). In order for the microscale domain evolution to represent the situation accurately, the reconstruction strategy selected must be appropriate.

Food structure representation at each scale

Domain selection is a process that involves the real food structure representation at each individual scale. There are various ways this can be achieved. Three common strategies are to generate a domain, create a simplified domain, or use the actual real food structure. For the application of multiscale food drying modeling, how the microscale domain represents the real food structure is of particular interest.

To generate a domain can be an appropriate strategy but requires an initial time investment to achieve the domain. Generating a microscale heterogeneous domain is a complex process. Abera et al. (2013) created a representative domain of fruit tissue using a cell-generating algorithm. They compared the generated domain to Verboven et al. (2008) work. The model was able to generate different types of tissue and the inclusion of cells, cell walls, and pores. For more general cases, other cell generation algorithms have been produced (Abera et al., 2014; Gibson et al., 2011; Merks, Guravage, Inzé, & Beemster, 2011). Depending on the application, generating a domain can be an effective approach.

Creating a simplified domain can be considered as a hybrid method between the generated and the actual domain. Generic software packages such as MATLAB can be used in conjugation with imaging methods to create a simplified representation of a product's microstructure. This is the most common approach in the literature and appears in various forms. Rahman et al. (2018) created a simplified microscale domain with clear identification of cell and intercellular spaces. They performed a statistical analysis of the developed geometrical model and microscopic images to determine the accuracy of the proposed method.

The microstructure of foods can be modeled directly. Many imagery techniques and methods exist to model the products directly over multiple spatial scales (Ho et al., 2013). Typically, when such imagery techniques are used, much post-processing is required. Commonly, application-specific custom-built software is utilized. Commercial versions also exist, such as Simpleware scan IP 7, as demonstrated by Kashkooli et al. (2016) for the application of multiscale modeling of lithium battery electrodes. Such software packages can create the exact microscale structure of a computational domain. This approach generally leads to a very accurate model but also a computationally demanding model.

2.5.2 Model formulation

Multiscale model formulation has a few key processes that set it apart from traditional single-scale modeling. The model consists of a method of downscaling and upscaling, in addition to its spatial and temporal coupling. The classical techniques of homogenization and multigrid are discussed in addition to the more modern frameworks of heterogeneous multiscale modeling and the equation-free framework. A model's spatial and temporal coupling are strongly linked to the upscaling and

downscaling techniques but this will be covered in more detail in our discussion of the solution techniques.

2.5.3 Homogenization

Homogenization is a traditional mathematical method which allows differential equations to be upscaled (Hornung, 2012). The homogenization methodology takes a few forms in literature with various variations existing for individual applications. Homogenization is centered around working on a family of functions, commonly denoted as u_ϵ (with u being a variable field such as temperature or moisture), to achieve the upscaling of an equation. In this notation ϵ represents the spatial scale parameter. Homogenization is best understood through examples (Pavliotis & Stuart, 2008). If we consider a 1D steady state conduction problem:

$$\frac{d}{dx} \left(k(x) \frac{dT(x)}{dx} \right) = f(x), \quad \text{for } x \in (0, L) \quad (2.2)$$

$$T(0) = T(L) = 0 \quad (2.3)$$

where $k(x)$ is the thermal conductivity, $T(x)$ is the dependent variable (i.e., temperature or moisture), $f(x)$ is a source term, and $T(0)$ and $T(L)$ are being a set of boundary conditions for the bounded domain of $x \in (0, L)$.

If the domain is considered as a heterogeneous and periodic material consisting of a series of subdomains (periodic unit cells), then the problem contains two length scales, a macroscale and a microscale. The reference problem turns into a multiscale problem. The small parameter ϵ signifies the ratio between the macroscale x and the microscale y , and then results in

$$y = \frac{x}{\epsilon} \quad (2.4)$$

with the resulting microscale problem:

$$\frac{d}{dy} \left(k(y) \frac{dT^\epsilon(y)}{dy} \right) = f(x) \quad \text{in } y \in (0, 1) \quad (2.5)$$

$$T^\varepsilon(0) = T^\varepsilon(1) \quad (2.6)$$

$$\int_0^1 T^\varepsilon(y) dy = 0 \quad (2.7)$$

Homogenization theory revolves around the limit

$$T^\varepsilon \xrightarrow[\varepsilon \rightarrow 0]{} T^0 \quad (2.8)$$

This limit involves considering the scale parameter, epsilon, tending to zero. This implies that the heterogeneity vanishes, leading to an equivalent homogeneous material (Pavliotis & Stuart, 2008). The homogenized global/macroscale problem results in

$$\frac{d}{dx} \left(k^0(y) \frac{dT^0(x)}{dx} \right) = f(x), \quad \text{for } x \in (0, L) \quad (2.9)$$

$$T(0) = T(L) = 0 \quad (2.10)$$

In order to derive the limit, the microscale temperature function T^ε is developed as the following expansion:

$$T^\varepsilon(x, y) = T_1(x) + \varepsilon T_2(x, y) + L(\varepsilon^2) + \dots \quad (2.11)$$

with the space derivatives of

$$\frac{d}{dx} = \frac{\partial}{\partial x} + \frac{1}{\varepsilon} \frac{\partial}{\partial y} \quad (2.12)$$

Performing a formal expansion will result in the homogenized macroscopic property k^0 as

$$k^0 = k(y) + k(y) \frac{\partial}{\partial y} \omega(y) \quad (2.13)$$

The homogenized variable is equal to the average of the microscopic variable plus a corrective term. The reader is directed to Hornung (2012) or Perré (2007) for

examples of applying homogenization to simple and well-known equations and problems.

Homogenization is constructed to produce macroscale results from a microscale heterogeneous model (Perré, 2007). This makes it ideal for multiscale food drying modeling and, as a result, homogenization has been the most commonly applied method thus far in the field. It should be noted that, currently, multiscale food drying literature is limited or nonexistent. However, individually, multiscale drying literature of other materials and multiscale food dehydration literature (excluding external heat sources) has been published to a certain degree recently (Kohout & Stepanek, 2007; Li, Lv, Wang, Zhao, & Yang, 2015; Li & Wang, 2016).

The majority of the multiscale models for drying has been conducted on timber. A series of works has been published for the various length scales for timber (Perré, Rémond, Colin, Mougel, & Almeida, 2012; Perré, Rémond, & Turner, 2013). Readers are directed to Perré (2007) for a breakdown of the homogenization and an in-depth description of the transport which occurs in these studies. In addition, Perré (2015) provides insight into when it is appropriate to use two or three state variable equations for multiscale transport modeling. These studies are focused on convection drying with simple and complex models (with the inclusion of product variation for the complex models, i.e., for timber sapwood or heartwood) being the focus of the work. The software TransPore was utilized to achieve the multiscale formulation and solve the model. Carr et al. (2013) produced a particularly insightful multiscale model for timber drying in the hygroscopic range. The model couples the heat and mass transfer at a microscopic level while using homogenization. The work uses a unit cell to represent the fine-scale domain as a heterogeneous periodic structure. However, the model is only applicable for the hygroscopic range and the initial FW of the product is not considered. This limits its applicability to food as the initial FW concentration is important within the process.

Thus far multiscale food modeling has been conducted for dehydration (Fanta et al., 2013; Ho et al., 2014). This excludes any external heat source and greatly reduces the deformation or shrinkage when compared to drying. The work published again utilizes homogenization and has primarily featured upscaled models. Gas and vapor transport have been investigated separately at a microscopic scale by Fanta et al. (2014) and Ho et al. (2011), respectively. These studies have been produced on 2D

and 3D microscale work for generated domains of pears. The 2D microscopic results limit the research applications because of the transport within the intercellular space; these issues were raised and discussed within Fanta et al. (2013). The research was later extended to a 3D microscale domain structure to remove the issues entirely. Multiscale dehydration models are at the forefront of the multiscale food modeling and create a strong theory base for future complex multiscale models for food drying.

Homogenization has the ability to incorporate a materials heterogeneous structure at a reasonable computational cost. In traditional homogenization approaches, the upscaling operation is performed just once. This means that homogenization is more computationally efficient than concurrent approaches where the upscaling and downscaling operations are performed repeatedly. For food drying the current macroscale approach uses lumped cell and pore properties, in addition to utilizing the single lumped value throughout the tissue (Nguyen, Verboven, Scheerlinck, Vandewalle, & Nicolaï, 2006). This is not ideal as large variations can exist within a product due to its structural heterogeneity. Considering multiphase nature of transport that takes place during drying, some key material properties which should be scaled include the effective density, effective thermal conductivity and effective specific heat. These properties influence the macroscale energy conservation and hence the model. The properties which require scaling will depend on the drying technology as well as the purpose of the model.

Homogenization is currently the dominant traditional mathematical technique used to achieve an upscaled model for modeling dehydration and drying. The models are increasing in complexity as computational resources and the knowledge of microscopic transport improve. As in traditional homogenization upscaling is done only once, it is unable to incorporate any microstructural changes which occurs throughout the drying process. Homogenization is expected to be utilized for many years to come to achieve multiscale models in partnership with some generalized frameworks to achieve concurrent or two-way coupled multiscale models.

2.5.4 Multigrid and extended multigrid

The extended multigrid framework is one of the earliest examples of applying a classical mathematical technique. As the name suggests, it is based on the classical

multigrid technique and there are various versions, such as the multiscale multigrid. The basic concept for multigrid was originally introduced by Fedorenko (1973) before becoming practical (Brandt, 1977). Brandt (2002) extended the technique to the application of multiscale modeling. In its classical form the technique is only directed toward capturing the fine-scale details. This limited the technique to linear scaling. Brandt's extension shares this limitation to a certain degree, but it does allow sublinear coupling (Weinan, 2011). The traditional technique was designed for algebraic equations that arise from discretizing partial differential equations and has a general procedure of:

- Interpolation—the current values of interest on the coarse-scale results are used to initialize or constrain the microscale.
- Equilibration—run the fine-level model (on small windows) for the required number of steps.
- Restriction—project the variables at the fine level back to the coarse level.

This procedure is shared by the extended multigrid framework. One major advantage of the extended variation is that the coarse and fine scales can be very different and very distant (Weinan, 2011). In addition, problems with different physics at various levels can be incorporated. It is a generalized approach and has a very similar procedure as the equation-free framework.

The extended multigrid or multiscale multigrid is not the first choice for multiscale food drying. Though variations in the literature have been applied in concurrent models on heterogeneous media (i.e., multigrid homogenization [Boffy & Venner, 2014; Cecot & Oleksy, 2015; Fish & Belsky, 1995a, 1995b] or multiscale finite element methods [Hou & Wu, 1997]), all share a similar methodology. In recent times, the multiscale multigrid framework has been applied to multiscale boundary turbulent flow, in particular in DNS or LNS simulations (Gravemeier, Gee, Kronbichler, & Wall, 2010; Gravemeier & Wall, 2010).

Boundary flow for food drying is still a large research area which has yet to be explored in depth (Defraeye, Radu, & Derome, 2016). The reader is directed to Defraeye et al. (2016) for further insight into this area. Multigrid could have potential

for multiscale modeling of boundary flow or multiscale transport; however, HMM and the equation-free framework have more potential for concurrent models.

2.5.5 Heterogeneous multiscale modeling

HMM has become one of the most common and well-known multiscale frameworks. It is a general framework for constructing multiscale models and is considered a very helpful guide (Weinan et al., 2007). It was first proposed by Weinan and Engquist (2003) and has since received significant attention. HMM is only a framework, and applying it to specific problems can be a highly complex and non-trivial task (Weinan et al., 2007). It has a very similar methodology to computational homogenization, although the two often appear in different fields, computational mathematics and computational mechanics, respectively (Matouš, Geers, Kouznetsova, & Gillman, 2017). HMM has been discussed and reviewed in great depth (Weinan et al., 2007). HMM is a top-down framework built for dual or higher multiscale models. Its formulation is constructed around having an incomplete macroscale model, commonly represented as

$$\partial_t U = L(U; D) \quad (2.14)$$

where U denotes the state variable field (i.e., temperature or moisture), D denotes the data needed to complete the model (i.e., fluxes or diffusion). The coupled microscale model can be represented as

$$\partial_t u = L(u; U) \quad (2.15)$$

Within this representation the macroscale variable U is transferred to the microscale model (through an assumption, constant, or interpolation). Representing this HMM approach in its basic theoretical form results in

$$F(U, D) = 0 \quad (2.16)$$

$$f(u, d) = 0 \quad ; \quad d = d(U) \quad (2.17)$$

where d denotes the data required to initiate the microscale mode (i.e., heat, temperature, or moisture). HMM is only interested in the final results of the macroscale model, the microscale model being supplementary (Weinan, 2011). It contains two

main components, a macroscale solver and a procedure for estimating the missing macroscale data D using the microscale model. This results in the state variables, U and u , being restricted and compressed between the scales throughout the simulation; thus providing a strategy for formulating the downscaling and upscaling of the model. In addition, the data, d , required between the scales must be constrained and estimated to complete the framework.

HMM or a variation of HMM has been used largely in many fields such as soft matter, biological science, material science, and mathematics. Heterogeneous porous media have only been modeled to a certain degree using this framework (Arjmand & Runborg, 2016). Lin et al. (2017) constructed a HMM-inspired framework for heterogeneous heat transfer and phase transition applications. They coupled a single state variable of temperature within the concurrent framework. Additionally, the framework has the ability to be applied to phase transition applications by allowing the effective properties (i.e., density, thermal conductivity and/or specific heat) to be updated at each fine scale data exchange point. For heterogeneous material, more research exists on computational homogenization than on HMM. Lin et al.'s approach and methodology has been applied to various types of problems; for example, thermal (Larsson, Runesson, & Su, 2010; Özdemir, Brekelmans, & Geers, 2008) and diffusion (Nilenius, Larsson, Lundgren, & Runesson, 2014). Computational homogenization has been directly applied to problems of porous media (Sandström, Larsson, & Runesson, 2016; Zhuang, Wang, & Zhu, 2015) and biological tissue (Breuls, Sengers, Oomens, Bouten, & Baaijens, 2002).

The HMM approach is an example of a concurrent multiscale framework and requires much more computational resources as the scaling operations occur multiple times throughout the simulation. For food drying, a concurrent approach has the ability to incorporate the microstructural changes which occur throughout the drying process. The relationship between the microstructural changes and the properties of the product is not clearly understood from the limited literature available (Rahman et al., 2016). However, it is well documented that a product's structure heavily affects its quality (Ko & Gunasekaran, 2007; Witek et al., 2010). To achieve a concurrent HMM approach, various parameters require scaling back and forth between the scales. A brief outline of some key variables that could be scaled in a concurrent application is given in Figure 2.3. To create a consistent model the source term as well as the boundary

conditions should be downscaled. Depending on the purpose of the model the phase specific fluxes, material properties and cell deformation should be scaled. The upscaling of the phase specific fluxes will contribute to the mass as well as the energy conservation. Furthermore, upscaling the material properties will influence the energy conservation and scaling of the deformation will be capable of capturing the microstructural changes (anisotropic shrinkage). In addition, the loosely bound water flux should be scaled separately to capture the true transport process. With HMM's ability to include the microstructural changes, it holds the great potential for multiscale research in food drying.

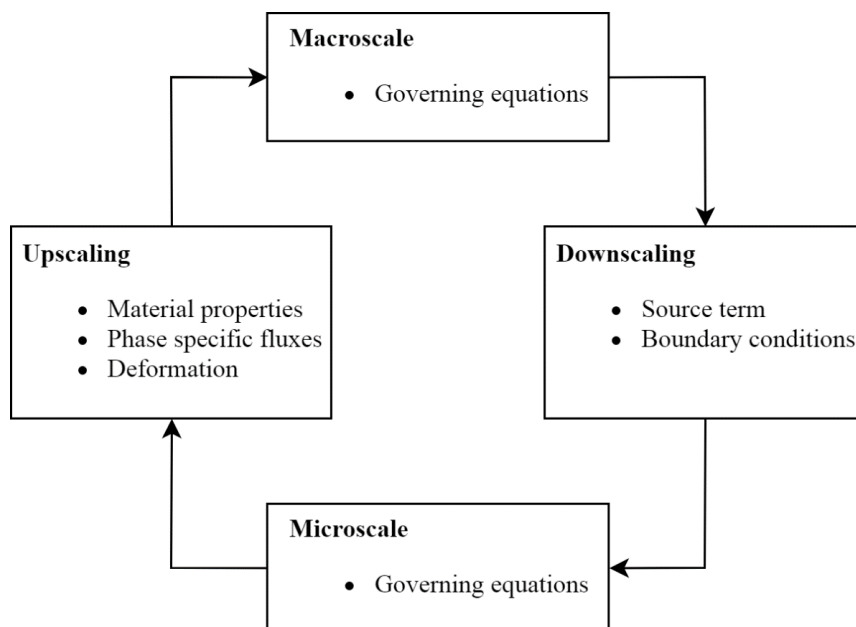


Figure 2.3. Concurrent food drying modeling approach.

2.5.6 Equation-free framework

The equation-free framework is a bottom-up modeling approach (Kevrekidis, Gear, & Hummer, 2004; Weinan, 2011). It was proposed by Kevrekidis et al. (2003) drawing on the work of Theodoropoulos, Qian, and Kevrekidis (2000) and has seen major advancements since then (Roberts & Kevrekidis, 2007; Samaey, Roose, & Kevrekidis, 2005). It is commonly used when the macroscale model is unknown or not well understood. This is one of its greatest advantages. The basic theoretical

formulation of the equation-free framework considers the microscopic evolution law and appropriate time stepper as

$$\partial_t u(x, t) = f(u(x, t)), u(x, t + dt) = s(u(x, t), dt) \quad (2.18)$$

with $u(x, t)$ denoting the microscopic state variables, x and t as the independent microscopic variables, and dt as the microscale time step. The equation-free framework assumes a macroscopic model exists, but its closed form is unknown. Hence the macroscopic model with its own time step can be represented as

$$\partial_t U(X, t) = F(U(X, t)), U(X, t + \delta t) = S(U(X, t), \delta t) \quad (2.19)$$

with $U(X, t)$ representing the set of macroscopic state variables, X and t being the macroscopic independent variables, and δt being the size of the coarse time step (macroscale). The framework is centered on the development of a coarse time stepper and can be considered instead of stochastic time integration in the space-time domain. This coarse time stepper can be represented as:

$$\bar{U}(X, t + \delta t) = \bar{S}(X, t), \delta t \quad (2.20)$$

with δt being the coarse time stepper. As the macroscopic equation does not exist, this representation is only an approximation of the time stepper; hence the bars are included in the equation to clarify this. The framework consists of three major operations: lifting, evolving/simulating, and restricting. Lifting involves the development of appropriate initial conditions at a microscale specifically mapping the macro to micro variables, a version of downscaling for this bottom-up framework. Evolving utilizes the microscopic model with constraints to evolve the results over the time step. Restricting is the equation-free version of upscaling where the microscopic model projects the required details onto the macroscopic model and hence the macroscopic variables are computed from the microscopic state (Samaey et al., 2005). These require two separate operators, a lifting operator, denoted as μ , and a restricting operator, denoted as M :

$$\begin{aligned} \mu : U(X, t) &\rightarrow u(x, t) = \mu(U(X, t)) \\ M : u(x, t) &\rightarrow U(X, t) = M(u(x, t)) \end{aligned} \quad (2.21)$$

A series of small subset domains are contained within the microscale model and are interpolated to achieve the multiscale model. In the simplest form these subdomains are contained within grid points, utilizing a gap-tooth scheme to project the results on the unknown macroscopic domain. In complex systems these grid points become boxes and the gap-tooth scheme is paired with projective integration to enable patch dynamics to be applied (Samaey, Roberts, & Kevrekidis, 2009).

The equation-free framework has been applied to heterogeneous problems (Bunder, Roberts, & Kevrekidis, 2017; Samaey, Kevrekidis, & Roose, 2006) with the use of buffer regions to apply common boundary conditions at a microscopic scale (Samaey et al., 2006). However, the framework has not been applied to drying. Much has been published on macroscale modeling in the drying literature, with few details remaining unknown at this scale. This makes the equation-free framework less incisive as it loses its major advantage (Kevrekidis et al., 2003). However, when information is known about the macroscopic model, the generalized equation-free framework can be modified and applied. In particular, knowledge of the structure of the unavailable equation can be used to modify the time derivative based upon the flux which is known from the microscopic simulator in space (Samaey et al., 2005). For more details about the equation-free framework for the application of the conservation laws in a generalized form, the reader can refer to Weinan and Engquist (2003).

The ultimate goal of multiscale modeling will be to achieve a multiscale model, where all phenomena are modeled at a microscale and the macroscale contains the up-scaled results. However, due to the lack of multiscale modeling in the food drying space, this is currently unfeasible. Furthermore, the limited microscale food drying literature will exaggerate the task. However, two or more generalized frameworks can be combined to apply multiscale modeling to a specific problem. Such approaches are expected to become useful tools in the study of systems with nonlinear material behavior (Kapellos, Alexiou, & Payatakes, 2010).

2.5.7 Other methods

There are many other multiscale methods in existence. Following the trend of modeling, hybrid methods are beginning to surface. These hybrid methods will attempt to merge two or more general frameworks to create a specific framework for a particular application. One recent example of this is the EDMM framework (Carr et al., 2016). The EDMM is thought to be a hybrid method between HMM and DMM.

DMM is also known as double porosity or dual porosity model and is a quite specific framework for a domain that contains two subdomains occupied by a homogeneous material. The EDMM approach generalizes the framework which most notably defines the macroscopic flux as the average of the microscopic fluxes within the microscale domain.

2.6 SOLUTION TECHNIQUE

Formulating the multiscale problem is one aspect of the model, another is the solution technique. For multiscale modeling this includes the spatial and temporal coupling. The multiscale-specific aspects of these topics will be investigated in relation to the subdomains, state variables, and fluxes. The detailed solution techniques of multiscale modeling are discussed below.

2.6.1 Spatial coupling

Spatial coupling refers to how the fine and coarse scales are connected. A multiscale framework provides a guide to compress or reconstruct the state variables (moisture or temperature) from one scale to another, but there are many components which must be considered when applying these guides to specific models and creating a solution technique.

Boundary conditions are one of the most important components of multiscale modeling. The model contains two major sets of boundary conditions, a set between the subdomains and a set at the boundary of the macroscale domain. These deal with the phase-specific fluxes and/or independent state variables (i.e., moisture and temperature). They are considered in a model's formulation and solution technique. The set of boundary conditions between the subdomains are of particular interest for multiscale modeling. Currently there are some common mathematics boundary conditions such as Dirichlet and Neumann that are commonly used in these scenarios. A Dirichlet condition treats the variables (temperature or moisture) as fixed (i.e., results between the scales are equal, micro to the macro). This can be represented as

$$u(x, t) = C; U(X, t) = C \quad (2.22)$$

where u and U are state variables, x , X , and t are the independent variables and C represents a generic constant (Note that the upper case represents the macroscale variables and the lower case denotes the microscale variables). A Neumann condition

prescribes the derivative of the boundary variables as fixed (also known as a heat flux boundary condition). This can be represented as

$$\frac{\partial u}{\partial x}(x, t) = C; \frac{\partial U}{\partial x}(X, t) = C \quad (2.23)$$

Dirichlet is quite a straight-forward approach and is commonly used in many different modeling applications. A Neumann condition also appears regularly in the literature and can be used to create an energy-consistent model between a microscale and a macroscale (Lin et al., 2017). Other traditional boundary conditions such as Cauchy or Robin conditions exist. Traditionally these mathematical boundary conditions are macroscopic in nature; however, they have been applied to microscopic domains in the literature (Samaey et al., 2009). The equation-free framework includes buffer regions to compensate for this.

Boundary conditions for multiscale heterogeneous material has received attention recently from Carr, Turner, and Perré (2017). A corrected set of macroscopic boundary condition was derived through volume-averaging and an average plus perturbation decomposition. Their work demonstrates a Robin condition should be applied at a macroscale when a Dirichlet condition is present at a microscale. Yue and Weinan (2007) investigated boundary conditions for the HMM framework, concluding that a weighted average was a more robust method for the HMM framework. The weight average considers the function is smooth, but it vanishes at the boundary, hence resulting in a more robust approach. Other works for weakly periodic boundary conditions (Sandst  m, Larsson, & Runesson, 2014), properties or boundary effects (Rabinovich, Dagan, & Miloh, 2012), and cell boundary errors (Arjmand & Runborg, 2016) have been investigated for multiscale modeling over the years. In the majority of cases for multiscale food drying, a Neumann condition would be the desired boundary condition between the scales. A Neumann condition is also known as a heat flux and would aid in convergence while allowing an energy-consistent model.

Boundary conditions are one type of method to achieve appropriate interactions between subdomains. Other methods exist to achieve different interactions, such as buffer regions, to shield the internal region from the boundary layer artifacts (Samaey et al., 2006), transition regions, or interfaces to account for imperfect interfaces (Javili, Kaessmair, & Steinmann, 2014; Javili, Steinmann, & Mosler, 2017), or oversampling for higher accuracy models by reducing the effect of artificial boundary conditions

(Chu, Efendiev, Ginting, & Hou, 2008; Hou & Wu, 1997; H. Zhang, Fu, & Wu, 2009). Furthermore, there are alternative methods, such as handshake interaction, which can be incorporated to improve the interactions of the spatial scales (Weinan et al., 2007). Yousefzadeh and Battiato (2017) presented a unique hybrid method for the spatial scale boundary interaction for finite volume. Their research contains a novel nonoverlapping, tightly coupled hybrid algorithm capable of modeling reactive transport in fractured and porous media. Selecting boundary conditions for a multiscale model is a model-specific scenario, though each multiscale framework provides some guidance.

2.6.2 Patch dynamics

Patch dynamics is an example of a specific spatial coupling solution technique. Patch dynamics is defined as a short-time, short-space scheme designed to be paired with a large-space, short-time framework (Gear & Kevrekidis, 2003; Ioannis G Kevrekidis et al., 2003). There are two core components of the scheme, the gap-tooth scheme and projective integration. The gap-tooth scheme is when a domain's macroscopic behavior is sufficiently smooth in space, a series of microscopic simulations in a number of small subdomains can be performed to reduce the complexity (Samaey et al., 2009). These microscopic simulations must be coupled with appropriate interpolation to achieve the scheme. The projective integration technique allows the macroscale domain to be extrapolated over a long-time step in the future. This is represented in Figure 2.4.

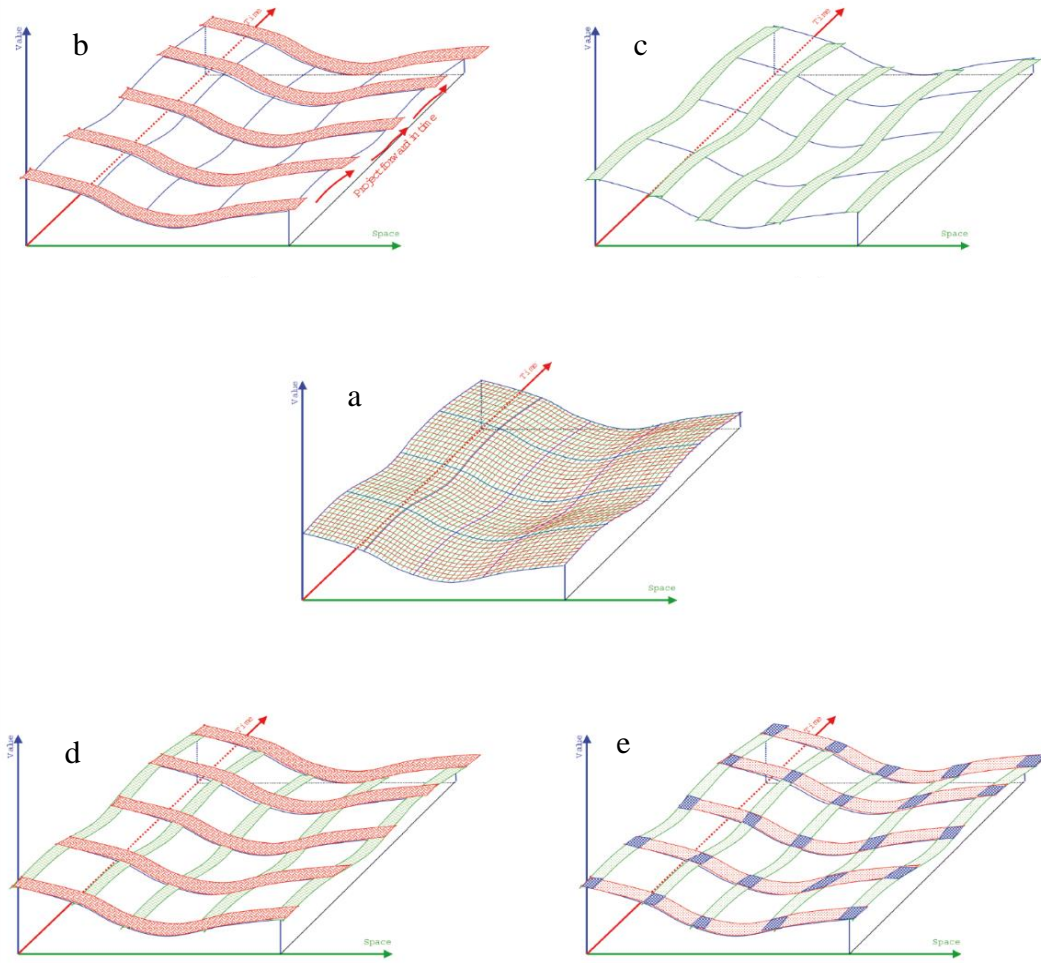


Figure 2.4. Visual representation of patch dynamics. (a) Full microscale simulation, (b) Coarse integration, (c) Gap-tooth scheme, (d & e) Combining the gap-tooth scheme and coarse integration to create patch dynamics. From “Equation-free, coarse-grained multiscale computation: Enabling microscopic simulators to perform system-level analysis,” by I.G. Kevrekidis, C.W. Gear, J.M. Hyman, P.G. Kevrekidis, O. Runborg, and C. Theodoropoulos, 2003, Communications in Mathematical Sciences, p. 737. Copyright 2003 by International Press of Boston, Inc.

Over the years, patch dynamics has been applied to homogenization problems and heterogeneity situations while evolving (Hyman, 2005; Roberts, MacKenzie, & Bunder, 2014). Samaey et al. (2005) utilized the scheme for a parabolic homogenization problem with non-linear reactions in order to understand the gap-tooth scheme. The effective microscopic behavior was modeled over the macroscopic space and time. The work was later extended to investigate the buffer regions in more depth, and it applied and investigated the accuracy of the scheme for a diffusion homogenization problem with periodic heterogeneity (Samaey et al., 2006). Dirichlet

boundary conditions were utilized and the results showed the algorithm can be applied to a large number of applications. Buffer regions are examples of a scale-interaction method and are commonly imposed to temporarily shield the internal region of a fine-scale domains from the boundary artifacts. In addition, they are utilized to impose traditional macroscopic boundary conditions on the microscopic domain (Kevrekidis et al., 2003; Samaey et al., 2006).

Buffer regions are strongly linked to the original equation-free framework and are shown in Figure 2.5. The figure represents the gap-tooth/patch dynamics coupling for a 1D situation. More recently patch dynamics has been applied to microscale heterogeneity (Bunder et al., 2017). The scheme captures the macroscale emergent dynamics of the microscale heterogeneous lattice system, and the results demonstrate that the system could be applied to a range of microscale heterogeneity problems.

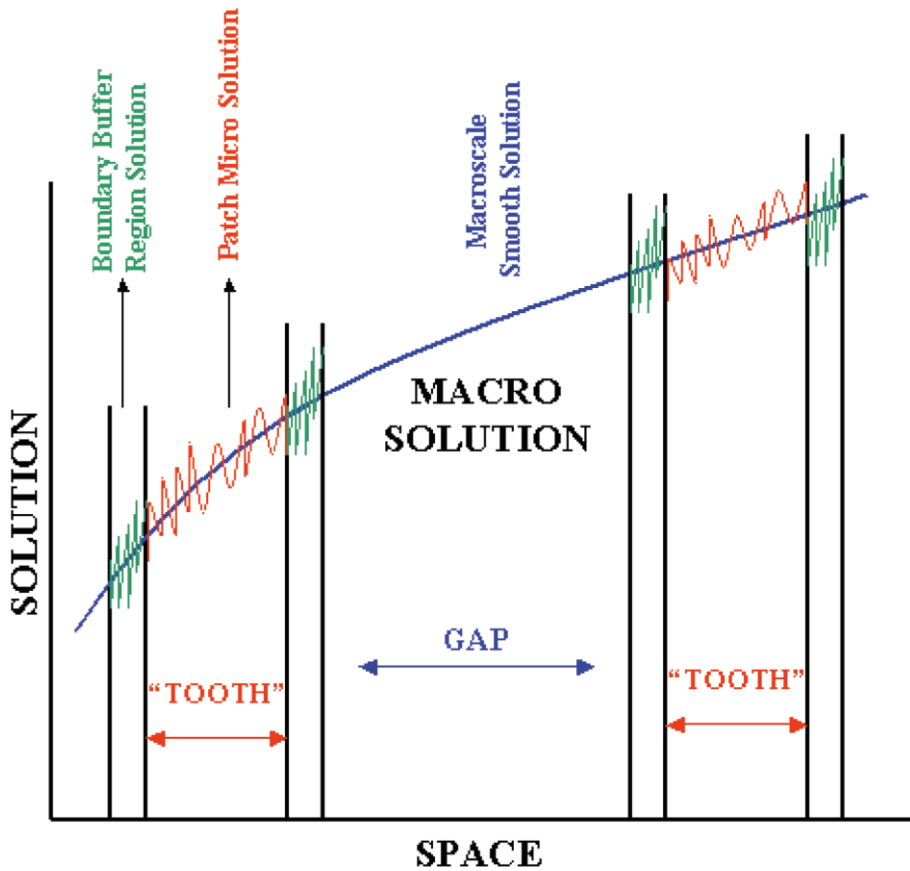


Figure 2.5. A schematic summary of the gap-tooth/patch dynamics nomenclature in 1D. From “Equation-free, coarse-grained multiscale computation: Enabling microscopic simulators to perform system-level analysis,” by I.G. Kevrekidis, C.W. Gear, J.M. Hyman, P.G. Kevrekidis, O. Runborg, and C. Theodoropoulos, 2003, Communications in Mathematical Sciences, p.738. Copyright 2003 by International Press of Boston, Inc.

Patch dynamics is an example of a spatial solution technique to achieve multiscale coupling. Patch dynamics or the use of gap-tooth/patch dynamics schemes with projective integration has great potential for multiscale modeling. A patch dynamics scheme could, for example, take multiscale modeling for complex drying technologies to the next level by accounting for the nonuniformity of certain drying technologies.

2.7 TEMPORAL COUPLING

Another important aspect of the solution technique is temporal coupling. Temporal coupling is considered to be the incorporation of each scale time step. Formulating a time step for each scale is a highly non-trivial task. It can be heavily influenced by a model's framework, physics, coupling type, and spatial coupling. In particular, each framework offers some guidance or methods of developing appropriate time steps. Additionally, separate strategies do exist to add or modify the framework strategies for specific applications; for example, seamless coupling (Weinan, 2011; Weinan, Ren, & Vanden-Eijnden, 2009). These additional strategies can both reduce and increase the computational cost of a model. Strategies for temporal couplings have no set naming scheme. A clear naming scheme was used by Lockerby, Duque-Daza, Borg, and Reese (2013) and will be followed here. A visual representation of the most common strategies for micro to macro temporal couplings can be seen in Figure 6 with the frameworks being included within this figure.

The basic and most obvious approach is for the micro and macro time step to be the same. This method includes no scale separation and has a high computational cost. This is represented as in Figure 6 (a) or can be defined as a fully coupled scheme. An improvement on this can be seen in Figure 6 (b), which shows an intermittent coupling strategy. The microscale time step is small compared to the macro time step. The microscale is simulated for the entire model, but information is exchanged less often. An alternative name for this method is a continuous microscale-solution (Lockerby et al., 2013). Evolving the microscale solution for the entire transient solution can be computationally demanding. Figure 6 (c) represents the multigrid and HMM time-step approach which is an evolution of this concept (Weinan, 2011). The information

between spatial scale is exchanged in the same way as a continuous micro-scheme; however, the microscale domain is only evolved around the exchange steps (where information is exchanged from one spatial scale to another). This results in periods of the microscale time domain being skipped. It should be noted that these skipped portions within the microscale model can introduce additional issues as the microscale domain will require reinitialization after each micro time break. An alternative to this approach is shown in Figure 6 (e) for the seamless HMM variate. In this scheme the micro and macro time steps are shown in different scales (t and τ). The seamless strategy bypasses the difficulty of HMM and contains a continuous microscale model. Figure 6 (f) demonstrates the continuous intermittent coupling scheme proposed by Lockerby et al. (2013) work. The scheme adaptability gives it a range of applicability of the seamless strategy, while maintaining the macroscale time-step efficiency of the HMM approach (Lockerby et al., 2013). The equation-free framework is centrally focused around its time stepper and is shown in Figure 6 (d). It shares the multigrid style of temporal coupling with information between exchanged back and forth at each macro time step. Formulating appropriate time steps is a highly nontrivial task for multiscale modeling.

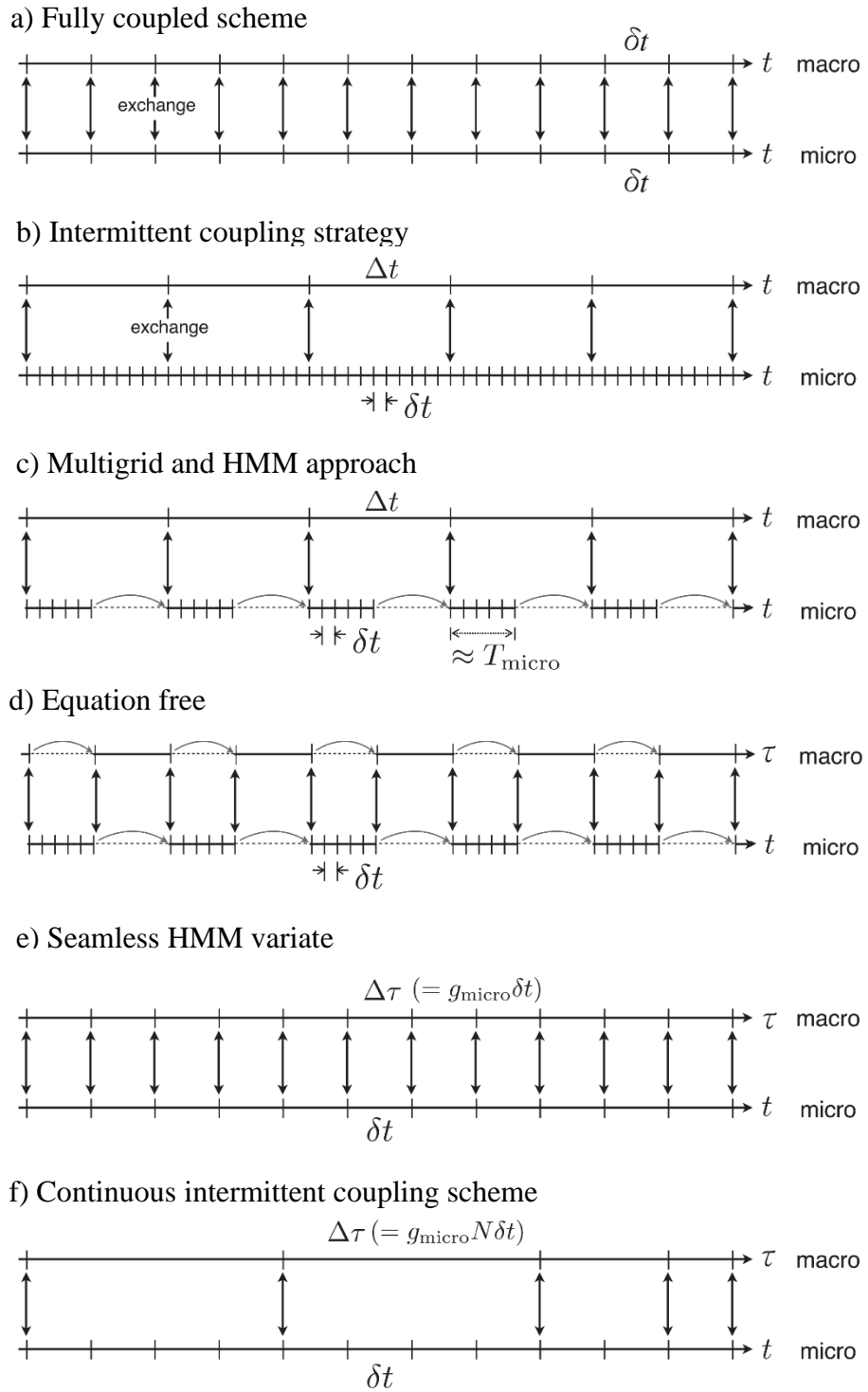


Figure 2.6. Temporal coupling. (a) Fully coupled scheme, (b) Intermittent coupling strategy, (c) Multigrid and HMM approach, (d) Equation free, (e) Seamless HMM variate, (f) Continuous intermittent coupling scheme (Adapted from “Time-Step Coupling for Hybrid Simulations of Multiscale Flows,” by D. A. Lockerby, C. A. Duque-Daza, M. K. Borg, and J. M. Reese, 2012 in Journal of Computational Physics, 237, p.346. Copyright 2012 by Elsevier Inc).

2.8 OTHER FACTORS FOR MULTISCALE MODELING

Multiscale modeling is very complex. Many different aspects must be considered when formulating a model, particularly the framework, desired spatial scale, time steps, governing physics at each scale, their coupling, concurrent or sequential coupling, and the sub domains' interaction between scales. All play an important role in the development of a multiscale model. There are a few other considerations which must be kept in mind when formulating such a model, such as computational resources and software, and balance of accuracy over cost and errors.

Though multiscale modeling does largely cut down on computational resources compared to modeling a comparable simulation incorporating multiple length scales, it is still more computation-heavy compared to a traditional continuum or macroscale approach. In partnership the software used to achieve the multiscale model goals is important to consider. Whether the model is product/technology-specific, generalized, or contains a simple or complex domain will dictate this decision. Commercial finite element and finite volume software packages exist where one- or two-way models can be achieved. In comparison, purpose-built software such as TransPore (Perré & Turner, 1999) or DryKiln_CRP (Colin, Rémond, & Perré, 2016), more general/math-based or inhouse software can be utilized.

The balance of accuracy versus desired results often dictates the formulation of theoretical modeling. The common impression is the more complex the model the better the model is. This is not always the reality. In real life, accuracy must be balanced with cost. A model which is highly complex may be more accurate, but it is likely to cost more in terms of time and resources. This balance is key to formulating a model. Commonly industry requires what is referred to as a "quick and dirty model." This refers to a low-cost model with a lower accuracy that still achieves its goal. Academia on the other hand trends toward more complex models with a higher accuracy and therefore a higher cost. For example, a researcher may construct a multiphase drying model for a particular problem when in industry an equivalent single-phase model would be constructed to model the same problem. Both achieve the end goal, one more complex and resource-heavy than the other.

Errors are another important consideration for modeling. Traditionally in theoretical modeling there are four types of error, round-off error, iteration error, solution error, and model error. These are generic forms of errors and often overlooked

in modeling, depending on the field. For multiscale modeling an additional modeling error occurs in the form of scaling error. These errors are extremely important to consider when formulating a model.

2.9 CHALLENGES FOR MULTISCALE MODELING

Multiscale modeling for food drying is still in its infancy. Current knowledge of the fundamental phenomena which occur at a microscale is limited. This has slowed the progress of multiscale modeling in the field. Adopting a framework to formulate a multiscale model is ideal. Various methods exist for representing food structure within a domain. Currently, traditional techniques such as homogenization have been used to achieve basic one-way coupled food dehydration and drying multiscale models. All multiscale frameworks presented within this review have potential for different aspects of multiscale modeling for food drying; in particular, multigrid for boundary flow modeling and HMM and equation-free for transport and deformation. The HMM framework is more established and clear in literature. The top-down approach suits the field as a large amount of information is already known at a macro level. In contrast, the equation-free framework is a bottom-up approach with its central advantage being that it does not require much information to be known at a macroscale. The equation-free framework is similar in nature to the multigrid in certain aspects. Its formulation is less established in the literature and has seen vast improvements over the years. A complete bottom-up approach would be desirable where the macroscale observations are direct results of the transport and deformation from the finer scales. However, with the current lack of knowledge at micro and finer scales, such an approach seems out of reach. A HHM framework is more feasible to establish the first concurrent multiscale models within the field.

Spatial and temporal couplings are extremely important to the model formulation and solution technique containing multiple levels of complexities. Each framework provides a guide or suggestion as to how to formulate these couplings, because model coupling is a very problem-specific scenario dictated by the technology and material in the model. Boundary conditions, boundary interaction, domain representation, and appropriate time steps all play an important role to achieve the multiscale model. Achieving an appropriate concurrent scheme for the large number of variables, which are required for theoretical food drying modeling, is a major concern. Food drying contains multiple phenomena paired with its heterogeneous microstructure requiring a

unique coupling scheme. The development of such a scheme paired with a multiscale framework will aid to establish multiscale modeling for food drying.

2.10 FUTURE DIRECTIONS

The implementation of multiscale modeling for food drying will be key for the next generation of food drying research as researchers aim for uncovering the actual micro level physics involved in drying process. However, developing a multiscale model for food drying is a difficult task as drying involves simultaneous heat and mass transfer with continuous phase change. Beside this complexity, food material is very complex due to its heterogeneous cellular structure. To develop an accurate multiscale model, the structural heterogeneity of food material needs to be considered. Therefore, a correct approach could be to first develop an actual heterogeneous microscale food domain and then connect the domain to the macroscale through a multiscale modeling framework. For multiscale modeling formulation, two approaches can be considered: a one way coupled technique or a concurrent approach. The construction of a one way coupled model, with the use of homogenization, would allow the heterogeneous structure of food material to be incorporated for a reasonable cost. This type of multiscale model would be applicable to food dehydration, material science, drying or post-harvest storage. It should be noted that literature on traditional homogenization application in different fields already exists. The limitation of this approach is that the scaling operation occurs only once. Therefore, if the materials microstructure changes significantly during drying, this cannot be captured in this technique. A concurrent approach provides a platform to incorporate the microstructural changes within a model allowing the properties to be changed throughout the simulation. This style of model is much more computationally demanding and should only be considered if the deformation is large. A concurrent model would have higher degree of precision and more potential applications. This type of model would be directly applicable to drying, post-harvest storage and groundwater modeling.

2.11 CONCLUSION

In this paper, a comprehensive review of the formulation and solution techniques for multiscale models for food drying is presented. Food structure, scale definitions, and the current status of multiscale modeling are discussed. The review investigated

and evaluated three concurrent frameworks, multigrid, HMM, and the equation-free framework in terms of their formulation and couplings. It was concluded that the HMM framework has immediate potential for establishing multiscale modeling for food drying; however, the development of a concurrent coupling scheme is required for food drying. Spatial and temporal coupling were also investigated, in addition to the specific solution technique of patch dynamics. This review has presented multiscale frameworks in order to aid in establishing multiscale modeling within food drying.

2.12 ACKNOWLEDGMENTS

This study was funded by the Department of Education and Training (AUS) through a Research Training Program (Stipend) Domestic (RTP) scholarship and Advanced Queensland Fellowship (AQF). This work is supported by the Australian Research Council (DP170100474).

2.13 AUTHOR CONTRIBUTIONS

All authors made substantial contributions to the article. The work was conceptualized by A.K. and Z.W. Manuscript preparation and drafting was carried out by Z.W. M.J.S. and M.I.H.K assisted in drafting, organizing, and critically revising the work. All authors contributed in editing and revising the work before final approval by A.K.

REFERENCES

- Abera, M. K., Fanta, S. W., Verboven, P., Ho, Q. T., Carmeliet, J., & Nicolai, B. M. (2013). Virtual fruit tissue generation based on cell growth modelling. *Food and Bioprocess Technology*, 6, 859-869. <https://doi.org/10.1007/s11947-011-0775-4>
- Abera, M. K., Verboven, P., Defraeye, T., Fanta, S. W., Hertog, M. L., Carmeliet, J., & Nicolai, B. M. (2014). A plant cell division algorithm based on cell biomechanics and ellipse-fitting. *Annals of Botany*, 114, 605-617. <https://doi.org/10.1093/aob/mcu078>
- Aregawi, W. A., Abera, M. K., Fanta, S. W., Verboven, P., & Nicolai, B. (2014). Prediction of water loss and viscoelastic deformation of apple tissue using a multiscale model. *Journal of Physics: Condensed Matter*, 26, 464111. <https://doi.org/10.1088/0953-8984/26/46/464111>
- Arjmand, D., & Runborg, O. (2016). A time dependent approach for removing the cell boundary error in elliptic homogenization problems. *Journal of Computational Physics*, 314, 206-227. <https://doi.org/10.1016/j.jcp.2016.03.009>
- Boffy, H., & Venner, C. H. (2014). Multigrid solution of the 3D stress field in strongly heterogeneous materials. *Tribology International*, 74, 121-129. <https://doi.org/10.1016/j.triboint.2014.02.019>
- Brandt, A. (1977). Multi-level adaptive solutions to boundary-value problems. *Mathematics of Computation*, 31, 333-390. <https://doi.org/10.1090/S0025-5718-1977-0431719-X>
- Brandt, A. (2002). Multiscale scientific computation: Review 2001. In *Multiscale and multiresolution methods* (pp. 3-95): Springer. https://doi.org/10.1007/978-3-642-56205-1_1
- Breuls, R. G. M., Sengers, B. G., Oomens, C. W. J., Bouten, C. V. C., & Baaijens, F. P. T. (2002). Predicting local cell deformations in engineered tissue constructs: A multilevel finite element approach. *Journal of Biomechanical Engineering*, 124, 198-207. <https://doi.org/10.1115/1.1449492>

- Bunder, J. E., Roberts, A. J., & Kevrekidis, I. G. (2017). Good coupling for the multiscale patch scheme on systems with microscale heterogeneity. *Journal of Computational Physics*, 337, 154-174. <https://doi.org/10.1016/j.jcp.2017.02.004>
- Centre, D., Herremans, E., Verboven, P., Ampofo-Asiamah, J., & Nicolaï, B. (2014). Characterization of the 3-D microstructure of mango (*Mangifera indica* L. cv. Carabao) during ripening using X-ray-computed microtomography. *Innovative Food Science & Emerging Technologies*, 24, 28-39. <https://doi.org/10.1016/j.ifset.2013.12.008>
- Car, R., & Parrinello, M. (1985). Unified approach for molecular dynamics and density-functional theory. *Physical Review Letters*, 55, 2471. <https://doi.org/10.1103/PhysRevLett.55.2471>
- Carr, E. J., Perré, P., & Turner, I. W. (2016). The extended distributed microstructure model for gradient-driven transport: A two-scale model for bypassing effective parameters. *Journal of Computational Physics*, 327, 810-829. <https://doi.org/10.1016/j.jcp.2016.10.004>
- Carr, E. J., & Turner, I. W. (2014). Two-scale computational modelling of water flow in unsaturated soils containing irregular-shaped inclusions. *International Journal for Numerical Methods in Engineering*, 98, 157-173. <https://doi.org/10.1002/nme.4625>
- Carr, E. J., Turner, I. W., & Perré, P. (2013). A dual-scale modeling approach for drying hygroscopic porous media. *Multiscale Modeling & Simulation*, 11, 362-384. <https://doi.org/10.1137/120873005>
- Carr, E. J., Turner, I. W., & Perré, P. (2017). Macroscale modelling of multilayer diffusion: Using volume averaging to correct the boundary conditions. *Applied Mathematical Modelling*, 47, 600-618. <https://doi.org/10.1016/j.apm.2017.03.044>
- Caurie, M. (2011). Bound water: Its definition, estimation and characteristics. *International Journal of Food Science & Technology*, 46, 930-934. <https://doi.org/10.1111/j.1365-2621.2011.02581.x>

- Cecot, W., & Oleksy, M. (2015). High-order FEM for multigrid homogenization. *Computers & Mathematics with Applications*, 70, 1391-1400. <https://doi.org/10.1016/j.camwa.2015.06.024>
- Chen, J. J., Lau, S. K., Chen, L., Wang, S. J., & Subbiah, J. (2017). Modeling radio frequency heating of food moving on a conveyor belt. *Food and Bioproducts Processing*, 102, 307-319. <https://doi.org/10.1016/j.fbp.2017.01.009>
- Chen, J., Pitchai, K., Birla, S., Negahban, M., Jones, D., & Subbiah, J. (2014). Heat and mass transport during microwave heating of mashed potato in domestic oven: Model development, validation, and sensitivity analysis. *Journal of Food Science*, 79, E1991-E2004. <https://doi.org/10.1111/1750-3841.12636>
- Chu, J., Efendiev, Y., Ginting, V., & Hou, T. (2008). Flow-based oversampling technique for multiscale finite element methods. *Advances in Water Resources*, 31, 599-608. <https://doi.org/10.1016/j.advwatres.2007.11.005>
- Colin, J., Rémond, R., & Perré, P. (2016). Design and optimization of industrial woody biomass pretreatment addressed by DryKiln_CRP, a multiscale computational model: Particle, bed, and dryer levels. *Drying Technology*, 34, 1820-1830. <https://doi.org/10.1080/07373937.2016.1143483>
- Defraeye, T. (2014). Advanced computational modelling for drying processes – A review. *Applied Energy*, 131, 323-344. <https://doi.org/10.1016/j.apenergy.2014.06.027>
- Defraeye, T., Radu, A., & Derome, D. (2016). Recent advances in drying at interfaces of biomaterials. *Drying Technology*, 34, 1904-1925. <https://doi.org/10.1080/07373937.2016.1144062>
- Delele, M. A., Schenk, A., Tijskens, E., Ramon, H., Nicolaï, B. M., & Verboven, P. (2009). Optimization of the humidification of cold stores by pressurized water atomizers based on a multiscale CFD model. *Journal of Food Engineering*, 91, 228-239. <https://doi.org/10.1016/j.jfoodeng.2008.08.027>
- Fachinotti, V. D., Toro, S., Sánchez, P. J., & Huespe, A. E. (2015). Sensitivity of the thermomechanical response of elastic structures to microstructural changes.

International Journal of Solids and Structures, 69, 45-59.
<https://doi.org/10.1016/j.ijsolstr.2015.06.009>

Fanta, S. W., Abera, M. K., Aregawi, W. A., Ho, Q. T., Verboven, P., Carmeliet, J., & Nicolai, B. M. (2014). Microscale modeling of coupled water transport and mechanical deformation of fruit tissue during dehydration. *Journal of Food Engineering*, 124, 86-96. <https://doi.org/10.1016/j.jfoodeng.2013.10.007>

Fanta, S. W., Abera, M. K., Ho, Q. T., Verboven, P., Carmeliet, J., & Nicolai, B. M. (2013). Microscale modeling of water transport in fruit tissue. *Journal of Food Engineering*, 118, 229-237. <https://doi.org/10.1016/j.jfoodeng.2013.04.003>

Fedorenko, R. (1973). Iterative methods for elliptic difference equations. *Russian Mathematical Surveys*, 28, 129-195.
<https://doi.org/10.1070/RM1973v028n02ABEH001542>

Fish, J., & Belsky, V. (1995a). Multi-grid method for periodic heterogeneous media part 2: Multiscale modeling and quality control in multidimensional case. *Computer Methods in Applied Mechanics and Engineering*, 126, 17-38.
[https://doi.org/10.1016/0045-7825\(95\)00812-F](https://doi.org/10.1016/0045-7825(95)00812-F)

Fish, J., & Belsky, V. (1995b). Multigrid method for periodic heterogeneous media part 1: Convergence studies for one-dimensional case. *Computer Methods in Applied Mechanics and Engineering*, 126, 1-16. [https://doi.org/10.1016/0045-7825\(95\)00811-E](https://doi.org/10.1016/0045-7825(95)00811-E)

Fish, J., & Yu, Q. (2001). Multiscale damage modelling for composite materials: Theory and computational framework. *International Journal for Numerical Methods in Engineering*, 52, 161-191. <https://doi.org/10.1002/nme.276>

Fletcher, D. F., & Langrish, T. A. G. (2009). Scale-adaptive simulation (SAS) modelling of a pilot-scale spray dryer. *Chemical Engineering Research and Design*, 87(10), 1371-1378. <https://doi.org/10.1016/j.cherd.2009.03.006>

Garcia, A. L., Bell, J. B., Crutchfield, W. Y., & Alder, B. J. (1999). Adaptive mesh and algorithm refinement using direct simulation Monte Carlo. *Journal of Computational Physics*, 154(1), 134-155. <https://doi.org/10.1006/jcph.1999.6305>

Gear, C. W., & Kevrekidis, I. G. (2003). Projective methods for stiff differential equations: Problems with gaps in their eigenvalue spectrum. *SIAM Journal on Scientific Computing*, 24, 1091-1106.
<https://doi.org/10.1137/S1064827501388157>

Geers, M. G., Kouznetsova, V. G., Matouš, K., & Yvonnet, J. (2017). Homogenization methods and multiscale modeling: Nonlinear problems. *Encyclopedia of Computational Mechanics Second Edition*, 1-34.
<https://doi.org/10.1002/9781119176817.ecm2107>

Gibson, W. T., Veldhuis, J. H., Rubinstein, B., Cartwright, H. N., Perrimon, N., Brodland, G. W., . . . Gibson, M. C. (2011). Control of the mitotic cleavage plane by local epithelial topology. *Cell*, 144, 427-438.
<https://doi.org/10.1016/j.cell.2010.12.035>

Golestani, R., Raisi, A., & Aroujalian, A. (2013). Mathematical modeling on air drying of apples considering shrinkage and variable diffusion coefficient. *Drying Technology*, 31, 40-51. <https://doi.org/10.1080/07373937.2012.714826>

Gravemeier, V., Gee, M. W., Kronbichler, M., & Wall, W. A. (2010). An algebraic variational multiscale–multigrid method for large eddy simulation of turbulent flow. *Computer Methods in Applied Mechanics and Engineering*, 199, 853-864.
<https://doi.org/10.1016/j.cma.2009.05.017>

Gravemeier, V., & Wall, W. A. (2010). An algebraic variational multiscale–multigrid method for large-eddy simulation of turbulent variable-density flow at low Mach number. *Journal of Computational Physics*, 229, 6047-6070.
<https://doi.org/10.1016/j.jcp.2010.04.036>

Gross, R. A., & Kalra, B. (2002). Biodegradable polymers for the environment. *Science*, 297, 803-807. <https://doi.org/10.1126/science.297.5582.803>

Gulati, T., Zhu, H., & Datta, A. K. (2016). Coupled electromagnetics, multiphase transport and large deformation model for microwave drying. *Chemical Engineering Science*, 156, 206-228. <https://doi.org/10.1016/j.ces.2016.09.004>

- Ho, Q. T., Carmeliet, J., Datta, A. K., Defraeye, T., Delele, M. A., Herremans, E., . . . Nicolai, B. M. (2013). Multiscale modeling in food engineering. *Journal of Food Engineering*, 114, 279-291. <https://doi.org/10.1016/j.jfoodeng.2012.08.019>
- Ho, Q. T., Verboven, P., Fanta, S. W., Abera, M. K., Retta, M. A., Herremans, E., . . . Nicolaï, B. M. (2014). A multiphase pore scale network model of gas exchange in apple fruit. *Food and Bioprocess Technology*, 7, 482-495. <https://doi.org/10.1007/s11947-012-1043-y>
- Ho, Q. T., Verboven, P., Verlinden, B. E., Herremans, E., & Nicolaï, B. M. (2013). Multiscale modeling of transport phenomena in plant-based foods. *Process Systems Engineering: Dynamic Process Modeling*, 7, 469-492. <https://doi.org/10.1002/9783527631209.ch74>
- Ho, Q. T., Verboven, P., Verlinden, B. E., Herremans, E., Wevers, M., Carmeliet, J., & Nicolaï, B. M. (2011). A three-dimensional multiscale model for gas exchange in fruit. *Plant Physiology*, 155, 1158-1168. <https://doi.org/10.1104/pp.110.169391>
- Ho, Q. T., Verboven, P., Verlinden, B. E., & Nicolaï, B. M. (2010). A model for gas transport in pear fruit at multiple scales. *Journal of Experimental Botany*, 61, 2071-2081. <https://doi.org/10.1093/jxb/erq026>
- Hornung, U. (2012). *Homogenization and porous media* (Vol. 6): Springer Science & Business Media.
- Hou, T. Y., & Wu, X.-H. (1997). A multiscale finite element method for elliptic problems in composite materials and porous media. *Journal of Computational Physics*, 134, 169-189. <https://doi.org/10.1006/jcph.1997.5682>
- Huang, S., Méjean, S., Rabah, H., Dolivet, A., Le Loir, Y., Chen, X. D., . . . Schuck, P. (2017). Double use of concentrated sweet whey for growth and spray drying of probiotics: Towards maximal viability in pilot scale spray dryer. *Journal of Food Engineering*, 196, 11-17. <https://doi.org/10.1016/j.jfoodeng.2016.10.017>
- Hyman, J. M. (2005). Patch dynamics for multiscale problems. *Computing in Science & Engineering*, 7, 47-53. <https://doi.org/10.1109/MCSE.2005.57>

- Javili, A., Kaessmair, S., & Steinmann, P. (2014). General imperfect interfaces. *Computer Methods in Applied Mechanics and Engineering*, 275, 76-97. <https://doi.org/10.1016/j.cma.2014.02.022>
- Javili, A., Steinmann, P., & Mosler, J. (2017). Micro-to-macro transition accounting for general imperfect interfaces. *Computer Methods in Applied Mechanics and Engineering*, 317, 274-317. <https://doi.org/10.1016/j.cma.2016.12.025>
- Joardder, M. U. H., Kumar, C., & Karim, M. A. (2017a). Food structure: Its formation and relationships with other properties. *Critical Reviews in Food Science and Nutrition*, 57, 1190-1205. <https://doi.org/10.1080/10408398.2014.971354>
- Joardder, M. U. H., Kumar, C., & Karim, M. A. (2017b). Multiphase transfer model for intermittent microwave-convective drying of food: Considering shrinkage and pore evolution. *International Journal of Multiphase Flow*, 95, 101-119. <https://doi.org/10.1016/j.ijmultiphaseflow.2017.03.018>
- Kapellos, G. E., Alexiou, T. S., & Payatakes, A. C. (2010). Theoretical modeling of fluid flow in cellular biological media: An overview. *Mathematical Biosciences*, 225, 83-93. <https://doi.org/10.1016/j.mbs.2010.03.003>
- Kashkooli, A. G., Farhad, S., Lee, D. U., Feng, K., Litster, S., Babu, S. K., . . . Chen, Z. (2016). Multiscale modeling of lithium-ion battery electrodes based on nanoscale X-ray computed tomography. *Journal of Power Sources*, 307, 496-509. <https://doi.org/10.1016/j.jpowsour.2015.12.134>
- Kaya, A., Aydin, O., & Dincer, I. (2008). Experimental and numerical investigation of heat and mass transfer during drying of Hayward kiwi fruits (*Actinidia Deliciosa* Planch.). *Journal of Food Engineering*, 88(3), 323-330. <https://doi.org/10.1016/j.jfoodeng.2008.02.017>
- Kevrekidis, I. G., Gear, C. W., & Hummer, G. (2004). Equation-free: The computer-aided analysis of complex multiscale systems. *American Institute of Chemical Engineers Journal*, 50, 1346-1355. <https://doi.org/10.1002/aic.10106>
- Kevrekidis, I. G., Gear, C. W., Hyman, J. M., Kevrekidid, P. G., Runborg, O., & Theodoropoulos, C. (2003). Equation-free, coarse-grained multiscale computation: Enabling mocroscopic simulators to perform system-level analysis.

Communications in Mathematical Sciences, 1, 715-762.
<https://doi.org/10.4310/CMS.2003.v1.n4.a5>

Khan, M. I. H., Joardder, M. U. H., Kumar, C., & Karim, M. A. (2016). Multiphase porous media modelling: A novel approach to predicting food processing performance. *Critical Reviews in Food Science and Nutrition*, 58, 528-546. <https://doi.org/10.1080/10408398.2016.1197881>

Khan, M. I. H., & Karim, M. A. (2017). Cellular water distribution, transport, and its investigation methods for plant-based food material. *Food Research International*, 99, 1-14. <https://doi.org/10.1016/j.foodres.2017.06.037>

Khan, M. I. H., Kumar, C., Joardder, M. U. H., & Karim, M. A. (2017). Determination of appropriate effective diffusivity for different food materials. *Drying Technology*, 35, 335-346. <https://doi.org/10.1080/07373937.2016.1170700>

Khan, M. I. H., Nagy, S. A., & Karim, M. A. (2018). Transport of cellular water during drying: An understanding of cell rupturing mechanism in apple tissue. *Food Research International*, 105, 772-781. <https://doi.org/10.1016/j.foodres.2017.12.010>

Khan, M. I. H., Wellard, R. M., Nagy, S. A., Joardder, M. U. H., & Karim, M. A. (2017). Experimental investigation of bound and free water transport process during drying of hygroscopic food material. *International Journal of Thermal Sciences*, 117, 266-273. <https://doi.org/10.1016/j.ijthermalsci.2017.04.006>

Ko, S., & Gunasekaran, S. (2007). Error correction of confocal microscopy images for in situ food microstructure evaluation. *Journal of Food Engineering*, 79, 935-944. <https://doi.org/10.1016/j.jfoodeng.2006.03.014>

Kohout, M., & Stepanek, F. (2007). Multi-scale analysis of vacuum contact drying. *Drying Technology*, 25, 1265-1273. <https://doi.org/10.1080/073739301438741>

Konstankiewicz, K., Czachor, H., Gancarz, M., Król, A., Pawlak, K., & Zdunek, A. (2002). Cell structural parameters of potato tuber tissue. *International Agrophysics*, 16(2), 119-128. <https://doi.org/10.17221/2118-RAE>

- Kouznetsova, V., Brekelmans, W. A. M., & Baaijens, F. P. T. (2001). An approach to micro-macro modeling of heterogeneous materials. *Computational Mechanics*, 27, 37-48. <https://doi.org/10.1007/s004660000212>
- Kumar, C., Joardder, M. U. H., Farrell, T. W., & Karim, M. A. (2017). Investigation of intermittent microwave convective drying (IMCD) of food materials by a coupled 3D electromagnetics and multiphase model. *Drying Technology*, 36, 736-750. <https://doi.org/10.1080/07373937.2017.1354874>
- Larsson, F., Runesson, K., & Su, F. (2010). Variationally consistent computational homogenization of transient heat flow. *International Journal for Numerical Methods in Engineering*, 81(13), 1659-1686. <https://doi.org/10.1002/nme.2747>
- Li, Z., Lv, K., Wang, Y., Zhao, B., & Yang, Z. (2015). Multi-scale engineering properties of tomato fruits related to harvesting, simulation and textural evaluation. *LWT - Food Science and Technology*, 61, 444-451. <https://doi.org/10.1016/j.lwt.2014.12.018>
- Li, Z., & Wang, Y. (2016). A multiscale finite element model for mechanical response of tomato fruits. *Postharvest Biology and Technology*, 121, 19-26. <https://doi.org/10.1016/j.postharvbio.2016.07.008>
- Li, Z. Y., Wang, R. F., & Kudra, T. (2011). Uniformity issue in microwave drying. *Drying Technology*, 29, 652-660. <https://doi.org/10.1080/07373937.2010.521963>
- Lin, S., Smith, J., Liu, W. K., & Wagner, G. J. (2017). An energetically consistent concurrent multiscale method for heterogeneous heat transfer and phase transition applications. *Computer Methods in Applied Mechanics and Engineering*, 315, 100-120. <https://doi.org/10.1016/j.cma.2016.10.037>
- Lockerby, D. A., Duque-Daza, C. A., Borg, M. K., & Reese, J. M. (2013). Time-step coupling for hybrid simulations of multiscale flows. *Journal of Computational Physics*, 237, 344-365. <https://doi.org/10.1016/j.jcp.2012.11.032>
- Luan, D., Wang, Y., Tang, J., & Jain, D. (2016). Frequency distribution in domestic microwave ovens and its influence on heating pattern. *Journal of Food Science*, 82, 429-436. <https://doi.org/10.1111/1750-3841.13587>

Lunati, I., & Jenny, P. (2006). Multiscale finite-volume method for compressible multiphase flow in porous media. *Journal of Computational Physics*, 216, 616-636. <https://doi.org/10.1016/j.jcp.2006.01.001>

Mahiuddin, M., Khan, M.I.H., Kumar, C.; Rahman, M. M., and. Karim, M. A (2018) Shrinkage of food materials during drying: Current status and challenges, *Comprehensive Reviews in Food Science and Food Safety*, 17 (5), 1113-1126. <https://doi.org/10.1111/1541-4337.12375>

Matouš, K., Geers, M. G. D., Kouznetsova, V. G., & Gillman, A. (2017). A review of predictive nonlinear theories for multiscale modeling of heterogeneous materials. *Journal of Computational Physics*, 330, 192-220. <https://doi.org/10.1016/j.jcp.2016.10.070>

Merks, R. M., Guravage, M., Inzé, D., & Beemster, G. T. (2011). VirtualLeaf: an open-source framework for cell-based modeling of plant tissue growth and development. *Plant Physiology*, 155, 656-666. <https://doi.org/10.1104/pp.110.167619>

Morris, E. R., Nishinari, K., & Rinaudo, M. (2012). Gelation of gellan : A review. *Food Hydrocolloids*, 28, 373-411. <https://doi.org/10.1016/j.foodhyd.2012.01.004>

Mulet, A., Garcia Reverter, J., Bon, J., & Berna, A. (2000). Effect of shape on potato and cauliflower shrinkage during drying. *Drying Technology*, 18(6), 1201-1219. <https://doi.org/10.1080/07373930008917772>

Nguyen, T. A., Verboven, P., Scheerlinck, N., Vandewalle, S., & Nicolaï, B. M. (2006). Estimation of effective diffusivity of pear tissue and cuticle by means of a numerical water diffusion model. *Journal of Food Engineering*, 72(1), 63-72. <https://doi.org/10.1016/j.jfoodeng.2004.11.019>

Nilenius, F., Larsson, F., Lundgren, K., & Runesson, K. (2014). Computational homogenization of diffusion in three-phase mesoscale concrete. *Computational Mechanics*, 54, 461-472. <https://doi.org/10.1007/s00466-014-0998-0>

Novák, V., Kočí, P., Štěpánek, F., & Marek, M. (2011). Integrated multiscale methodology for virtual prototyping of porous catalysts. *Industrial and*

Özdemir, I., Brekelmans, W. A. M., & Geers, M. G. D. (2008). Computational homogenization for heat conduction in heterogeneous solids. *International Journal for Numerical Methods in Engineering*, 73, 185-204.
<https://doi.org/10.1002/nme.2068>

Pavliotis, G. A., & Stuart, A. M. (2008). *Multiscale methods: averaging and homogenization*. Springer Science & Business Media.

Perré, P. (2007). Multiscale aspects of heat and mass transfer during drying. *Transport in Porous Media*, 66, 59-76. <https://doi.org/10.1007/s11242-006-9022-2>

Perré, P. (2010). Multiscale modeling of drying as a powerful extension of the macroscopic approach: Application to solid wood and biomass processing. *Drying Technology*, 28, 944-959. <https://doi.org/10.1080/07373937.2010.497079>

Perré, P. (2015). The proper use of mass diffusion equations in drying modeling: Introducing the drying intensity number. *Drying Technology*, 33, 1949-1962.
<https://doi.org/10.1080/07373937.2015.1076836>

Perré, P., & Rémond, R. (2006). A dual-scale computational model of kiln wood drying including single board and stack level simulation. *Drying Technology*, 24, 1069-1074. <https://doi.org/10.1080/07373930600778106>

Perré, P., Rémond, R., Colin, J., Mougel, E., & Almeida, G. (2012). Energy consumption in the convective drying of timber analyzed by a multiscale computational model. *Drying Technology*, 30, 1136-1146.
<https://doi.org/10.1080/07373937.2012.705205>

Perré, P., Rémond, R., & Turner, I. (2013). A comprehensive dual-scale wood torrefaction model: Application to the analysis of thermal run-away in industrial heat treatment processes. *International Journal of Heat and Mass Transfer*, 64, 838-849. <https://doi.org/10.1016/j.ijheatmasstransfer.2013.03.066>

Perré, P., & Turner, I. W. (1999). Transpore: A generic heat and mass transfer computational model for understanding and visualising the drying of porous

media. *Drying Technology*, 17, 1273-1289.
<https://doi.org/10.1080/07373939908917614>

Rabinovich, A., Dagan, G., & Miloh, T. (2012). Boundary effects on effective conductivity of random heterogeneous media with spherical inclusions. *Physical Review E*, 86, 046601. <https://doi.org/10.1103/PhysRevE.86.046601>

Rahman, M. M., Gu, Y. T., & Karim, M. A. (2018). Development of realistic food microstructure considering the structural heterogeneity of cells and intercellular space. *Food Structure*, 15, 9-16. <https://doi.org/10.1016/j.foostr.2018.01.002>

Rahman, M. M., Joardder, M. U. H., Khan, M. I. H., Nghia, D. P., & Karim, M. A. (2016). Multi-scale model of food drying: Current status and challenges. *Critical Reviews in Food Science and Nutrition*, 58, 858-876. <https://doi.org/10.1080/10408398.2016.1227299>

Rahman, M. M., Kumar, C., Joardder, M. U. H., & Karim, M. A. (2018). A micro-level transport model for plant-based food materials during drying. *Chemical Engineering Science*, 187, 1-15. <https://doi.org/10.1016/j.ces.2018.04.060>

Roberts, A. J., & Kevrekidis, I. G. (2007). General tooth boundary conditions for equation free modeling. *SIAM Journal on Scientific Computing*, 29, 1495-1510. <https://doi.org/10.1137/060654554>

Roberts, A. J., MacKenzie, T., & Bunder, J. E. (2014). A dynamical systems approach to simulating macroscale spatial dynamics in multiple dimensions. *Journal of Engineering Mathematics*, 86, 175-207. <https://doi.org/10.1007/s10665-013-9653-6>

Rohan, E., Turjanicová, J., & Lukeš, V. (2017). A Darcy-Brinkman model of flow in double-porous media : Two-level homogenization and computational modelling. *Computers & Structures*. (In press)
<https://doi.org/10.1016/j.compstruc.2017.08.006>

Ryan, E. M., & Tartakovsky, A. M. (2011). A hybrid micro-scale model for transport in connected macro-pores in porous media. *Journal of Contaminant Hydrology*, 126, 61-71. <https://doi.org/10.1016/j.jconhyd.2011.06.005>

- Samaey, G., Kevrekidis, I. G., & Roose, D. (2006). Patch dynamics with buffers for homogenization problems. *Journal of Computational Physics*, 213, 264-287. <https://doi.org/10.1016/j.jcp.2005.08.010>
- Samaey, G., Roberts, A. J., & Kevrekidis, I. G. (2009). Equation-free computation: An overview of patch dynamics. *Multiscale Methods: Bridging the Scales in Science and Engineering* (pp. 216-247): Oxford University Press.
- Samaey, G., Roose, D., & Kevrekidis, I. G. (2005). The gap-tooth scheme for homogenization problems. *Multiscale Modeling & Simulation*, 4, 278-306. <https://doi.org/10.1137/030602046>
- Sandström, C., Larsson, F., & Runesson, K. (2014). Weakly periodic boundary conditions for the homogenization of flow in porous media. *Advanced Modeling and Simulation in Engineering Sciences*, 1, 12. <https://doi.org/10.1186/s40323-014-0012-6>
- Sandström, C., Larsson, F., & Runesson, K. (2016). Homogenization of coupled flow and deformation in a porous material. *Computer Methods in Applied Mechanics and Engineering*, 308, 535-551. <https://doi.org/10.1016/j.cma.2016.05.021>
- Senadeera, W., Bhandari, B. R., Young, G., & Wijesinghe, B. (2005). Modeling dimensional shrinkage of shaped foods in fluidized bed drying. *Journal of Food Processing and Preservation*, 29(2), 109-119. <https://doi.org/10.1111/j.1745-4549.2005.00017.x>
- Showalter, R. E. (1993). Distributed microstructure models of porous media. *Flow in Porous Media* (pp. 155-163). Birkhäuser, Basel
- Srikiatden, J., & Roberts, J. S. (2007). Moisture transfer in solid food materials: A review of mechanisms, models, and measurements. *International Journal of Food Properties*, 10, 739-777. <https://doi.org/10.1080/10942910601161672>
- Szymkiewicz, A., Lewandowska, J., Angulo-Jaramillo, R., & Butlańska, J. (2008). Two-scale modeling of unsaturated water flow in a double-porosity medium under axisymmetric conditions. *Canadian Geotechnical Journal*, 45, 238-251. <https://doi.org/10.1139/T07-096>

Tadmor, E. B., Ortiz, M., & Phillips, R. (1996). Quasicontinuum analysis of defects in solids. *Philosophical Magazine A*, 73, 1529-1563.
<https://doi.org/10.1080/01418619608243000>

Theodoropoulos, C., Qian, Y.-H., & Kevrekidis, I. G. (2000). “Coarse” stability and bifurcation analysis using time-steppers: A reaction-diffusion example. *Proceedings of the National Academy of Sciences*, 97, 9840-9843.
<https://doi.org/10.1073/pnas.97.18.9840>

Vadivambal, R., & Jayas, D. S. (2010). Non-uniform temperature distribution during microwave heating of food materials: A review. *Food and Bioprocess Technology*, 3, 161-171. <https://doi.org/10.1007/s11947-008-0136-0>

van der Sman, R., & Broeze, J. (2014). Multiscale analysis of structure development in expanded starch snacks. *Journal of Physics: Condensed Matter*, 26(46), 464103. <https://doi.org/10.1088/0953-8984/26/46/464103>

van der Sman, R. G. M., Vergeldt, F. J., Van As, H., van Dalen, G., Voda, A., & van Duynhoven, J. P. M. (2014). Multiphysics pore-scale model for the rehydration of porous foods. *Innovative Food Science & Emerging Technologies*, 24, 69-79.
<https://doi.org/10.1016/j.ifset.2013.11.008>

Verboven, P., Kerckhofs, G., Mebatsion, H. K., Ho, Q. T., Temst, K., Wevers, M., . . . Nicolaï, B. M. (2008). Three-dimensional gas exchange pathways in pome fruit characterized by synchrotron X-ray computed tomography. *Plant Physiology*, 147, 518-527. <https://doi.org/10.1104/pp.108.118935>

Vicent, V., Verboven, P., Ndoye, F.-T., Alvarez, G., & Nicolaï, B. (2017). A new method developed to characterize the 3D microstructure of frozen apple using X-ray micro-CT. *Journal of Food Engineering*, 212, 154-164.
<https://doi.org/10.1016/j.jfoodeng.2017.05.028>

Weinan, E. (2011). *Principles of multiscale modeling*: Cambridge University Press.

Weinan, E., & Engquist, B. (2003). The heterogenous multiscale methods. *Communications in Mathematical Sciences*, 1, 87-132.

- Weinan, E., Engquist, B., Li, X., Ren, W., & Vanden-Eijnden, E. (2007). Heterogeneous multiscale methods: A review. *Communications in Computational Physics*, 2, 367-450.
- Weinan, E., Ren, W., & Vanden-Eijnden, E. (2009). A general strategy for designing seamless multiscale methods. *Journal of Computational Physics*, 228, 5437-5453.
<https://doi.org/10.1016/j.jcp.2009.04.030>
- Witek, M., Węglarz, W., De Jong, L., Van Dalen, G., Blonk, J., Heussen, P., . . . Van Duynhoven, J. (2010). The structural and hydration properties of heat-treated rice studied at multiple length scales. *Food Chemistry*, 120(4), 1031-1040.
<https://doi.org/10.1016/j.foodchem.2009.11.043>
- Yousefzadeh, M., & Battiaito, I. (2017). Physics-based hybrid method for multiscale transport in porous media. *Journal of Computational Physics*, 344, 320-338.
<https://doi.org/10.1016/j.jcp.2017.04.055>
- Yue, X., & Weinan, E. (2007). The local microscale problem in the multiscale modeling of strongly heterogeneous media: Effects of boundary conditions and cell size. *Journal of Computational Physics*, 222, 556-572.
<https://doi.org/10.1016/j.jcp.2006.07.034>
- Zhang, H., Fu, Z., & Wu, J. (2009). Coupling multiscale finite element method for consolidation analysis of heterogeneous saturated porous media. *Advances in Water Resources*, 32, 268-279. <https://doi.org/10.1016/j.advwatres.2008.11.002>
- Zhang, W., Luan, D., Tang, J., Sablani, S. S., Rasco, B., Lin, H., & Liu, F. (2015). Dielectric properties and other physical properties of low-acyl gellan gel as relevant to microwave assisted pasteurization process. *Journal of Food Engineering*, 149, 195-203. <https://doi.org/10.1016/j.jfoodeng.2014.10.014>
- Zhang, Y., Cao, L., Feng, Y., & Wang, W. (2017). A multiscale approach and a hybrid FE-BE algorithm for heterogeneous scattering of Maxwell's equations. *Journal of Computational and Applied Mathematics*, 319, 460-479.
<https://doi.org/10.1016/j.cam.2017.01.017>

Zhuang, X., Wang, Q., & Zhu, H. (2015). A 3D computational homogenization model for porous material and parameters identification. *Computational Materials Science*, 96, 536-548. <https://doi.org/10.1016/j.commatsci.2014.04.059>

Chapter 3: Multiscale modelling for food drying: A homogenised diffusion approach

This chapter is originally published in **Journal of Food Engineering**.

Welsh, Z. G., Khan, M. I. H., & Karim, M. A. (2021). Multiscale modeling for food drying: A homogenized diffusion approach. *Journal of Food Engineering*, 292, 110252. doi:10.1016/j.jfoodeng.2020.110252.



Statement of Contribution of Co-Authors for Thesis by Published Paper

The following is the suggested format for the required declaration provided at the start of any thesis chapter which includes a co-authored publication.

The authors listed below have certified that:

1. they meet the criteria for authorship and that they have participated in the conception, execution, or interpretation, of at least that part of the publication in their field of expertise;
2. they take public responsibility for their part of the publication, except for the responsible author who accepts overall responsibility for the publication;
3. there are no other authors of the publication according to these criteria;
4. potential conflicts of interest have been disclosed to (a) granting bodies, (b) the editor or publisher of journals or other publications, and (c) the head of the responsible academic unit, and
5. they agree to the use of the publication in the student's thesis and its publication on the [QUT's ePrints site](#) consistent with any limitations set by publisher requirements.

In the case of this chapter:

Welsh, Z. G., Khan, M. I. H., & Karim, M. A. (2021). Multiscale modeling for food drying: A homogenized diffusion approach. *Journal of Food Engineering*, 292, 110252

Contributor	Statement of contribution
Zachary Welsh	
QUT Verified Signature	Generation of concept, model concept, model construction and model analysis, manuscript preparation, drafting and critically reviewing the manuscript
Date: 29/11/2020	
M. I. H. Khan QUT Verified Signature	Experimentation, manuscript drafting, data analysis, and critically revising the manuscript.
M. A. Karim	Supervision, concept refinement, manuscript revision, manuscript editing, author for correspondence and final approval

Principal Supervisor Confirmation

I have sighted email or other correspondence from all Co-authors confirming their certifying authorship.
(If the Co-authors are not able to sign the form please forward their email or other correspondence confirming the certifying authorship to the GRC).

Azharul Karim
Name

QUT Verified Signature

Signature

30/11/20
Date

3.1 ABSTRACT

Fruits and vegetables have a heterogeneous microstructure which dynamically changes during drying. Currently, food drying models approximate the material's structure through utilizing a representative elementary volume which adopts a larger scale of description and considers the fluid phases as fictitious continuums. This assumption limits the ability of the models to capture the heterogeneity of food material. The multiscale modeling is considered to have the ability to overcome this limitation and advance the understanding of the micro level transport processes. This research aims to develop a multiscale homogenization model for food drying. The homogenization was performed on the cellular structure of apple tissue considering intracellular (bound) water and free water separately to calculate the effective diffusivity for convective drying. The simulation was performed at three different drying temperatures (45°C , 60°C and 70°C), and the results were validated using experimental data. The homogenized diffusivity approach described the experimental data well and provides new insight into how to consider the heterogeneous structure of food material utilizing knowledge of the microstructural evolution.

3.2 INTRODUCTION

Plant-based food materials, particularly fruits and vegetables are heterogeneous with a porous structure composed of polymers, minerals, air and water, with a water content of up to 90% (Khan et al., 2017a; Joardder and Karim, 2019). During convective drying, food material can undergo significant modifications to its physical, chemical, and nutritional characteristics. These modifications occur across multiple length scales and are governed by the complex structure of the food material (Rahman et al., 2018a). Moisture resides mostly in three different locations within fruits and vegetables: (i) intracellular environments, termed as intracellular water (ICW); (ii) intercellular environments, usually referred to as free water (FW); and, (iii) inside the cell walls, known as strongly bound water (Khan and Karim, 2017; Khan et al., 2017b). The ICW, which migrate through three possible pathways: cell to cell, cell to pore or through progressive cell rupturing, has strong influence on cell deformation (Welsh et al., 2018; Mahiuddin et al., 2018).

Traditionally, partial differential equations have been used to describe the simultaneous heat transport, mass transport, and associated deformation during food drying. Various models have been developed considering food as a single-phase material (Golestani et al., 2013), a multiphase material (Purlis, 2019; Khan et al., 2017c), or with/without deformation (Defraeye and Radu, 2018). Whitaker (1977) theory forms the foundation of many of these drying models. The theory considered the heat, mass, momentum conservation equations of each phase (solid, liquid water, water vapor, and air) at microscale, and then used the concept of a representative elementary volume (REV) to develop a mechanistic model at the macroscale. The mathematical models were constructed based on some key assumptions. Some of these assumptions are: local thermal equilibrium is present, the domain is a rigid structure and the absence of ICW (Wang et al., 2007). As this approach does not consider the ICW transport separately, it fails to incorporate the heterogeneity of food materials. A visual representation of the cellular water distribution for the conceptual domain of the Whitaker (1977) approach and a representation of the actual domain of food materials can be seen in Figure 3.1 (b) and Figure 3.1 (a), respectively. To overcome this issue, various empirical relationships are embedded within the models to approximate the material. This generates a dramatic demand in physical and mechanical characterization of each sample being studied (Perré, 2007). Despite this fact, this assumption is still being used in many current modeling strategies.

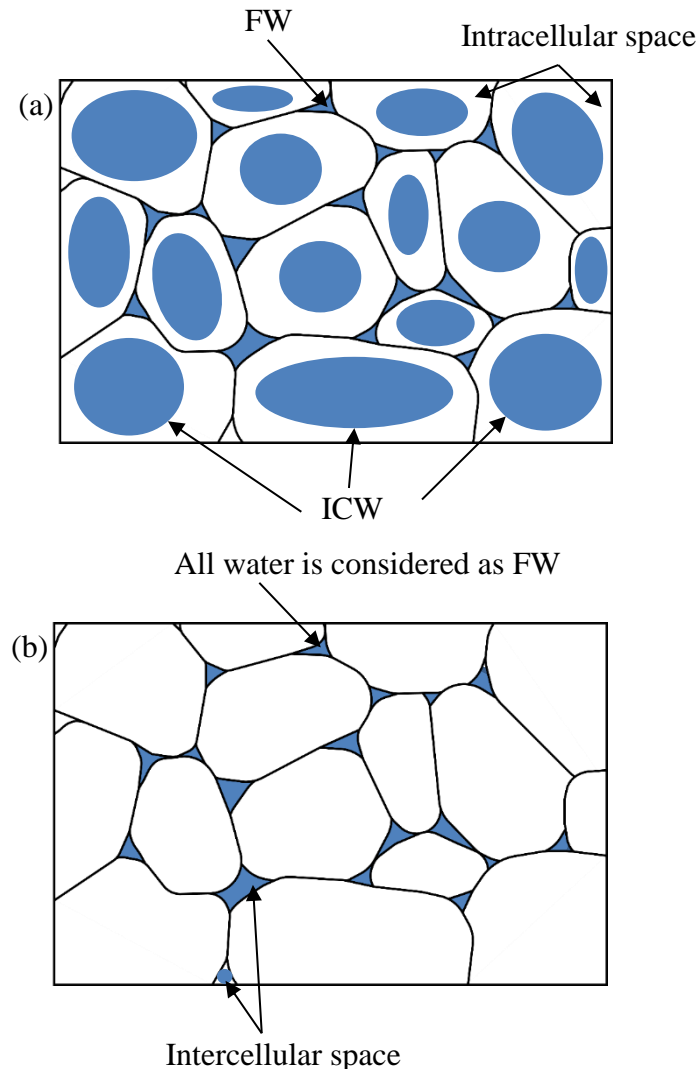


Figure 3.1. Schematic representation of the cellular water inside food materials considering two subdomains (intracellular spaces and intercellular spaces), (a) simplified representation of the real water distribution within food material, demonstrating where ICW and free water (denoted as blue) can be found, (b) REV approach demonstrating water is only considering as ‘free water’.

Multiscale modeling can address these concerns and model a more realistic description of the physics of drying. Multiscale modeling is a series of sub-models that investigate a product’s behavior over multiple spatial scales, allowing substantial physics to be modeled while saving on computational resources (Welsh et al., 2018). Multiscale modeling is still new for food drying, though it has been applied to the dehydration aspects of food material (Aregawi et al., 2014) and timber drying (Perré, 2007; Carr et al., 2013). However, these works are significantly different from food drying as drying process involves simultaneous heat and mass transport with

significant physical, chemical, and morphological changes (Rahman et al., 2018b). Compared to drying, dehydration models describe mass transport with its associated deformation without any external heat source (Welsh et al., 2018). Aregawi et al. (2014) predicted the water loss and viscoelastic deformation of food material through applying multiscale modeling. The work investigated the dehydration of apple tissue simulated as a cylinder in crossflow with an air velocity of 0.01 m/s, temperature of 25°C and a high relative humidity of 97%. These air properties indicate that the model cannot be directly applied to food drying at higher temperatures (60-70°C). Fanta et al. (2013) investigated the microscale coupled water transport and deformation of fruit tissue during dehydration. The research demonstrated that effective properties could be computed for the application of a multiscale modeling framework. Carr et al. (2013) applied multiscale modeling to model timber drying considering the material heterogeneity and presented a dual scale approach for simulating the drying of porous media. However, fruits and vegetables have unique deformation under an external heat source, restricting the applicability of these previous approaches. To capture the heterogeneously distributed water in fruit and vegetables, multiscale modeling can be applied for determining the heterogeneous diffusivity.

The estimation of effective diffusivity coefficients in many current modeling studies involves an experimental investigation and curve fitting techniques to develop a simple empirical relationship. This technique lumps the various mass transport mechanisms, such as liquid and vapor diffusion, capillary flow, and Knudsen flow, which act separately but coexist (Lentzou et al., 2019). The effective diffusivity has been extensively described by an Arrhenius type relation (temperature dependent),

$$D_{\text{eff}} = D_0 e^{-\frac{E_a}{RT}} \quad (3.1)$$

where D_0 is an integration constant (m^2/s), R is the universal gas constant ($\text{kJ/mol}\cdot\text{K}$), T is temperature (K) and E_a is the activation energy (kJ/mol). Both the integration constant and activation energy must be obtained from an experimental investigation which has resulted in numerous works to describe each food material and their associated cultivars (Rodrigues and Mauro, 2008; Kaya et al., 2007; Vega-Gálvez et al., 2008; Kara and Doymaz, 2015). In addition, these curve fitting techniques often consider a perfect geometry with no deformation often causing the predictive model

and experimental data to significantly deviate in the latter stages of drying (Tzempelikos et al., 2015).

Multiscale modeling provides an alternative approach to calculate the diffusivity by explicitly considering the material's heterogeneity rather than the use of a simple empirical relationships. In this work, we apply multiscale modeling approach to determine the diffusivity by considering the heterogeneously distributed water within food material during drying. Homogenization was applied on a representation of the cellular structure of apple tissue with ICW and FW considered separately in order to calculate the effective diffusivity. To demonstrate the strength of considering the heterogeneous structure, three drying temperatures (45°C, 60°C and 70°C) and three diffusivity evaluation methods (temperature dependent, moisture dependent and homogenized diffusivity) were investigated for Granny Smith apples. Finally, the study was validated with experimental data (Khan et al., 2018a).

3.3 MODEL DEVELOPMENT

The model we consider describes two spatial scales, a microscale and a macroscale, represented in Figure 3.2. The transport model was developed using an axisymmetric coordinate system, as shown in Figure 3.2 (b). The temperature and moisture dependent diffusivity approaches were only utilized in the macroscale model, whereas the homogenized diffusivity was considered for both microscale and macroscale. Based on the calculated Reynolds number of hot air at a velocity of 0.7 m/s, the fluid flow was considered laminar (See Appendix A for details). Therefore, the variations of the heat and mass transfer coefficients were neglected. The macroscale was developed based on some assumptions: (1) internal convective flow and heat generation can be neglected, (2) drying air properties are constant, (3) axisymmetric heating occurs, (4) moisture is only evaporated from the surface and (5) thermal equilibrium exists between all phases. Homogenization was applied to the microscale domain (Figure 3.2c) to calculate the effective homogenized diffusion (described in Homogenized effective diffusivity)

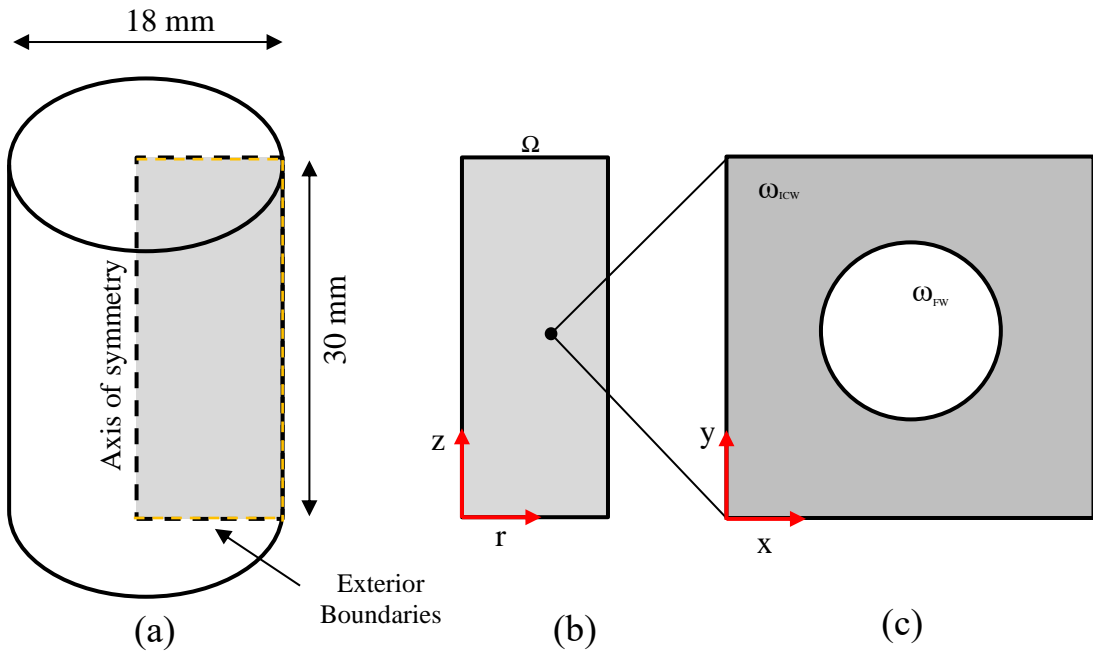


Figure 3.2. Geometries (a) whole sample, (b) axisymmetric macroscale domain and (c) microscale domain.

3.3.1 Macroscale mass conservation

The macroscale mass transport equation, based on Fick's law of diffusion, can be written as (Golestani et al., 2013)

$$\frac{\partial C}{\partial t} + \frac{1}{r} \frac{\partial}{\partial r} \left[-D_{i,eff} r \frac{\partial C}{\partial r} \right] + \frac{\partial}{\partial z} \left[-D_{i,eff} \frac{\partial C}{\partial z} \right] = 0 \quad (3.2)$$

where C is the instantaneous moisture concentration (mol/m^3), t is the time (s) and $D_{i,eff}$ is the effective moisture diffusivity (m^2/s) with $i=T,M,H$ denoting the temperature dependent, moisture dependent and homogenized diffusivity respectively.

3.3.2 Microscale mass conservation

To formulate the two-scale model, a microscale model was introduced to represent the heterogeneous structure of the food material. This assumption holds when the scale parameter (ε) trends to zero, implying the heterogeneities vanish, leading to a homogeneous material (Pavliotis & Stuart, 2008). The scale parameter is the ratio between the microscale characteristic length (l) and the macroscale

characteristic length (L), $\varepsilon=l/L$. This assumption is essential when deriving the model via homogenization and is commonly known as the separation of scales (Auriault et al., 2010; Carr & Turner, 2014). Within the model, cell wall water was not taken into consideration. During drying, the samples are commonly dried up to the equivalent moisture content where certain proportion of water remains within the dried sample. Apple parenchyma contains only a small proportion of cell wall water (only 2-4%) (Khan et al., 2016), which is usually not removed during drying as it is strongly bounded with the solid material. Its transportation causes cell wall collapses, mechanical instability and overall tissue collapse (Khan and Karim, 2017). In this research, the apple samples were also dried to the equilibrium moisture content (roughly 10-15%) for proper preservation. To reach this moisture content, the cell wall water was not required to be modeled and therefore was not considered within the study. Consequently, the microscale domain consists of two subdomains, ICW denoted as ω_{ICW} and FW denoted as ω_{FW} , demonstrated in Figure 3.2. The macroscale mass transport, as shown in Equation (3.2), has a coupled microscale mass transport equation defined as,

$$\frac{\partial}{\partial t} c(x, y, t) + \nabla \cdot (-D(x, y) \nabla c(x, y, t)) = 0 \quad (3.3)$$

where c is the microscale concentration (mol/m^3) and D is the cellular diffusivity (m^2/s) equaling D_{ICW} if $x, y \in \omega_{ICW}$ and D_{FW} if $x, y \in \omega_{FW}$.

3.3.3 Macroscale energy balance

The macroscale energy balance was considered utilizing Fourier's law of heat transfer, (Golestani et al., 2013)

$$\rho c_p \frac{\partial T}{\partial t} + \frac{1}{r} \frac{\partial}{\partial r} \left[-k r \frac{\partial T}{\partial r} \right] + \frac{\partial}{\partial z} \left[-k \frac{\partial T}{\partial z} \right] = 0 \quad (3.4)$$

where T is the instantaneous temperature (K), ρ is the density of apple tissue (kg/m^3), c_p is the specific heat of the material ($\text{J}/(\text{kg}\cdot\text{K})$) and k is the thermal conductivity of the material ($\text{W}/(\text{m}\cdot\text{K})$).

3.3.4 Boundary conditions

The mass flux at the exterior boundaries was considered as,

$$-D_{i,eff} \left(\frac{\partial C}{\partial r}, \frac{\partial C}{\partial z} \right) \Big|_{\mathbf{n}} = h_m \frac{(p_{v eq} - p_{v air})}{RT} \quad (3.5)$$

where h_m is the mass transfer coefficient (m/s), $p_{v eq}$ is the equilibrium vapor pressure, $p_{v air}$ is the vapor air pressure of ambient air (Pa), \mathbf{n} is the unit vector normal to the boundary and R is the universal gas constant (J/(mol·K)). The equilibrium vapor pressure can be defined from the sorption isotherm for apple tissue for any given point within a sample. The equilibrium vapor pressure, $p_{v eq}$ (Pa), for apple is defined as (Ratti et al, 1989),

$$p_{v eq} = p_{v sat}(T) \exp(-0.182M_{db}^{-0.696} + 0.232e^{-43.949M_{db}} M_{db}^{0.0411} \ln[p_{v sat}(T)]) \quad (3.6)$$

where $p_{v sat}$ is the saturated vapor pressure of water (Pa) and M_{db} is the moisture content (kg/kg dry basis). The saturated vapor pressure is defined as (Vega-Mercado et al., 2001)

$$p_{v sat} = \exp \left[\frac{-5800.2206}{T} + 1.3915 - 0.0486T + \left[0.4176 \times 10^{-4}T^2 - 0.1445 \times 10^{-7}T^3 + 6.546 \ln(T) \right] \right] \quad (3.7)$$

The heat transfer boundary condition on the exterior boundaries considered both convective heat transfer and heat lost due to evaporation at the surface, is defined as,

$$-k \left(\frac{\partial T}{\partial r}, \frac{\partial T}{\partial z} \right) \Big|_{\mathbf{n}} = h_T(T_{air} - T) - h_m \frac{(p_{v eq} - p_{v air})}{RT} \lambda M_w \quad (3.8)$$

with h_T being the heat transfer coefficient (W/(m²·K)), T_{air} is the drying air temperature (K), M_w molar mass of water (kg/mol) and λ is the latent heat of evaporation (J/kg). The last boundary condition is the symmetric condition, defined as

$$-D_{i,eff} \left(\frac{\partial C}{\partial r}, \frac{\partial C}{\partial z} \right) \Big|_{\mathbf{n}} = 0 \quad (3.9)$$

$$-k \left(\frac{\partial T}{\partial r}, \frac{\partial T}{\partial z} \right) \Big|_{\mathbf{n}} = 0 \quad (3.10)$$

3.3.5 Food material properties

The thermophysical properties of specific heat, c_p (J/(kg·K)), and thermal conductivity, k (W/(m·K)), of the food material were considered as a function of wet bases moisture content (M_{wb}) (Białobrzewski, 2006):

$$c_p = 1000(1.4 + 3.22M_{wb}) \quad (3.11)$$

$$k = 0.148 + 0.493M_{wb} \quad (3.12)$$

3.3.6 Diffusion approaches

This research considered three effective diffusivity approaches; temperature dependent, shrinkage dependent and homogenization diffusion.

Temperature dependent effective diffusivity

The temperature dependent diffusivity approach for food drying is defined through an Arrhenius-type relationship to the temperature, considered as:

$$D_{T,eff} = D_0 e^{-\frac{E_a}{RT}} \quad (3.13)$$

where D_0 is an integration constant (m²/s) and E_a is the activation energy (J/mol). Both the integration constant and activation energy were obtained from the experimental investigation (Feng et al., 2000).

Shrinkage dependent effective diffusivity

Shrinkage dependent effective diffusivity can be considered as a function of moisture content for products undergoing deformation defined as (Kumar et al., 2015; Karim & Hawlader, 2005):

$$\frac{D_{ref}}{D_{M,eff}} = \left(\frac{b_o}{b} \right)^2 \quad (3.14)$$

where D_{ref} is a reference diffusivity (m²/s), b_0 is the initial product's thickness (m) and b is the product's thickness (m) at time t (s). The thickness ratio was considered as (Desmorieux & Moyne, 1992):

$$b = b_0 \left[\frac{\rho_w + M_{wb} \rho}{\rho_w + M_{0wb} \rho} \right] \quad (3.15)$$

where ρ_w is density of water (kg/m^3) and M_{0wb} is the wet bases initial moisture content.

Calculating the reference diffusivity, integration constant and activation energy

The cylindrical sample had an initial height to diameter (H/D) ratio of 1.67. Ghisalberti and Kondjoyan (1999) investigated the effect of body shape, dimension and position in flow of a short cylinder in airflow. The work demonstrated marginal difference between a cylinder with a H/D ratio of 1.2 and an infinite cylinder at the associated Reynolds number and Nusselt number within this work (Appendix A). Therefore the sample was considered as an infinite cylinder in crossflow (Ghisalberti and Kondjoyan, 1999). Additionally, the samples were considered as isotropic, under Fick's law, with no volume change, uniform initial moisture content and negligible external resistance. The reference diffusivity from the experimental investigation was calculated by the following expression (Feng et al., 2000),

$$M^* = \frac{M(t) - M_e}{M_o - M_e} = \frac{4}{b_1^2} \exp \left(-\frac{b_1^2 D_{ref} t}{r_{avg}^2} \right) \quad (3.16)$$

where M^* is the moisture content slope (kg/kg), b_1 is the first root for Bessel function of first kind of zero order and r_{avg} is the average of the cylinder (m) during the duration of drying under consideration. The integration constant and activation energy were calculated through the Arrhenius plot (Srikiatden & Roberts, 2005).

Homogenized effective diffusivity

The 2D homogenized effective diffusivity can be denoted as a tensor,

$$D_{H,eff} = \begin{bmatrix} \frac{1}{\omega} \int_{\omega} D(x, y) \left(\frac{\partial u_1}{\partial x} + 1 \right) d\omega & \frac{1}{\omega} \int_{\omega} D(x, y) \frac{\partial u_2}{\partial x} d\omega \\ \frac{1}{\omega} \int_{\omega} D(x, y) \frac{\partial u_1}{\partial y} d\omega & \frac{1}{\omega} \int_{\omega} D(x, y) \left(\frac{\partial u_2}{\partial y} + 1 \right) d\omega \end{bmatrix} \quad (3.17)$$

$$\mathbf{e}_1 = \begin{bmatrix} 1 \\ 0 \end{bmatrix}, \quad \mathbf{e}_2 = \begin{bmatrix} 0 \\ 1 \end{bmatrix} \quad (3.18)$$

where ω is the area of the macroscale domain, u_1 and u_2 are the corrective factors and the solution of the periodic cell problem:

$$\nabla \cdot (D \nabla(u_j + \mathbf{e}_j)) = 0 \quad j = 1, 2 \quad (3.19)$$

$$u_j \text{ is } \omega\text{-periodic} \quad (3.20)$$

$$\frac{1}{\omega_A} \int_{\omega_A} u_j d\omega = 0 \quad (3.21)$$

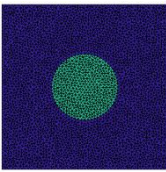
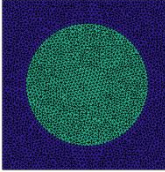
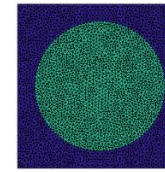
The solution of the corrective factors, Equation (3.19), is unique only up to an additive constant (Auriault et al., 2010), requiring the zero mean constraint, Equation (3.21), to achieve a single unique solution. However, the effective homogenized diffusion tensor only requires the gradient of u_j , therefore any of these unique solutions are suitable (Carr & Turner, 2014).

3.3.7 Microscale domain – Considering predefined deformation

An individual microscale domain was used for each drying temperature, as shown in Table 3.1, which was constructed based on the author's previous work on cellular water transport during drying (Khan et al., 2018a). The microscale domains must represent the heterogeneous structure of food material at their associated drying temperatures (Rahman et al., 2018c). However, homogenization does not preserve the orientation of the microscale sub-domains (location of intercellular spaces). This allows the intercellular spaces to be grouped and represented as a circle. The ratio between sub-domains within the microscale is the key factor to represent materials heterogeneity. ICW's ability to transport through progressive cell rupturing (Khan et al., 2018b) does add complexities to representing this ratio. Khan et al. (2018) investigated the percentages of ICW and FW throughout the entire drying cycle. The study demonstrated that no progressive cell rupturing occurred during convective drying at 45°C. This translated into an average FW content of 17.19% over the entire drying cycle (Table 3.1). However, at 60°C moderate progressive cell rupturing occurred and at 70°C progressive cell rupturing occurred quickly and regularly throughout the experiments. This cell rupturing dynamically changed the microstructure and increased the average FW content over the drying cycle for these drying temperatures. Based on the findings of Khan et al. (2018) research, the average

FW content was calculated for each associated drying temperature, Table 3.1. This resulted in the construction of individual microscale domains and introduced predefined cellular deformation into the approach.

Table 3.1. Microscale domains for each drying temperature where the blue subdomain denotes ICW (ω_{ICW}) and the green subdomain denotes FW (ω_{FW}).

Temperature	45°C	60°C	70°C
Microscale domains			
Average FW (%)	17.19 %	37.20%	45.30%

3.3.8 Cellular Diffusion Properties – ICW and FW

To complete the microscale model, the cellular diffusivity was required for each sub-domain. FW is located within ω_{FW} and is clearly defined in literature as 2.6×10^{-5} (m²/s) (Datta, 2007). However, the cellular diffusivity for ICW is not explicitly defined for fruits and vegetables. Individual functions do exist for the capillary diffusion within potatoes and Granny Smith apples for multiphase models (Ni, 1997; Kumar et al., 2016). However, these functions have been constructed utilizing macroscale effective diffusivity results not through microscale research.

This research conducted an ICW diffusivity investigation for drying at 45°C and the most appropriate value was used for the remaining drying temperatures. As the microscale domains consider the average FW content, the diffusivity of ICW must also be averaged over the entire drying cycle. An optimization investigation based on the minimization of the distance (*OF*) between the simulated and experimental moisture drying curves for $D_{H,eff}$ was used with the objective function denoted as

$$OF(D_{H,eff}) = \int \left[\overline{M}_{db,exp}(t) - \overline{M}_{db,num}(t, D_{H,eff}) \right]^2 dt \quad (3.22)$$

where $\overline{M}_{db,exp}$ is the average dry bases moisture content from the experimental investigation and $\overline{M}_{db,num}$ is the average moisture content (dry bases). The Levenberg-Marquardt algorithm was utilized due to its superior convergence rate associated with the least-square-type problems.

3.4 INPUT PARAMETERS

The input parameters can be seen in Table 3.2.

Table 3.2. Input parameters

Parameter	Value (unit)	Reference
Density of apple, ρ	837 (kg/m ³)	Mavroudis et al., (1998)
Density of water, ρ_w	995 (kg/m ³)	Cengel 2003
Initial moisture content, M_0	6.4 (kg/kg db)	This study
Initial sample temperature, T_0	296 (K)	This study
Equilibrium moisture content, M_e	0.2 (kg/kg db)	Białobrzewski (2006)
Initial wet bases moisture content, M_{0wb}	0.86 (kg/kg wb)	This study
Latent heat of evaporation, λ	2358600 (J/kg)	Cengel (2003)
Universal gas constant, R	8.314 (J/(mol·K))	Cengel and Boles (2002)
Molar mass of water, M_w	0.018016 (kg/mol)	Cengel and Boles (2002)
Partial vapor pressure, p_{vair}	2000 (Pa)	This study

Average sample radius during drying, r_{avg}	0.0055 (m)	This study
Initial sample thickness, b_0	0.03 (m)	This study
Heat transfer coefficient, h_T	15.21 (W/(m ² ·K))	This study
Mass transfer coefficient, h_m	0.01 (m/s)	This study
Reference diffusivity 45°C, $D_{ref\ 45}$	3.76×10^{-10} (m ² /s)	This study
Reference diffusivity 60°C, $D_{ref\ 60}$	5.12×10^{-10} (m ² /s)	This study
Reference diffusivity 70°C, $D_{ref\ 70}$	6.74×10^{-10} (m ² /s)	This study
Integration constant, D_0	9.92×10^{-7} (m ² /s)	This study
Activation energy, E_a	20871 (J/mol)	This study

3.5 SIMULATION METHODOLOGY

The modeling solution procedure can be found in Figure 3.3. The temperature and moisture dependent diffusivities were calculated through the experimental investigation utilized the pre-existing techniques within food drying literature (denoted within the pink subsection of Figure 3.3). The homogenized diffusivity was calculated through applying homogenization on a microscale model. This is novel for the field food drying (denoted within the orange subsection of Figure 3.3). The macroscale model was solved in COMSOL Multiphysics 5.3a and the finite element homogenization was solved using MATLAB R2018a with Gmsh (Geuzaine and Remacle, 2009) for microscale geometry creation. The macroscale mesh contained 1922 elements with a minimum skewness quality of 0.71. Additionally, an implicit backward differentiation formula with variable discretization and an automatic step-size selection was utilized for the temporal solver. Also, the *free* time step option was used to allow an adaptive time step to be chosen based on the local error estimates within COMSOL.

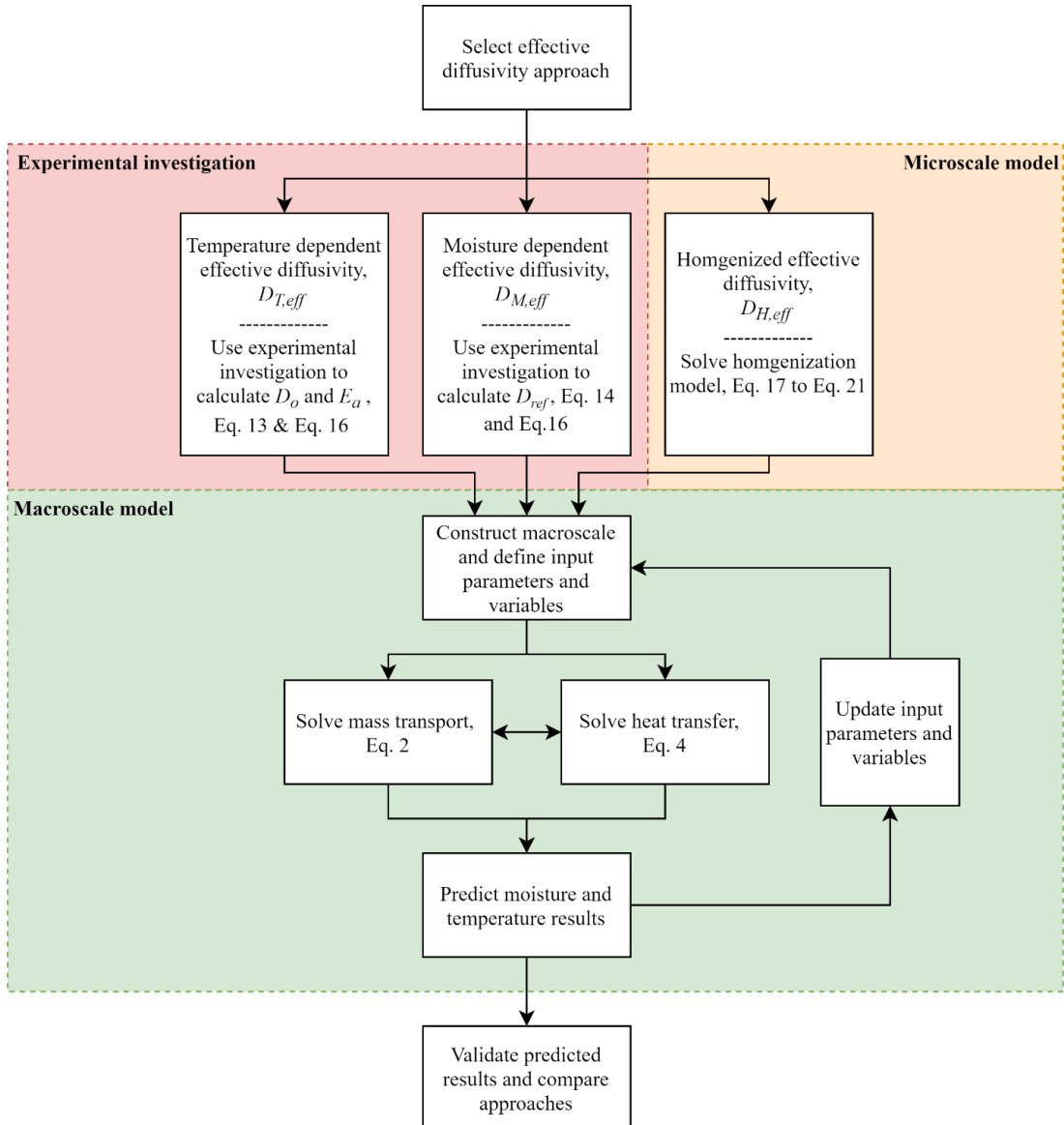


Figure 3.3. Modeling solution procedure.

3.6 EXPERIMENTAL INVESTIGATION

Fresh Granny Smith apples were collected from a local market (Woolworths) in Brisbane, Australia, and stored in a refrigerator at 4 °C until the drying experiments. The apples used were harvested at commercial maturity, as informed by the supermarket. The samples were prepared based on the standard sample preparation procedure (ASABE and Home). Firstly, the materials were washed and cut into cylindrical slices of 30 mm in length and 18 mm in diameter using a fruit sample preparation tool [a stainless-steel Cork Borer (JH-1225)]. To maintain consistency, all

samples were prepared from the mesocarp of pulp (skin off) portions of a Granny Smith apple. Then, the prepared samples were placed horizontally on the tray of the dryer and then dried in a multi-tray cabinet dryer (temperature range 35-70 °C, 220-240v, 50Hz, 245W). In this dryer, drying air flowed perpendicularly to the drying surfaces of the samples. The dryer was started about 30 min before each drying run to obtain steady-state drying conditions (Khan et al., 2018b). The drying experiments were performed at temperatures 45 °C, 60 °C, and 70 °C with 60% relative humidity (equivalent to 0.014 kg/m³ absolute humidity). Generally, standard hot-air or convective drying is conducted at temperatures between 40 °C to 80 °C. In this study, three different temperatures (45 °C, 60 °C, and 70 °C) were selected within this range to observe the effect of temperature on the drying kinetics. All drying experiments were performed in a laboratory at Queensland University of Technology, Brisbane, Australia where the relative humidity was maintained at 60%. The hot air was supplied with an airspeed of 0.7 m/s. Total 0.30 kg (30 samples) of sliced apple was used and each sample was taken from the dryer in 30 mins intervals, and immediately weighed using a digital electronic balance (model BB3000; Mettler-Toledo AG, Grefensee, Switzerland). The balance had a measurement range of 0-100 g with an accuracy of 0.01 g. All weight measurements were completed within 10 seconds during the drying process. This experimental procedure was replicated three times. The temperatures were measured by four fiber optic thermal sensors, which were connected to a fiber optical 4-channel thermometer monitor (OPTO con AG, Germany) and the data was recorded. The four optical fiber thermal sensors were placed at different locations across the sample thickness. The first sensor was placed at the center of the sample (at 9 mm depth from the surface), the second one was placed at 6 mm, third was placed at 3 mm depth from the surface and the fourth sensor was placed on the surface of the sample. The four-sensor data were then averaged and considered for further analysis. The detailed drying experimental procedure and some of the results can be found in the authors' previous publication (Khan et al., 2018a).

3.7 RESULTS

This study investigated the drying kinetics using three effective diffusivity approaches, temperature dependent, moisture dependent and homogenized diffusivity. Additionally, an ICW diffusivity investigation was also conducted. The predicted results were compared to the experimental data of Khan et al. (2018) to validate the model.

3.7.1 Drying kinetics

The study utilized a Levenberg-Marquardt algorithm to find the optimal diffusivity for ICW. The objective function, Equation (3.22), minimized the discrepancy between the experimental and simulated results of the average moisture content for drying at 45°C. The optimization investigation found that the optimal ICW diffusivity for Granny Smith apples was $1.74 \times 10^{-10} \text{ m}^2/\text{s}$. This resulted in an effective isotropic diffusivity tensor of $2.45 \times 10^{-10} \text{ m}^2/\text{s}$ (for drying at 45°C), which was consistent with existing literature falling within the expected range of 10^{-11} - $10^{-9} \text{ m}^2/\text{s}$ for most food material (Saravacos and Maroulis, 2001; Panagiotou et al., 2004). This effective diffusivity can also be compared to 1.22×10^{-10} - $4.29 \times 10^{-10} \text{ m}^2/\text{s}$ for Apple Pomace for the temperature range of 50-80°C (Kara and Doymaz, 2015), 0.713×10^{-11} - $7.66 \times 10^{-10} \text{ m}^2/\text{s}$ for Red Delicious apples at a temperature range of 35-55°C (Beigi, 2016) and $4.9779 \times 10^{-10} \text{ m}^2/\text{s}$ for Granny Smith apples at 40°C (Cruz et al., 2015). The majority of food drying studies have been conducted at a macroscale. Therefore, limited literature exists to compare the ICW diffusivity ($1.74 \times 10^{-10} \text{ m}^2/\text{s}$). Literature reported the ICW diffusivity of fresh Granny Smith apples (high moisture content) as $3.8 \times 10^{-10} \text{ m}^2/\text{s}$ (Sibgatullin et al., 2007). Additionally, it is known that as the moisture content within the sample decreases, the effective water diffusivity also decreases (Dadmohammadi and Datta, 2019). This trend is demonstrated in macroscale multiphase models in association with the capillary diffusivity decreasing with the decreasing moisture content (Datta, 2007; Kumar et al., 2016). The average ICW diffusivity of this study ($1.74 \times 10^{-10} \text{ m}^2/\text{s}$) aligns with the expected trend (as it is an average). However, the model could be slightly underpredicting its magnitude. The presented model simplifies certain aspects of drying, i.e. consideration of idealized

cells in material structure and no shrinkage, which could be contributing to the underprediction. The investigated ICW diffusivity was then used to predict the moisture content for the homogenization approach.

Figure 3.4 shows the dry bases (db) moisture content profiles at different drying temperatures during drying. The average moisture content [Equation (A.1)] for each diffusivity approach was plotted with respect to time and compared to the experimental data to validate the model. The accuracy of the approaches was evaluated based on the mean absolute error (MAE) between the predicted results and the experimental data, Table 3.3. The moisture contents for all three diffusivity approaches demonstrate good agreements with the experimental results at 45°C and 60°C with low MAEs, as shown in Figure 3.4 (a) and Figure 3.4 (b), respectively. Looking closely at the predicted results, while drying at 45°C, the temperature dependent approach described the experimental data more accurately in the early stages of drying (up to 120 mins), Figure 3.4 (a). However, the approach tended to overpredict the moisture content from the middle stages to the end of drying process with an overall MAE of 0.09 kg/kg db. Also, at 45°C the moisture dependent approach performed very similar to the temperature dependent approach with a MAE of 0.11 kg/kg db. At 60°C, the temperature dependent approach predicted the moisture content reasonably well (MAE of 0.09 kg/kg db) and the moisture dependent approach over predicted the early stages and under predicted the latter stages of drying resulting in a MAE of 0.12 kg/kg db, Figure 3.4(b).

The homogenized diffusivity approach was able to predict drying at 45°C and 60°C very accurately, achieving MAEs under 0.06 kg/kg db. The approach considered the heterogeneous structure at each drying temperature with the same constant diffusivities for ICW and FW. All three diffusivity approaches failed to describe the early stages of drying at higher temperatures (70°C), Figure 3.4 (c), reporting high MAEs ranging from 0.33 to 0.51 kg/kg db, Table 3.3 . Drying at a temperature of 70°C resulted in a large amount of cellular deformation through progressive cell rupturing causing the ratio between ICW and FW to drastically oscillate (Khan et al., 2018a). This was unable to be captured by any diffusivity approach. Additionally, drying at higher temperatures can cause certain deformation to occur, such as case hardening and crust formation, which influences the moisture migration. At 70°C, a large

difference in moisture content can exist between the core and surface of the product producing a shell layer on the exterior transport boundary (Karunasena et al., 2015). This shell layer is an additional barrier for moisture transport causing the water to only exit the product via internal evaporation as water vapor. Additionally, within the shell layer vapor generation is enhanced leading to a higher vapor diffusivity (Gulati and Datta, 2015). Case hardening is commonly associated with food materials with high starch contents, such as potatoes, but the phenomena has also been reported in apple tissue. Bai et al. (2002) investigated apple tissue during convective drying at 60-65°C and uncovered case hardening had occurred with evidence within the tissue's microstructure. Figure 3.5 demonstrates that there was a large difference in moisture content between the core and surface within the macroscale model after 60 minutes of drying. However, the models did not incorporate the effects of the shell layer adequately contributing to their inability to predict the experimental data at 70°C. When considering two cellular subdomains (FW and ICW), the homogenization model only moderately predicted drying at higher temperatures. To overcome this issue, the microscale could consider a third subdomain, consisting of the shell layer, to accurately represent the cellular structure which can occur at higher temperatures.

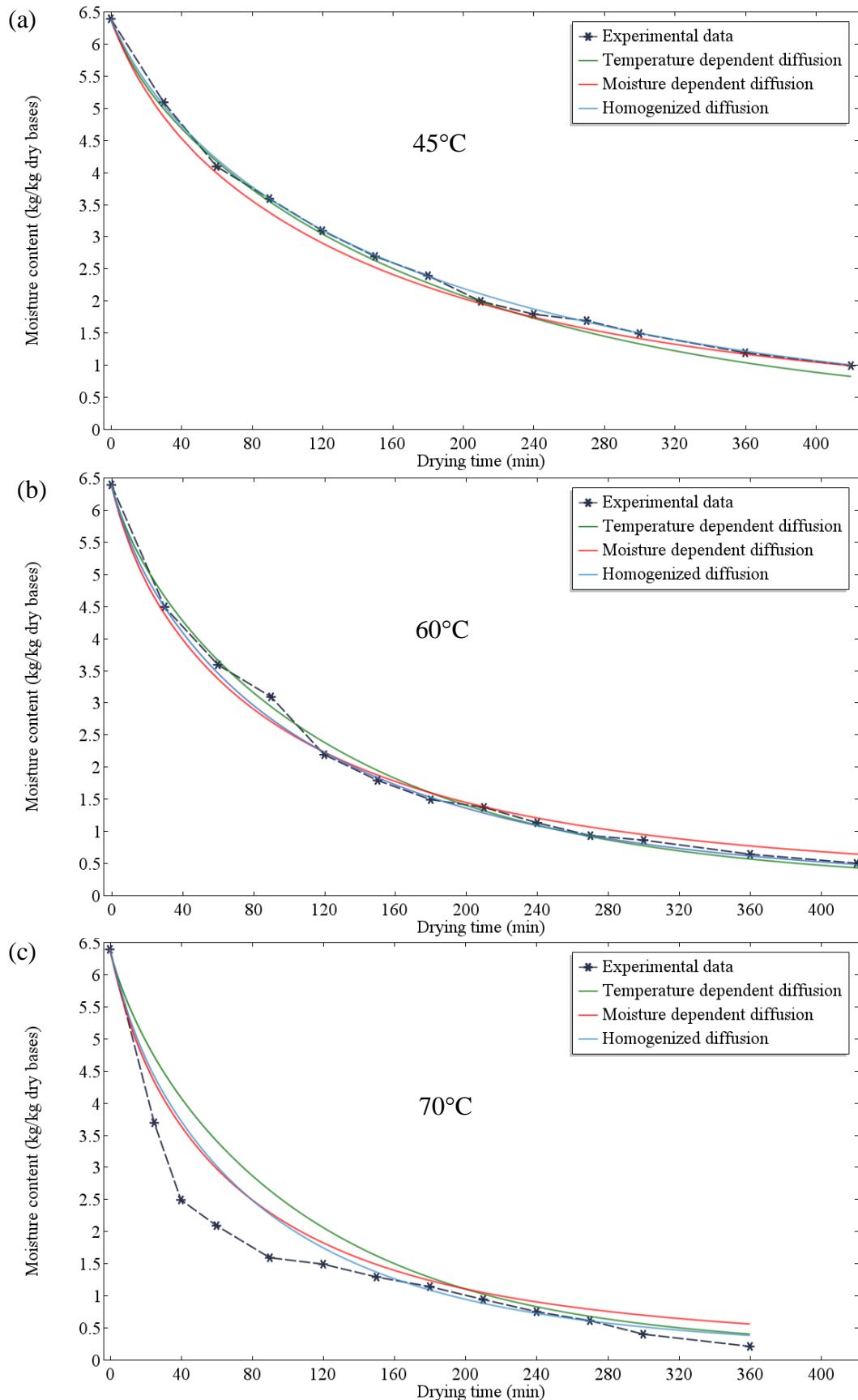


Figure 3.4. Moisture content curves for each diffusivity approach at different drying temperatures, a) 45°C, b) 60°C, c) 70°C

Table 3.3. Summary of the mean absolute error (MAE) between the model predictions and experimental data

MAE	Diffusivity approach	Drying temperature		
		45°C	60°C	70°C
Average moisture Content (Figure 3.4)	Temperature dependent diffusivity	0.09 kg/kg db	0.09 kg/kg db	0.51 kg/kg db
	Moisture dependent diffusivity	0.11 kg/kg db	0.12 kg/kg db	0.39 kg/kg db
	Homogenized diffusivity	0.04 kg/kg db	0.06 kg/kg db	0.33 kg/kg db
Average temperature (Figure 3.6)	Temperature dependent diffusivity	0.86 °C	3.00 °C	2.01 °C
	Moisture dependent diffusivity	0.58 °C	1.52 °C	1.47 °C
	Homogenized diffusivity	0.31 °C	2.65 °C	2.07 °C
$MAE = \frac{1}{N} \sum_{n=1}^{\infty} Y_{\text{exp}}^n - Y_{\text{num}}^n ,$ where Y is either M_{db} or T (moisture content and temperature respectively) and N is the number of experimental data points.				

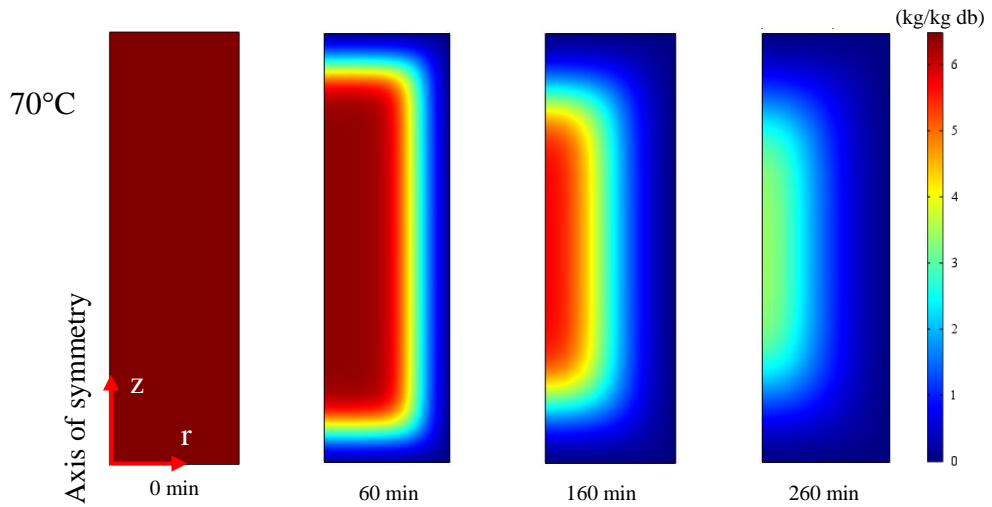


Figure 3.5. The axisymmetric moisture profile (kg/kg dry bases) at different drying times for the homogenized diffusivity approach for drying at 70°C.

3.7.2 Temperature profiles

The results of the temperature profile for the developed model can be seen in Figure 3.6. The average temperature [Equation (A.1)] of each diffusivity approach was plotted with respect to time and compared to the experimental data to validate the models. Within the macroscale energy balance, the food material's thermal conductivity and specific heat are functions of moisture. Therefore, the trends which exist within the moisture content curves are mirrored within the average temperature profiles. All other aspects within the energy balance are the same between the different diffusivity approaches. At 45°C all three diffusivity approaches described the experimental data well after 50 minutes of drying with MAEs less than 0.86°C. Additionally, the homogenized approach predicted the results the best with a MAE of 0.31°C, Figure 3.6 (a). All approaches tended to overpredict the average temperature initially, however, the duration of the overprediction decreased as the drying temperature increased. For drying at 45°C the overprediction occurred for the first 65 minutes, whereas for drying at 70°C the duration of the overprediction was 15 minutes. At 60°C all diffusivity approaches under predicted the average temperature after 25 minutes, with MAEs ranging from 1.52°C to 3°C, Figure 3.6 (b). At 70°C all diffusivity approaches accurately predicted the latter stages of drying but failed to capture the middle stage (40-100 min), Figure 3.6 (c). This follows the trend uncovered in the moisture profile results.

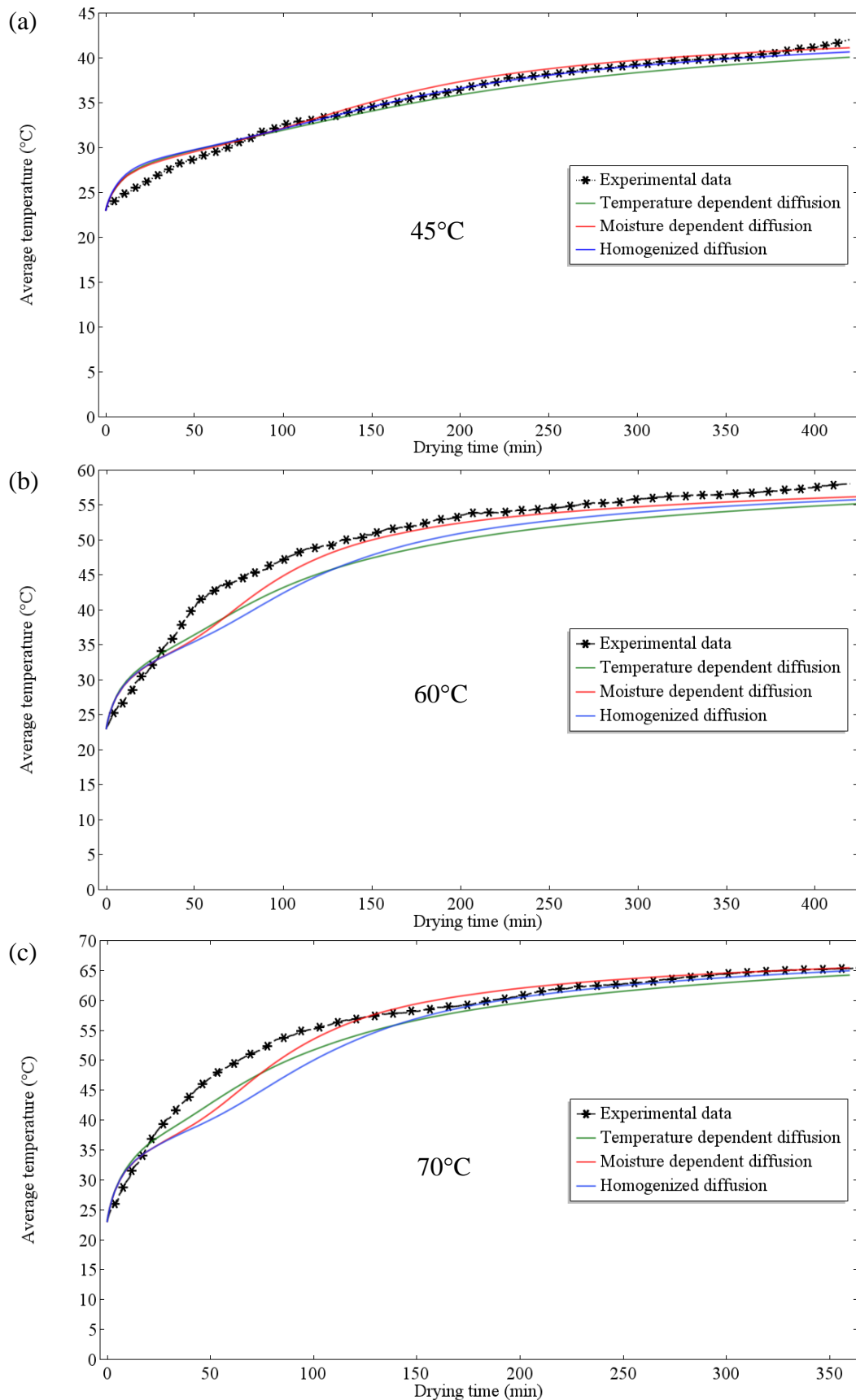


Figure 3.6. Average temperature for each diffusivity approach at different drying temperatures, a) 45°C, b) 60°C, c) 70°C

3.8 DISCUSSION

3.8.1 Comparison of diffusivity approaches

The homogenized diffusivity model provides new insight into how to take the heterogeneous structure of food material into consideration utilizing knowledge of the microstructural evolution. The approach was able to achieve good agreement with the experiment data and achieved similar results to the current diffusivity approaches for drying at low to medium temperatures. All three diffusivity approaches created the same axisymmetric concentration profile, as demonstrated in Figure 3.5. Within this distribution, moisture still resides within the center of the sample, whereas the outside is completely dry. This moisture profile is typical for convective drying and consistent with existing literature (Kumar et al., 2015) providing an additional form of model validation. Each diffusivity approach calculated the effective diffusivity differently. The temperature dependent approach heavily depends on the experimental conditions requiring the integration constant (D_0) and the activation energy (E_a) to be calculated experimentally, as shown in Equation (3.13). The moisture dependent approach requires the reference diffusivity (D_{ref}) to be known at each drying temperature to construct its property [Equation (3.14)]. These variables depend on the specific sample being dried (i.e. apple or carrot) and the drying conditions (Kara and Doymaz, 2015). Thus, every sample in every drying condition being predicted must be experimentally investigated to create accurate variables for the study. This can create a dramatic demand in physical and mechanical characterizations of the sample (Perré, 2007). On the other hand, the homogenization approach considers the heterogeneously distributed water and could hold potential to move towards less empirical based models while improving their prediction capabilities. In addition, the curve fitting techniques for the temperature and moisture dependent diffusivity approaches often consider a perfect geometry with no deformation causing the predictive model and experimental data to significantly deviate in the latter stages of drying (Tzempelikos et al., 2015). This assumption is embedded within the selection of the radius of the sample in Equation (3.16), which is key to calculating the integration constant, activation energy and reference diffusivity, influencing the accuracy of these approaches. This study utilized the average radius (r_{avg}) considering a basic level of deformation embedded within the property, improving the accuracy of the predicted

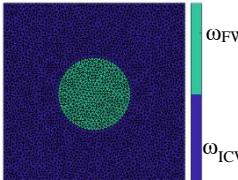
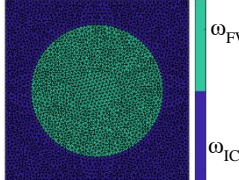
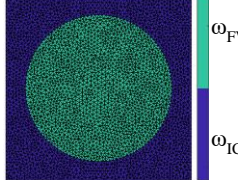
results in the latter stages of drying. It is also very common to consider the initial radius which can cause the simulation to significantly deviate from the experimental results.

The homogenized diffusivity approach considered constant cellular diffusivity properties, an individual microscale at each drying temperature (predefined deformation) and a limited ICW diffusivity investigation. Although the diffusivity of ICW within fruits and vegetables is not explicitly defined in the literature, an optimization investigation was able to uncover a suitable average for drying at various temperatures by utilizing the experimental results of drying at 45°C. To construct the microscale domains, knowledge of the microscale evolution was required. This achieved through considering the average FW content of Khan et al. (2018) work. Utilizing these experimental results, a separate microscale domain was constructed for each drying temperature. As a result, the homogenized approach was able to describe convective drying at 45°C and 60°C very accurately. However, the approach only moderately predicted drying at 70°C. The temperature and moisture dependent approaches were also unable to adequately predict the moisture content at this temperature. Drying at higher temperatures can cause the creation of a crust or dried shell, alternating the cellular structure and increasing the vapor diffusivity within the region (Gulati and Datta, 2015). Additionally, a large amount of progressive cell rupturing occurs in the middle stages of drying (Khan et al., 2018). These changes to the cellular microstructure heavily influenced the magnitude of diffusivity and were only moderately captured by considering the average heterogeneous structure with no consideration of the dried shell layer within the microscale domain. A microscale domain which dynamically changes or deforms should be considered at higher drying temperatures to incorporate these large changes to the heterogeneous structure. This would require the scales (microscale and macroscale) to be fully coupled removing the requirement of the knowledge of the microstructural evolution but it should be noted this would also increase the computational cost. The current homogenized approach treats the scales as independent and $D_{H,eff}$ is precomputed as demonstrated in Figure 3.3.

The homogenized diffusivity approach provides an alternative technique for the commonly used diffusivity techniques. By keeping the cellular diffusivity properties of ICW and FW the same for all drying temperatures, the strength of considering the heterogeneous structure is demonstrated. A comparison of the three diffusivity

approaches can be found in Table 3.4. The temperature and moisture dependent approaches resulted in diffusivity ranges, varying with the temperature and moisture respectively. Whereas, the homogenized diffusivity approach created an average isotropic diffusivity matrix [Equation (3.17)] due to the configuration of the microscale domains. All effective diffusivity results were similar to pre-existing literature on apples (Khan et al., 2017a) and fell within the expect effective diffusivity range of 10^{-9} - 10^{-11} m²/s for most food material (Saravacos and Maroulis, 2001; Panagiotou et al., 2004). Additionally, the effective diffusivities found were less than the self-diffusion of water at each associated drying temperature as expected (Lentzou et al., 2019).

Table 3.4. Effective diffusivity results of different approaches.

Diffusivity (m ² /s)	Temperatures		
	45°C	60°C	70°C
$D_{T,eff}$	2.18×10^{-10} - 3.33×10^{-10} m ² /s	2.16×10^{-10} - 4.87×10^{-10} m ² /s	2.16×10^{-10} - 5.96×10^{-10} m ² /s
$D_{M,eff}$	2.19×10^{-10} - 3.78×10^{-10} m ² /s	2.43×10^{-10} - 5.15×10^{-10} m ² /s	3.12×10^{-10} - 6.78×10^{-10} m ² /s
$D_{H,eff}$	 $\begin{bmatrix} 2.45 \times 10^{-10} & 0 \\ 0 & 2.45 \times 10^{-10} \end{bmatrix}$ m ² /s	 $\begin{bmatrix} 3.81 \times 10^{-10} & 0 \\ 0 & 3.81 \times 10^{-10} \end{bmatrix}$ m ² /s	 $\begin{bmatrix} 5.199 \times 10^{-10} & 0 \\ 0 & 5.199 \times 10^{-10} \end{bmatrix}$ m ² /s

3.9 CONCLUSION

A homogenized diffusivity approach was developed for convective drying of plant-based food materials. The approach considered the heterogeneously distributed water (ICW and FW) to determine the diffusivity utilizing individual microscale domains with cellular diffusivity properties. The results were compared with two existing diffusivity methods (temperature and moisture dependent diffusivity). Additionally, the models were validated by comparing the simulated results with experimentally determined moisture content and temperature profiles. The homogenized approach was able to describe convective drying at 45°C and 60°C accurately with low MAEs, but only moderately described drying at higher temperatures (70°C). Drying at 70°C causes large microstructure deformation which the homogenized approach could not fully capture. The homogenized diffusivity model provides new insight into how to consider the heterogeneously distributed water of food material utilizing knowledge of the microstructural evolution. Additionally, the model is a step towards a more mechanistic approach to determine diffusivity which will aid in developing advanced food drying processes.

3.10 ACKNOWLEDGEMENTS

The authors would like to thank Prof. Matthew J. Simpson for his valuable suggestions and guidance. This study was funded by the Department of Education and Training (AUS) through a Research Training Program (Stipend) Domestic (RTP) scholarship. The second author acknowledges the supports from the Advance Queensland Fellowship Project (AQF) (the grant ID: 02073-2015-30358/15)

3.11 MODEL AVAILABILITY

The models described in this article can be obtained from the corresponding author upon request.

REFERENCES

- Aregawi, W.A., Abera, M.K., Fanta, S.W., Verboven, P., Nicolai, B., 2014. “Prediction of water loss and viscoelastic deformation of apple tissue using a multiscale model.”. *J.Phys. Condens. Matter* 26, 464111. <https://doi.org/10.1088/0953-8984/26/46/464111>.
- J. Asabe and A. Home, “American Society of Agricultural and Biological Engineers”.
- Auriault, J.-L., Boutin, C., Geindreau, C., 2010. Homogenization of coupled phenomena in heterogenous media. John Wiley & Sons.
- Bai, Y., Rahman, M.S., Perera, C.O., Smith, B., Melton, L.D., 2002. “Structural Changes in Apple Rings during Convection Air-Drying with Controlled Temperature and Humidity.”. *J. Agric. Food Chem.* 50(11), 3179-3185. <https://doi.org/10.1021/jf011354s>, 2002/05/01.
- Beigi, M., 2016. “Influence of drying air parameters on mass transfer characteristics of apple slices.”. *Heat Mass tran.* 52(10), 2213-2221. <https://doi.org/10.1007/s00231-015-1735-8>, 2016/10/01.
- Białobrzeski, I., 2006. “Simulation of changes in the density of an apple slab during drying.”. *Int. Commun. in Heat Mass Tran.* 33(7), 880-888. <https://doi.org/10.1016/j.icheatmasstransfer.2006.02.017>, 2006/08/01.
- Carr, E.J., Turner, I.W., 2014. “Two-scale computational modelling of water flow in unsaturated soils containing irregular-shaped inclusions.”. *Int. J. for Numer. Methods Eng.* 98, 157-173. <https://doi.org/10.1002/nme.4625>.
- Carr, E.J., Turner, I.W., Perré, P., 2013. “A dual-scale modeling approach for drying hygroscopic porous media”. *Multiscale Model. Simul.* 11, 362-384. <https://doi.org/10.1137/120873005>.
- Cengel, Y., 2003. Heat, Transfer Mass: A practical approach. Mc-Graw Hill Education, Columbus, GA, USA.
- Cengel, Y.A., & Boles, M.A., 2002. “Thermodynamics: an engineering approach.”. Sea, 1000, 8862.

Cruz, A.C., Guiné, R.P.F., Gonçalves, J.C., 2015. "Drying Kinetics and Product Quality for Convective Drying of Apples (cvs. Golden Delicious and Granny Smith)",. Int. J. Fruit Sci. 15(1), 54-78. <https://doi.org/10.1080/15538362.2014.931166>, 2015/01/02.

Dadmohammadi, Y., Datta, A.K., 2019. "Prediction of effective moisture diffusivity in plant tissue food materials over extended moisture range,". Dry. Technol. 1-15. <https://doi.org/10.1080/07373937.2019.1690500>.

Datta, A.K., 2007. "Porous media approaches to studying simultaneous heat and mass transfer in food processes. II: Property data and representative results,". J. Food Eng. 80(1), 96-110. <https://doi.org/10.1016/j.jfoodeng.2006.05.012>.

Defraeye, T., Radu, A., 2018. "Insights in convective drying of fruit by coupled modeling of fruit drying, deformation, quality evolution and convective exchange with the airflow,". Appl. Therm. Eng. 129, 1026-1038. <https://doi.org/10.1016/j.applthermaleng.2017.10.082>.

Desmorieux, H., Moyne, C., 1992. "Analysis of dryers performance for tropical foodstuffs using the characteristic drying curve concept,". Drying 92, 834-843.

Fanta, S.W., Abera, M.K., Ho, Q.T., Verboven, P., Carmeliet, J., Nicolai, B.M., 2013. "Microscale modeling of water transport in fruit tissue,". J. Food Eng. 118, 229-237. <https://doi.org/10.1016/j.jfoodeng.2013.04.003>.

Feng, H., Tang, J., John Dixon-Warren, S., 2000. "Determination of moisture diffusivity of red delicious apple tissues by thermogravimetric analysis,". Dry. Tech. 18 (6), 1183-1199. <https://doi.org/10.1080/07373930008917771>, 2000/07/01.

Geuzaine, C., Remacle, J.F., 2009. "Gmsh: A 3-D finite element mesh generator with built-in pre-and post-processing facilities,". Int. J. Numer. Methods Eng. 79 (11), 1309-1331. <https://doi.org/10.1002/nme.2579>.

Ghisalberti, L., Kondjoyan, A., 1999. "Convective heat transfer coefficients between air flow and a short cylinder. Effect of air velocity and turbulence. Effect of body shape, dimensions and position in the flow,". J. Food Eng. 42 (1), 33-44. [https://doi.org/10.1016/S0260-8774\(99\)00100-4](https://doi.org/10.1016/S0260-8774(99)00100-4), 1999/10/01/.

- Golestani, R., Raisi, A., Aroujalian, A., 2013. "Mathematical modeling on air drying of apples considering shrinkage and variable diffusion coefficient,". Dry. Technol. 31, 40-51. <https://doi.org/10.1080/07373937.2012.714826>.
- Gulati, T., Datta, A.K., 2015. "Mechanistic understanding of case-hardening and texture development during drying of food materials,". J. Food Eng. 166, 119-138. <https://doi.org/10.1016/j.jfoodeng.2015.05.031>, 2015/12/01.
- Joardder, M.U., Karim, M., 2019. "Development of a porosity prediction model based on shrinkage velocity and glass transition temperature,". Dry. Technol. 37 (15), 1988-2004. <https://doi.org/10.1080/07373937.2018.1555540>.
- Kara, C., Doymaz, İ., 2015. "Effective moisture diffusivity determination and mathematical modelling of drying curves of apple pomace,". Heat Mass Tran. 51 (7), 983-989. <https://doi.org/10.1007/s00231-014-1470-6>.
- Karim, M.A., Hawlader, M., 2005. "Drying characteristics of banana: theoretical modelling and experimental validation,". J. Food Eng. 70 (1), 35-45. <https://doi.org/10.1016/j.jfoodeng.2004.09.010>.
- Karunasena, H.C.P., Gu, Y.T., Brown, R.J., Senadeera, W., 2015. "Numerical Investigation of Case Hardening of Plant Tissue During Drying and Its Influence on the Cellular-Level Shrinkage,". Dry. Technol. 33 (6), 713-734. <https://doi.org/10.1080/07373937.2014.982759>, 2015/04/26.
- Kaya, A., Aydin, O., Demirtas, C., 2007. "Drying kinetics of red delicious apple,". Biosyst. Eng. 96 (4), 517-524. <https://doi.org/10.1016/j.biosystemseng.2006.12.009>.
- Khan, M.I.H., Farrell, T., Nagy, S.A., Karim, M.A., 2018a. "Fundamental Understanding of Cellular Water Transport Process in Bio-Food Material during Drying,". Sci. Rep. 8 (1), 15191. <https://doi.org/10.1038/s41598-018-33159-7>, 2018/10/12.
- Khan, M.I.H., Farrell, Troy, Nagy, S.A., Karim, M.A., 2018b. "Transport of cellular water during drying: An understanding of cell rupturing mechanism in apple tissue,". Food Res. Int. 105, 772-781. <http://doi.org/10.1016/j.foodres.2017.12.010>, 2018/03/01/.

Khan, M.I.H., Kumar, C., Joardder, M.U.H., Karim, M.A., 2017c. "Multiphase porous media modelling: A novel approach of predicting food processing performance,". Crit. Rev. in Food Sci. Nutr. 58, 528-546. <https://doi.org/10.1080/10408398.2016.1197881>.

Khan, M.I.H., Karim, M., 2017. "Cellular water distribution, transport, and its investigation methods for plant-based food material,". Food Res. Int. 99, 1-14. <https://doi.org/10.1016/j.foodres.2017.06.037>.

Khan, M.I.H., Wellard, R.M., Nagy, S.A., Joardder, M.U.H., Karim, M. A., 2016. "Investigation of bound and free water in plant-based food material using NMR T2 relaxometry,". Innovat. Food Sci. & Emerg. Technol. 38, 252-261. <https://doi.org/10.1016/j.ifset.2016.10.015>, 2016/12/01/.

Khan, M.I.H., Kumar, C., Joardder, M. U. H., Karim, M. A., 2017a. "Determination of appropriate effective diffusivity for different food materials,". Dry. Technol. 35, 335-346. <https://doi.org/10.1080/07373937.2016.1170700>.

Khan, M.I.H., Wellard, R.M., Nagy, S.A., Joardder, M., Karim, M., 2017b. "Experimental investigation of bound and free water transport process during drying of hygroscopic food material,". Int. J. Therm. Sci. 117, 266-273. <https://doi.org/10.1016/j.ijthermalsci.2017.04.006>.

Kumar, C., Millar, G.J., Karim, M.A., 2015. "Effective Diffusivity and Evaporative Cooling in Convective Drying of Food Material,". Dry. Technol. 33 (2), 227-237. <https://doi.org/10.1080/07373937.2014.947512>, 2015/01/25

Kumar, C., Joardder, M.U.H., Farrell, T.W., Karim, M.A., 2016. "Multiphase porous media model for intermittent microwave convective drying (IMCD) of food,". Int. J. Therm. Sci. 104, 304-314. <https://doi.org/10.1016/j.ijthermalsci.2016.01.018>.

Lentzou, D., Boudouvis, A.G., Karathanos, V.T., Xanthopoulos, G., 2019. "A moving boundary model for fruit isothermal drying and shrinkage: An optimization method for water diffusivity and peel resistance estimation,". J. Food Eng. 263, 299-310. <https://doi.org/10.1016/j.jfoodeng.2019.07.010>.

Mahiuddin, M., Khan, M.I.H., Kumar, C., Rahman, M.M., Karim, M., 2018. "Shrinkage of food materials during drying: Current status and challenges,".

Compr. Rev. Food Sci. Food Saf. 17 (5), 1113-1126.
<https://doi.org/10.1111/1541-4337.12375>.

Mavroudis, N.E., Gekas, V., Sjöholm, I., 1998. "Osmotic dehydration of apples—effects of agitation and raw material characteristics,". J. Food Eng. 35 (2), 191-209. [https://doi.org/10.1016/S0260-8774\(98\)00015-6](https://doi.org/10.1016/S0260-8774(98)00015-6).

Ni, H., January, 1997. Multiphase moisture transport in porous media under intensive microwave heating. PhD. Cornell University.

Panagiotou, N., Krokida, M., Maroulis, Z., Saravacos, G., 2004. "Moisture diffusivity: literature data compilation for foodstuffs,". Int. J. Food Prop. 7 (2), 273-299. <https://doi.org/10.1081/JFP-120030038>.

Pavliotis, G.A., Stuart, A., 2008. Multiscale methods: averaging and homogenization. Springer Science & Business Media.

Perré, P., 2007. "Multiscale aspects of heat and mass transfer during drying,". Transport in Porous Media 66, 59-76. <https://doi.org/10.1007/s11242-006-9022-2>.

Purlis, E., 2019. "Modelling convective drying of foods: A multiphase porous media model considering heat of sorption,". J. Food Eng. 263, 132-146. <https://doi.org/10.1016/j.jfoodeng.2019.05.028>.

Rahman, M.M., Joardder, M.U., Khan, M.I.H., Pham, N.D., Karim, M., 2018a. "Multiscale model of food drying: Current status and challenges,". Crit. Rev. Food Sci. Nutr. 58 (5), 858-876. <https://doi.org/10.1080/10408398.2016.1227299>.

Rahman, M., Kumar, C., Joardder, M. U., Karim, M., 2018b. "A micro-level transport model for plant-based food materials during drying,". Chem. Eng. Sci. 187, 1-15. <https://doi.org/10.1016/j.ces.2018.04.060>.

Rahman, M.M., Gu, Y., Karim, M., 2018c. "Development of realistic food microstructure considering the structural heterogeneity of cells and intercellular space,". Food Struct. 15, 9-16. <https://doi.org/10.1016/j.foostr.2018.01.002>.

- Ratti, C., Crapiste, G., Rotstein, E., 1989. "A new water sorption equilibrium expression for solid foods based on thermodynamic considerations,". J. Food Sci. 54 (3), 738-742. <https://doi.org/10.1111/j.1365-2621.1989.tb04693.x>.
- Rodrigues, A.E., Mauro, M.A., 2008. "Effective diffusion coefficients behavior in osmotic dehydration of apple slices considering shrinking and local concentration dependence,". J. Food Process. Eng. 31 (2), 207-228. <https://doi.org/10.1111/j.1745-4530.2007.00148.x>.
- Saravacos, G.D., & Maroulis, Z.B., 2001. Transport properties of foods. CRC Press.
- Sibgatullin, T., De Jager, P., Vergeldt, F., Gerkema, E., Anisimov, A., Van As, H., 2007. "Combined analysis of diffusion and relaxation behavior of water in apple parenchyma cells,". Biophysics 52 (2), 196-203. <https://doi.org/10.1134/S0006350907020091>.
- Srikiatden, J., Roberts, J., 2005. "Moisture loss kinetics of apple during convective hot air and isothermal drying,". Int. J. Food Prop. 8 (3), 493-512. <https://doi.org/10.1080/10942910500267737>.
- Tzempelikos, D.A., Mitrakos, D., Vouros, A.P., Bardakas, A.V., Filios, A.E., Margaris, D.P., 2015. "Numerical modeling of heat and mass transfer during convective drying of cylindrical quince slices,". J. Food Eng. 156, 10-21. <https://doi.org/10.1016/j.jfoodeng.2015.01.017>.
- Vega-Gálvez, A., Miranda, M., Bilbao-Sáinz, C., Uribe, E., Lemus-Mondaca, R., 2008. "Empirical modeling of drying process for apple (Cv. Granny Smith) slices at different air temperatures,". J. Food Process. Preserv. 32 (6), 972-986. <https://doi.org/10.1111/j.1745-4549.2008.00227.x>.
- Vega-Mercado, H., Marcela Góngora-Nieto, M., Barbosa-Cánovas, G.V., 2001. "Advances in dehydration of foods,". J. Food Eng. 49 (4), 271-289. [https://doi.org/10.1016/S0260-8774\(00\)00224-7](https://doi.org/10.1016/S0260-8774(00)00224-7), 2001/09/01.
- Wang, W., Chen, G., Mujumdar, A. S., 2007. "Physical interpretation of solids drying: An overview on mathematical modeling research,". Dry. Technol. 25 (4), 659-668. <https://doi.org/10.1080/07373930701285936>.

Welsh, Z., Simpson, M.J., Khan, M.I.H., Karim, M., 2018. "Multiscale Modeling for Food Drying: State of the Art,". Compr. Rev. Food Sci. Food Saf. 17 (5), 1293-1308. <https://doi.org/10.1111/1541-4337.12380>.

Whitaker, S., 1977. Simultaneous heat, mass, and momentum transfer in porous media: a theory of drying. In: Advances in Heat Transfer, vol. 13. Elsevier, pp. 119-203.

Chapter 4: A multiscale temporal investigation for food material during drying

This chapter is under review to **Food Research International**.

Welsh, Z. G., Khan, M. I. H., Simpson, M. J., & Karim, M. A. (2020). A multiscale approach to estimate the cellular diffusivity during food drying. *Food Research International* (Under review).



Statement of Contribution of Co-Authors for Thesis by Published Paper

The following is the suggested format for the required declaration provided at the start of any thesis chapter which includes a co-authored publication.

The authors listed below have certified that:

1. they meet the criteria for authorship and that they have participated in the conception, execution, or interpretation, of at least that part of the publication in their field of expertise;
2. they take public responsibility for their part of the publication, except for the responsible author who accepts overall responsibility for the publication;
3. there are no other authors of the publication according to these criteria;
4. potential conflicts of interest have been disclosed to (a) granting bodies, (b) the editor or publisher of journals or other publications, and (c) the head of the responsible academic unit, and
5. they agree to the use of the publication in the student's thesis and its publication on the [QUT's ePrints site](#) consistent with any limitations set by publisher requirements.

In the case of this chapter:

Welsh, Z. G., Khan, M. I. H., Simpson, M. J., & Karim, M. A. (2020). A multiscale approach to estimate the cellular diffusivity during food drying. *Food Research International* (Under review).

Contributor	Statement of contribution
Zachary G. Welsh	Generation of concept, model concept, model construction and model analysis, manuscript preparation, drafting and critically reviewing the manuscript.
QUT Verified Signature	
Date: 2/12/2020	
M. I. H. Khan	Assisted in drafting, organising and critically revising the manuscript.
M. J. Simpson	Assisted in drafting, and critically revising the manuscript.
M. A. Karim	Supervision, concept refinement, manuscript revision, manuscript editing, author for correspondence and final approval

Principal Supervisor Confirmation

I have sighted email or other correspondence from all Co-authors confirming their certifying authorship.
(If the Co-authors are not able to sign the form please forward their email or other correspondence confirming the certifying authorship to the GRC).

Name

QUT Verified Signature

Signature

Date

4.1 ABSTRACT

Theoretical models for food drying commonly utilize an effective diffusivity solved through curve fitting based on experimental data. This creates models with limited predictive capabilities which are often unable to consider any variations in the material, experimental set up and/or drying conditions. Multiscale modeling is one approach which can help transition to a more physics-based model minimizing the empirical information required while improving the model's predictive capabilities. However, to enable an accurate scaling operation, multiscale models require diffusivity at a fine scale (microscale). Measuring these properties is experimentally costly and time consuming as they are often temperature and/or moisture dependent and therefore dynamically change due to simultaneous heat transport, mass transport and deformation during food drying. This research conducts an inverse analysis on a multiscale homogenization food drying model to deduce the temporal diffusivity of intracellular water. The real cellular morphology was considered and appropriate assumptions to represent its cellular heterogeneity, in relation to time, were investigated. The work uncovered that a linear decrease in intracellular water content could be assumed and thus a function for its diffusivity was developed. The proposed function is in terms of sample temperature and intracellular water content opening the possibilities to be applied to various food materials.

4.2 INTRODUCTION

Plant-based food materials are structurally heterogeneous with moisture distributed throughout the material's various cellular environments (Rahman et al., 2018; Rahman et al., 2018). The largest proportion of water (around 80%) is located within intracellular spaces (inside cell vacuole), known as intracellular water (ICW) (Khan et al., 2016). During convective drying, the transportation of ICW causes dynamic modifications to the materials physical structure and nutritional characteristics affecting the products quality (Khan et al., 2018; Pham et al., 2020). Generally, when modeling moisture migration for food drying, all mass transport mechanisms are lumped and Fickian diffusion is assumed. The effective diffusivity is then solved through curve fitting techniques and the Arrhenius framework. The resulting models have limited predictive capabilities and are often unable to consider any variations in material, experimental set up and/or drying conditions

(Dadmoammadi & Datta, 2019). These condition-dependent properties generate a dramatic demand in physical and mechanical characterization of each product being dried (Perré, 2007). Additionally, within published literature, experimental moisture diffusivity data is sparse and often unreliable as they vary by 3-5 orders of magnitude for the same material (Dadmoammadi & Datta, 2019; Saravacos & Maroulis, 2001). Moving towards a more physics-based model will aid in improving its predictive capabilities while minimizing the empirical information required.

Multiscale modeling is an approach which can help transition towards a more mechanistic model by considering the dynamic water heterogeneity within the material (Welsh et al., 2021). Multiscale modeling is a series of sub-models which investigate a products behavior over multiple spatial scales, modeling a more realistic description of the underlying physics (Rahman et al., 2018). Recently, researchers have shown their immense interest in multiscale food drying modeling and provided some general background into the topic (Ho et al., 2013; Rahman et al., 2018; Welsh et al., 2018). However, to complete the scaling operation multiscale models require diffusivity at a fine scale (microscale) which has not been thoroughly investigated for food materials during drying. Most studies in the literature investigated bulk level moisture and/or temperature dependent diffusivities (Joardder et al., 2014; Khan et al., 2017; Kumar et al., 2015).

Cellular diffusivity properties can be either experimentally investigated or approximated utilizing an inverse problem (optimization). Sibgatullin et al. (2007) investigated the diffusion and relaxation behavior of water in fresh apple parenchyma cells using Nuclear Magnetic resonance (NMR) spectroscopy. Their approach distinguished two components, a slow relaxing component (assigned to the vacuole) for the restrictive diffusion and a fast component (other cell components) for the unrestricted diffusion component. However, this investigation was conducted for fresh apple tissue not food material during drying. Food drying models require temperature and/or moisture dependent properties to describe the complex simultaneous heat and mass transport which occurs. Additionally, investigating these properties experimentally can become time consuming and costly (Kumar et al., 2018). The alternative approach is to conduct an inverse analysis. If the phase morphology is correctly represented at a cell level, a complete scaling approach can be performed. However, instead of using the approach to predict macroscopic properties, an inverse

analysis can be conducted allowing the local (microscale) properties to be deduced from the macroscopic measurements (Perré et al., 2016). This approach has already been applied to the application of timber drying. Perré et al. (2016) presented a comprehensive strategy to predict different wood properties from anatomical images, particularly focusing on several meshless methods. A key step within the strategy was the representation of the structure which accounted for the local anisotropy and heterogeneity of the cell walls for the material. Inverse problems have also been utilized on macroscale theoretical models. Weres and Olek (2005) developed a finite element analysis strategy for inverse problems. The proposed algorithm was investigated and validated for two types of timber to identify the thermal conductivity, convective heat transfer coefficient, diffusion coefficient, equilibrium moisture content and convective mass transfer coefficient. Lentzou et al. (2019) used an inverse problem in a food drying model. The investigation estimated the effective macroscale diffusivity and mass transfer coefficient in a moving boundary model for fruit isothermal drying and shrinkage. However, an inverse study has not been applied in the context of multiscale food drying modeling to uncover the temporal cellular properties.

In this work, we conduct an inverse analysis to deduce the diffusivity of intracellular water while investigating the temporal heterogeneity of apple tissue during drying. The approach will apply multiscale modeling, specifically homogenization, for convective drying at 60°C. A temporal heterogeneity investigation will be performed to compare the real cellular water morphology and suitable assumptions which can represent the actual material. Finally, the most robust approach uncovered within the heterogeneity investigation will be utilized to construct the property for ICW diffusivity.

4.3 MODEL DEVELOPMENT

4.3.1 Drying model

The model utilized two spatial scales, a microscale and a macroscale, Figure 4.1. The macroscale transport model used an axisymmetric coordinate system and assumed the following: (1) internal convective flow and heat generation can be neglected, (2) drying air properties are constant, (3) axisymmetric heating occurs, (4)

moisture is only evaporated from the surface and (5) thermal equilibrium exists between all phases.

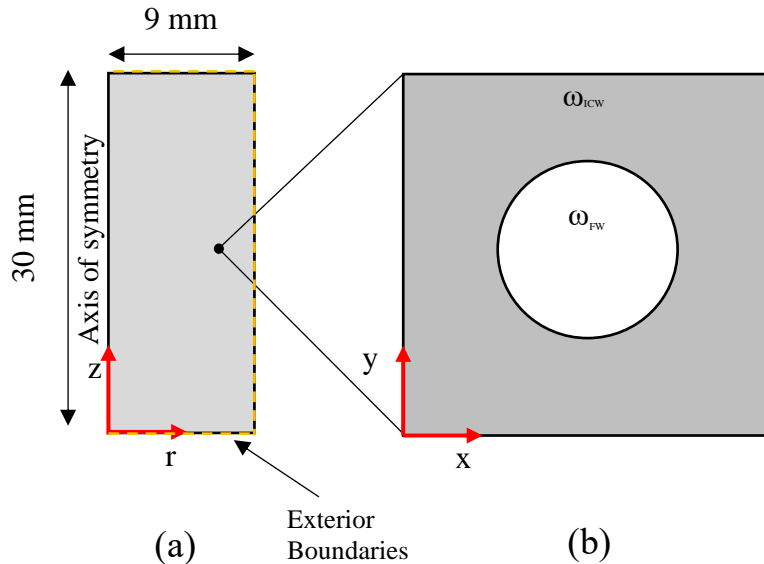


Figure 4.1. Domains (a) axisymmetric macroscale domain and (b) microscale domain.

4.3.2 Cellular structure representation within the microscale domain

The cellular structure of apple consists of a few key components: protoplast (composed of vacuole, tonoplast membrane and cytoplasm), the cell membrane, cell wall and intercellular space (Prawiranto et al., 2018). These components deform and change during drying due to the various transport mechanisms which occur separately but coexist (Lentzou et al., 2019). Additionally, drying at different temperatures can cause different cellular deformations (Khan et al., 2018; Mahiuddin et al., 2018). These mechanisms and modifications to the microstructure dictate how to represent the temporal heterogeneity of water and add complexities to accurately representing the structure. With this in mind, the microscale domain considered two subdomains, ICW denoted as ω_{ICW} and intercellular water [free water (FW)] denote as ω_{FW} (Khan & Karim, 2017), demonstrated in Figure 4.1. This groups the effects of the protoplast, cell membrane and cell wall within the ICW domain. Homogenization does not preserve to the location of intercellular spaces, therefore they were grouped and represented as a circle, Figure 4.1 (b) (Welsh et al., 2021). This circle was assumed to be located at the center of the microscale domain, requiring minimal microstructural

knowledge but forcing the homogenized diffusivity to be isotropic. The key factor to represent the spatial heterogeneity is the ratio between subdomains. The migration of ICW is the major part of the transport process during drying and its temporal representation is thoroughly investigated within the temporal heterogeneity investigation

4.3.3 Macroscale mass conservation

The macroscale mass transport equation solves for the instantaneous moisture concentration C (mol/m³), given by (Golestani et al., 2013),

$$\frac{\partial C}{\partial t} + \frac{1}{r} \frac{\partial}{\partial r} \left[-D_{eff} r \frac{\partial C}{\partial r} \right] + \frac{\partial}{\partial z} \left[-D_{eff} \frac{\partial C}{\partial z} \right] = 0 , \quad (4.1)$$

where t is the time (s) and D_{eff} is the effective moisture diffusivity (m²/s).

4.3.4 Microscale mass conservation

To represent the heterogeneous structure of the food material, a microscale was introduced at each point in the macroscale, Figure 4.1 (b). This assumption is valid when the scale parameter (ratio between the macroscale and microscale domain lengths) trends to zero, implying the homogeneities vanish, leading to a homogeneous material (Pavliotis & Stuart, 2008). This assumption is typically known as the separation of scales (Auriault et al., 2010; Carr & Turner, 2014) and is routine when deriving a model via homogenization. The coupled microscale mass transport equation expressed as,

$$\frac{\partial c}{\partial t} + \frac{\partial}{\partial x} \left(-D \frac{\partial c}{\partial x} \right) + \frac{\partial}{\partial y} \left(-D \frac{\partial c}{\partial y} \right) = 0 , \quad (4.2)$$

where c is the microscale concentration (mol/m³) and D is the cellular diffusivity (m²/s) equaling D_{ICW} if $x, y \in \omega_{ICW}$ and D_{FW} if $x, y \in \omega_{FW}$.

4.3.5 Macroscale energy balance

The macroscale energy balance solves for the instantaneous temperature T (K) based on Fourier's law of heat transfer, given by (Golestani et al., 2013),

$$\rho c_p \frac{\partial T}{\partial t} + \frac{1}{r} \frac{\partial}{\partial r} \left[-k r \frac{\partial T}{\partial r} \right] + \frac{\partial}{\partial z} \left[-k \frac{\partial T}{\partial z} \right] = 0, \quad (4.3)$$

where ρ is the density of apple tissue (kg/m^3), c_p is the specific heat of apple tissue ($\text{J}/(\text{kg}\cdot\text{K})$) and k is the thermal conductivity of apple tissue ($\text{W}/(\text{m}\cdot\text{K})$).

4.3.6 Boundary conditions

The mass flux at the exterior boundaries is given by,

$$\mathbf{n} \cdot \left[-D_{eff} \nabla C \right] = h_m \frac{(p_{v eq} - p_{v air})}{RT}, \quad (4.4)$$

where h_m is the mass transfer coefficient (m/s), $p_{v eq}$ is the equilibrium vapor pressure, $p_{v air}$ is the vapor air pressure of ambient air (Pa), \mathbf{n} is the unit vector normal to the boundary and R is the universal gas constant ($\text{J}/(\text{mol}\cdot\text{K})$). The sorption isotherm of apple tissue was used to derive the equilibrium vapor pressure, $p_{v eq}$ (Pa), given as (Ratti et al., 1989),

$$p_{v eq} = p_{v sat}(T) \exp(-0.182M_{db}^{-0.696} + 0.232e^{-43.949M_{db}} M_{db}^{0.0411} \ln[p_{v sat}(T)]) , \quad (4.5)$$

where $p_{v sat}$ is the saturated vapor pressure of water (Pa) and M_{db} is the moisture content (kg/kg dry basis). The saturated vapor pressure is (Vega-Mercado et al., 2001)

$$p_{v sat} = \exp \left[\frac{-5800.2206}{T} + 1.3915 - 0.0486T + \frac{0.4176 \times 10^{-4}T^2 - 0.1445 \times 10^{-7}T^3 + 6.546 \ln(T)}{T} \right]. \quad (4.6)$$

The heat transfer boundary condition on the exterior boundaries considered both convective heat transfer and heat lost due to evaporation at the surface, defined as,

$$\mathbf{n} \cdot \left[-k \nabla T \right] = h_T(T - T_{air}) - h_m \frac{(p_{v eq} - p_{v air})}{RT} \lambda M_w, \quad (4.7)$$

where h_T being the heat transfer coefficient ($\text{W}/(\text{m}^2\cdot\text{K})$), T_{air} is the drying air temperature (K), M_w molar mass of water (g/mol) and λ is the latent heat of evaporation (J/kg). The last boundary condition is the symmetric condition, defined as

$$\mathbf{n} \cdot \left[-D_{eff} \nabla C \right] = 0, \quad (4.8)$$

$$\mathbf{n} \cdot [-k \nabla T] = 0. \quad (4.9)$$

4.3.7 Homogenized effective diffusivity

The 2D homogenized effective diffusivity can be denoted as a tensor,

$$D_{\text{eff}} = \begin{bmatrix} \frac{1}{\omega} \int_{\omega} D(x, y) \left(\frac{\partial u_1}{\partial x} + 1 \right) d\omega & \frac{1}{\omega} \int_{\omega} D(x, y) \frac{\partial u_2}{\partial x} d\omega \\ \frac{1}{\omega} \int_{\omega} D(x, y) \frac{\partial u_1}{\partial y} d\omega & \frac{1}{\omega} \int_{\omega} D(x, y) \left(\frac{\partial u_2}{\partial y} + 1 \right) d\omega \end{bmatrix}, \quad (4.10)$$

and ω is the area of the macroscale domain, u_1 and u_2 are the corrective factors and the solution of the periodic cell problem:

$$\nabla \cdot (D \nabla (u_j + \mathbf{e}_j)) = 0, \quad j = 1, 2, \quad (4.11)$$

where,

$$\mathbf{e}_1 = \begin{bmatrix} 1 \\ 0 \end{bmatrix}, \quad \mathbf{e}_2 = \begin{bmatrix} 0 \\ 1 \end{bmatrix}, \quad (4.12)$$

$$u_j \text{ is } \omega\text{-periodic}, \quad (4.13)$$

$$\frac{1}{\omega} \int_A u_j d\omega = 0. \quad (4.14)$$

The solution u_j is unique only up to an additive constant, Equation (4.11) (Auriault et al., 2010). Therefore, requiring a zero mean constraint to achieve a single unique solution, Equation (4.14). However, the effective homogenized diffusion only requires the gradient of u_j , therefore any of these unique solutions are suitable (Carr & Turner, 2014).

4.3.8 Other input parameters

The input parameters used in the model are presented in Table 4.1.

Table 4.1. Input parameters

Parameter	Value (unit)	Reference
Density of apple, ρ	837 (kg/m ³)	Mavroudis, Gekas, and Sjöholm (1998)

Density of water, ρ_w	995 (kg/m ³)	Y. Cengel (2003)
Specific heat of apple, c_p	1000(1.4+3.22 M_{wb}) (J/(kg·K))	(Białobrzewski, 2006)
Thermal conductivity of apple, k	0.0148+0.0493 M_{wb} (W/(m·K))	(Białobrzewski, 2006)
Initial moisture content, M_0	6.4 (kg/kg dry bases)	This study
Initial sample temperature, T_0	296 (K)	This study
Equilibrium moisture content, M_e	0.2 (kg/kg dry bases)	Białobrzewski (2006)
Initial wet basis moisture content, $M_{0_{wb}}$	0.86 (kg/kg wet bases)	This study
Latent heat of evaporation, λ	2358600 (J/kg)	Y. Cengel (2003)
Universal gas constant, R	8.314 (J/(mol·K))	Y. A. Cengel and Boles (2002)
Molar mass of water, M_w	0.018016 (kg/mol)	Y. A. Cengel and Boles (2002)
Partial vapor pressure, $p_{v air}$	2000 (Pa)	This study
Heat transfer coefficient, h_T	19.98 (W/(m ² ·K))	This study
Mass transfer coefficient, h_m	0.018 (m/s)	This study
Diffusivity of FW, D_{FW}	$2.26 \times 10^{-5} \left[\frac{T}{273.15} \right]^{1.81}$ (m ² /s)	Pace (1962)

4.4 INVERSE PROBLEM

For the inverse problem, the effective diffusivity (D_{eff}) is unknown and therefore predicted through solving Fick's law of diffusion utilizing the experimental moisture curve over the entire drying period. To implement this, a Levenberg-Marquardt optimization algorithm coupled with the finite element method was applied. The optimization investigation was based on the minimization of the distance between the simulated and experimental moisture (OF) drying curves for D_{eff} with the objective function denoted as:

$$OF(D_{eff}) = \int \left[\overline{M}_{db,exp}(t) - \overline{M}_{db,num}(t, D_{i,eff}) \right]^2 dt, \quad (4.15)$$

where $\overline{M}_{db,exp}$ is the average experimental moisture content (dry bases) and $\overline{M}_{db,num}$ is the average predicted moisture content (dry bases) from the model. The Levenberg-Marquardt algorithm was used for its higher convergence rate in least-square-type problems (Lentzou et al., 2019). Two optimal scenarios were considered for the effective diffusivity, optimal scenario 1 achieving an Arrhenius relationship ($D_{1,eff}$) and optimal scenario 2 an average ($D_{2,eff}$), defined as

$$D_{1,eff} = D_0 e^{-\frac{E_a}{RT}}, \quad (4.16)$$

$$D_{2,eff} = \overline{D_{eff}}, \quad (4.17)$$

where D_o is an integration constant (m^2/s), E_a is the activation energy (J/mol) and $\overline{D_{eff}}$ is the average diffusivity (m^2/s). Once $D_{1,eff}$ and $D_{2,eff}$ were solved, the temporal heterogeneity investigation was employed to investigate suitable approaches to consider the dynamic heterogeneity of the material.

4.5 TEMPORAL HETEROGENEITY INVESTIGATION

The temporal heterogeneity investigation considered four approaches: approach 1: the actual cellular phase morphology, approach 2: the average phase morphology, approach 3: ICW content linearly decreases and approach 4: diffusivity by stages. All approaches and their associated phase morphologies are summarized in Figure 4.2.

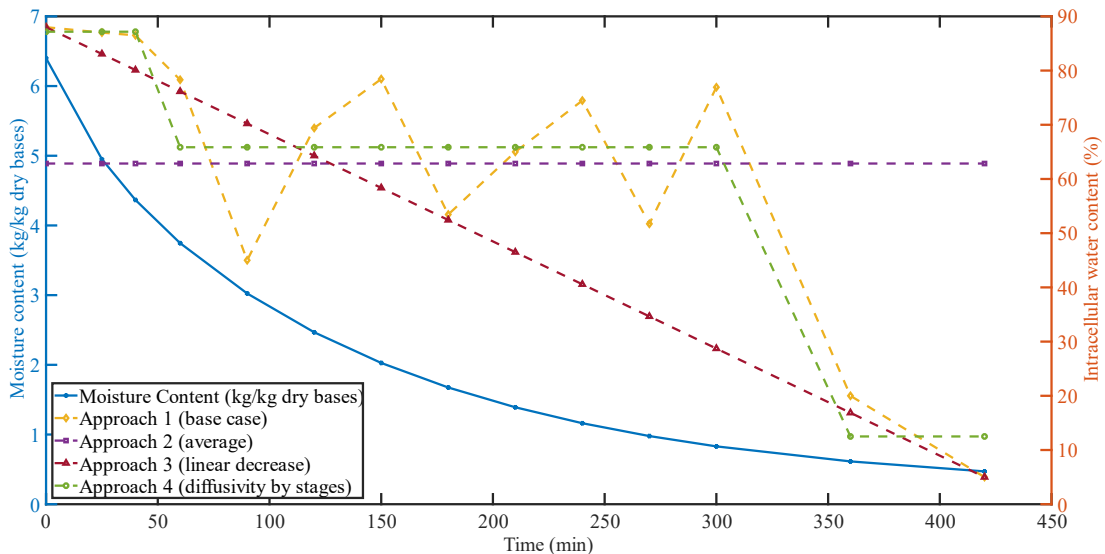


Figure 4.2. Water heterogeneity breakdown of ICW content and moisture content (kg/kg dry bases) with time.

Approach 1 considered the actual phase morphology based on the experimental results of Khan et al. (2018). This approach is the base case for the investigation. Khan et al. (2018) used NMR to investigate the cellular transport phenomena of apple tissue during convective drying at 60°C. Their results revealed that ICW migrates from intracellular spaces to intercellular spaces by cell walls progressively rupturing while drying at higher temperatures. Within Figure 4.2, the total amount of water (ICW + FW) is considered 100% at each point of the drying process. Looking closely at approach 1 in Figure 4.2 (base case), there are many fluctuations in the proportions of ICW and FW throughout the drying period. According to the arguments of Khan et al. (2018), these fluctuations are mainly caused by cells collapsing at different stages of drying. The peaks in the ICW content curve indicate the points where the cell membranes collapse. When cells collapse, water rushes out of the cells, moving from the intracellular spaces to intercellular spaces and thus becomes FW. Therefore, when cells collapse, the proportion of ICW drops rapidly and the proportion of FW increases accordingly. Approach 2-4 utilize various assumptions to approximate the dynamic heterogeneity of ICW. Approach 2 considers the average phase morphology with respect to time. This creates a single microscale domain and a constant diffusivity coefficient for the entire drying period. Considering constant diffusivity is very common in literature (Rahman et al., 2018) and therefore it was included within the

investigation as a comparison. Approach 3 assumes the dynamic heterogeneity can be approximated by the ICW content linearly decreasing as drying occurs. This is a basic assumption and aligns with previously published finding (Halder et al., 2011). Approach 4 introduces a new concept and considers diffusivity in three stages; stage 1: cells intact, stage 2: cell rupturing occurs and stage 3: ultimate cell rupturing. This approach assumes cell rupturing during stage 2 significantly influences the results and is a key interest of the model. Each stage is defined by the magnitude and fluctuations of ICW in the base case. Stage 1, when the cells are intact, occurs first and is when the ICW content experiences minimal deviation from its initial percentage. Stage 2, when cell rupturing occurs, exists in the middle stages of drying when the majority of fluctuations in ICW occur. Stage 3, ultimate cell rupturing, occurs in the latter stages of drying when the percentage of ICW drops off significantly. The stages are represented in Figure 4.2. Each approach will be investigated and evaluated on their ability to represent the base case, relative experimental cost and applicability to represent ICW diffusivity (D_{ICW}) as a function.

4.6 RELATIONSHIP DEVELOPMENT FOR THE DIFFUSIVITY OF INTRACELLULAR WATER

The relationship development for diffusivity of ICW (D_{ICW}) was conducted on the best approach uncovered within the temporal heterogeneity investigation. It was considered in terms of two variables, sample temperature (T_s) and ICW content (WC_{ICW}). Multiple regression with a logarithmic transformation was utilized and solved in MATLAB. After a brief investigation to determine the nature of the data, the initial function for D_{ICW} was assumed as,

$$D_{ICW} = \exp(\beta_0 + \beta_1 T_s + \beta_2 WC_{ICW} + \beta_3 T_s^2 + \beta_4 WC_{ICW}^2). \quad (4.18)$$

4.7 COMPUTATIONAL METHODOLOGY

Step by step procedure of developing and solving the equations is presented in Figure 4.3. The optimization and macroscale heat and mass transport model were solved in COMSOL Multiphysics 5.3a. Whereas, the homogenization and property development was solved using MATLAB 2018a coupled with Gmsh (Geuzaine &

Remacle, 2009) to construct the microscale domains. Once $D_{1,eff}$ and $D_{2,eff}$ were solved through the optimization procedure, the temporal heterogeneity investigation could be applied and the relationship for D_{ICW} could be developed.

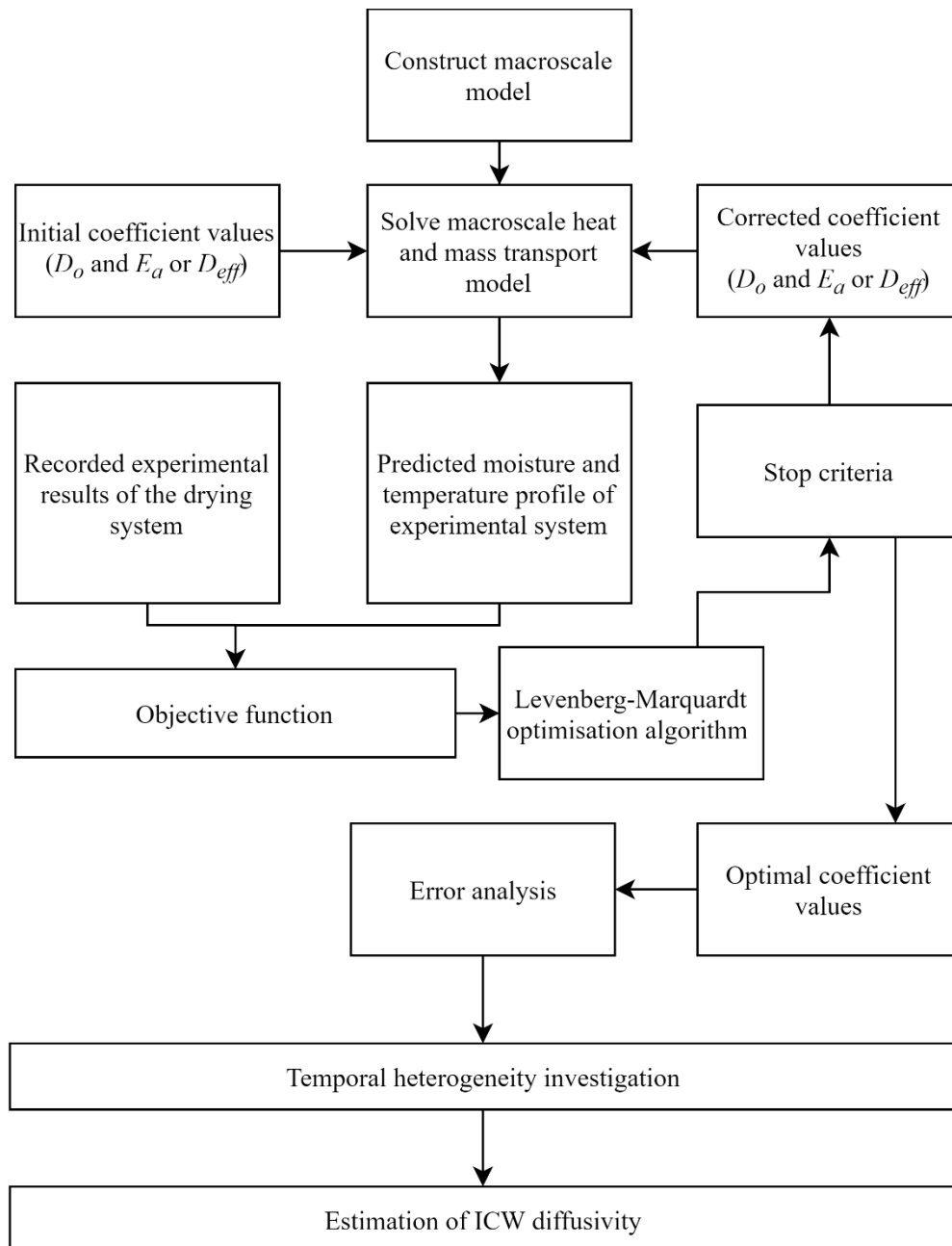


Figure 4.3. Computational Methodology

4.8 RESULTS

The results consist of three main parts: an inverse analysis of the food drying model, the temporal heterogeneity investigation and the estimation of ICW diffusivity.

The predicted results were compared to experimental data to validate the model (Khan et al., 2018). This study investigates convective drying at 60°C. All averages shown within the results were calculated using Equation C.1 within Appendix C.

4.8.1 Inverse analysis on the macroscale effective diffusivity

The results of the optimization investigation are presented in Figure 4.4 and Figure 4.5. The investigation considered two optimal scenarios: assuming an Arrhenius relationship is ideal [optimal scenario 1, Equation (4.16)] and assuming an average effective diffusivity ($\overline{D_{eff}}$) is sufficient [optimal scenario 2, Equation (4.17)]. Optimal scenario 1 assumes temperature is the dominant influencer on diffusivity. This resulted in a D_o of 8.77×10^{-7} m²/s and E_a of 20.871 kJ/mol. The results show that this approach predicted moisture transport accurately with a low mean relative error (MRE) of 5.96% (Figure 4.4). The average temperature profile also described the experimental data well with a MRE of 1.97%. The value for the integration constant (E_a) agrees with the existing literature falling within the expected range of 12.7-110 kJ/mol for various food and agricultural material (Zogzas et al., 1996). In particular, E_a for apple has been reported at 24.51 kJ/mol for drying at 40-60°C (Wang et al., 2007) and 29.65 kJ/mol for drying at 50-80°C (Kara & Doymaz, 2015).

The alternative approach (optimal scenario 2) found an optimal average effective diffusivity (D_{eff}) of 3.30×10^{-10} m²/s with MREs of 5% and 1.77% for the average moisture and temperature profiles respectively. This effective diffusivity was within the expected diffusivity range of 10^{-9} - 10^{-11} m²/s for most food material (Panagiotou et al., 2004; Saravacos & Maroulis, 2001). Additionally, the calculated effective diffusivities were less than the self-diffusion of water at 60 °C (4.748×10^{-9} m²/s) as expected (Lentzou et al., 2019). D_{eff} can also be compared to 0.713×10^{-11} - 7.66×10^{-10} m²/s for Red Delicious apples at a temperature range of 35-55°C (Beigi, 2016).

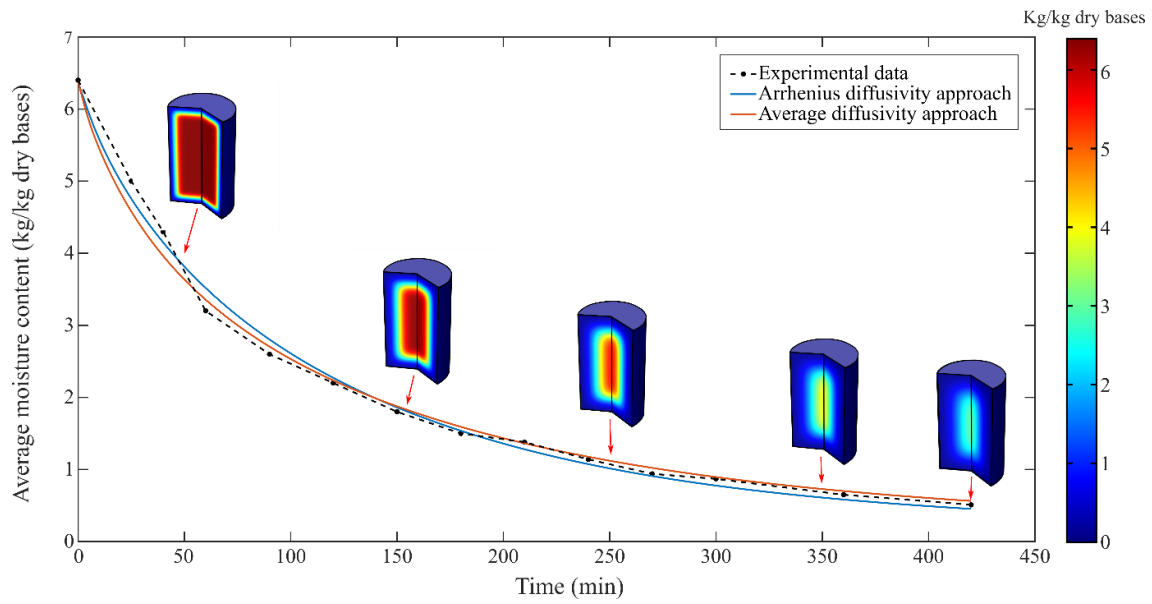


Figure 4.4. Average moisture content (kg/kg dry bases) for drying at 60 °C.

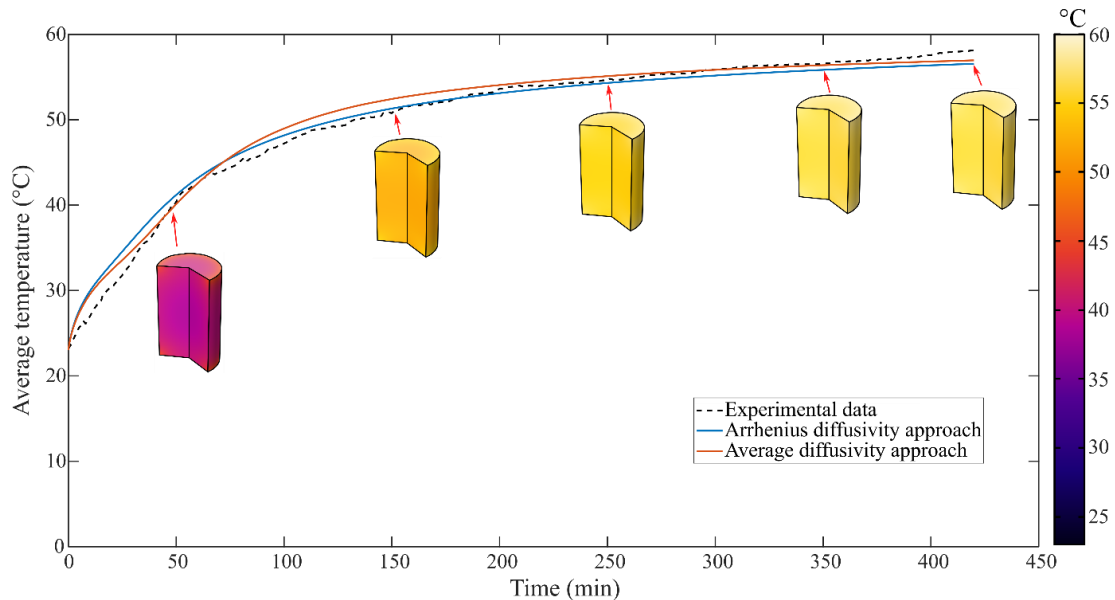


Figure 4.5. Average temperature (°C) for drying at 60 °C.

4.8.2 Temporal heterogeneity investigation

Investigating the temporal heterogeneity utilizing an inverse study can be complex. Due to the nature of the approach, the diffusivity of ICW is inversely calculated. This means all approaches essentially achieve the same macroscale diffusivity result. This can make it hard to evaluate the performance of each approach. However, each approach creates unique relationships for the diffusivity of ICW, and

not all these relationships can be easily described by functions for future models. The end goal of applying multiscale modeling is to move towards a more mechanistic modeling approach. This cannot be achieved without suitable property relationships at a microscale. Therefore, each approach is evaluated on their ability to represent the real cellular phase morphology (base case), relative experimental cost and applicability to represent ICW diffusivity (D_{ICW}) as a function.

The results of the temporal heterogeneity investigation can be seen within Figure 4.6 to Figure 4.9. Approach 1 considered previously published experimental results to create a base case of achieving an optimal Arrhenius relationship. The approach assumed optimal scenario 1 was ideal and the results can be seen in Figure 4.6. Within the experimental data, the FW content fluctuates, and when considering two subdomains at a microscale this trend is reflected in the diffusivity of ICW. The diffusivity initially increases, however, once cell rupturing occurs, the diffusivity oscillates. Towards the end, ultimate cell rupturing occurs causing the diffusivity of ICW to drastically drop to achieve the optimal Arrhenius trend. It should be noted, it is likely there is a few mechanisms occurring at the latter stage of drying contributing to the low diffusivity of the ICW subdomain. The ICW subdomain encompasses the protoplast, cell membrane and cell wall which are known to deform/change due to the drying process. Joardder et al. (2015) demonstrated that the cell wall thickness halved during convective drying of Granny Smith apples. Prawiranto et al. (2018) modeled the dehydration of cellular food tissue (at an air temperature of 25 °C). The work theorized and demonstrated that the dried material forms an additional barrier restricting the moisture within the sample in the later stages of dehydration. The presence of cell rupturing likely causes the additional restricting barrier to have a smaller effect on the diffusivity in the later stages of drying. However, it could still be contributing to the drastic drop off.

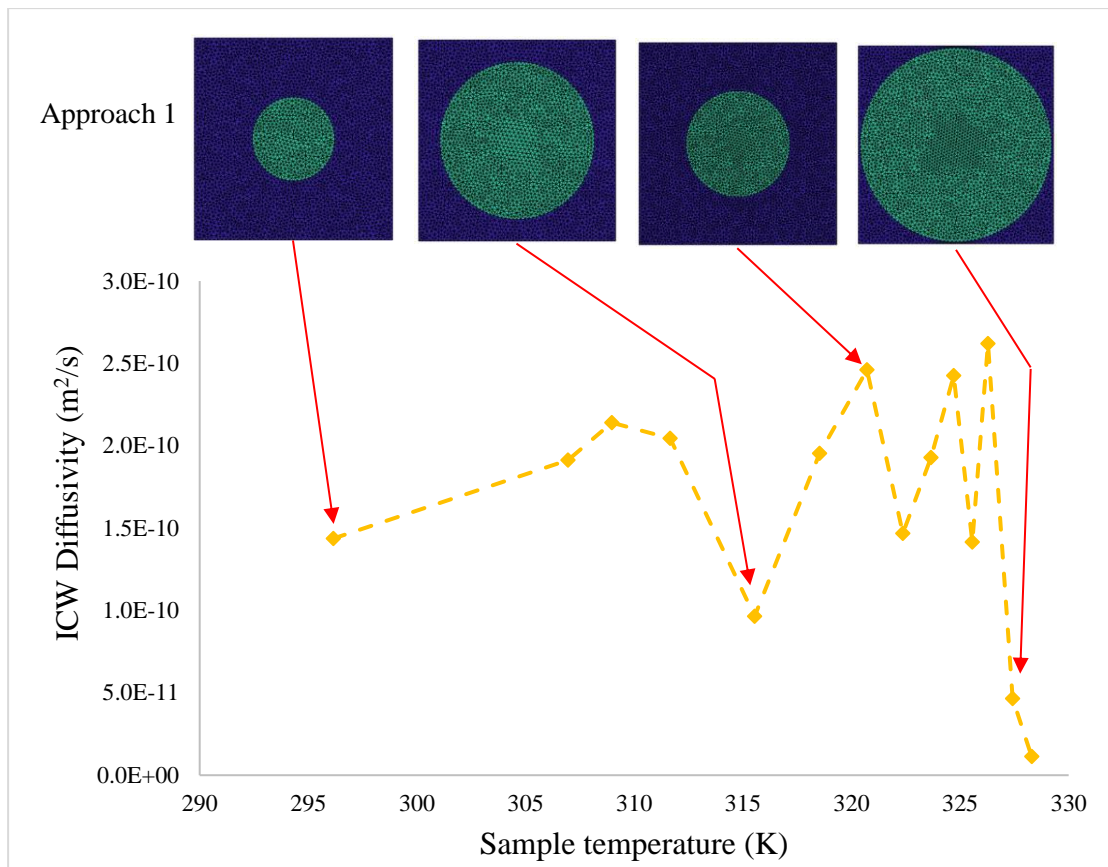


Figure 4.6. Diffusivity (m^2/s) of intracellular water for approach 1 (base case). The temporal evolution of the microscale domain can be seen along the top of the figure, purple denotes ICW and green denotes FW

Approach 2 considered the average ICW content from the base case to construct the microscale domain. The approach considered optimal scenario 2 and the results can be seen in Figure 4.7. Approach 2 resulted in a single microscale domain and a single D_{ICW} for the duration of drying. Considering the average diffusivity rather than the temperature dependent approach (Arrhenius relationship) resulted in slightly lower MREs, however the approach required comprehensive knowledge of the microstructural evolution of the sample (comprehensive experimental data). Specifically, approach 2 considers the average ICW content over the entire drying period to construct its microscale domain. Recording the ratio of cellular water content is not trivial and requires an NMR or similar approach (Khan et al., 2016). Approach 2 resulted in an average ICW diffusivity of $1.5 \times 10^{-10} \text{ m}^2/\text{s}$. Most literature on the diffusivity of food material during drying has only investigated the tissue level (macroscale) (Welsh et al., 2018). This adds complexity to comparing the average

ICW diffusivity uncovered. Research has been published on the ICW diffusivity of fresh Granny Smith apples (high moisture content) with a value of $3.8 \times 10^{-10} \text{ m}^2/\text{s}$ (Sibgatullin et al., 2007). Convective drying significantly effects the material's diffusion process due to the continuous moisture loss and cell ruptures. Additionally, it is known that the effective water diffusivity decreases with the decrease in the moisture content in the sample (Dadmoammadi & Datta, 2019). This trend is demonstrated in macroscale multiphase models in association with the capillary diffusivity decreasing with the decreasing moisture content (Datta, 2007; Kumar et al., 2016). The average diffusivity found in this study aligns with the expected trend.

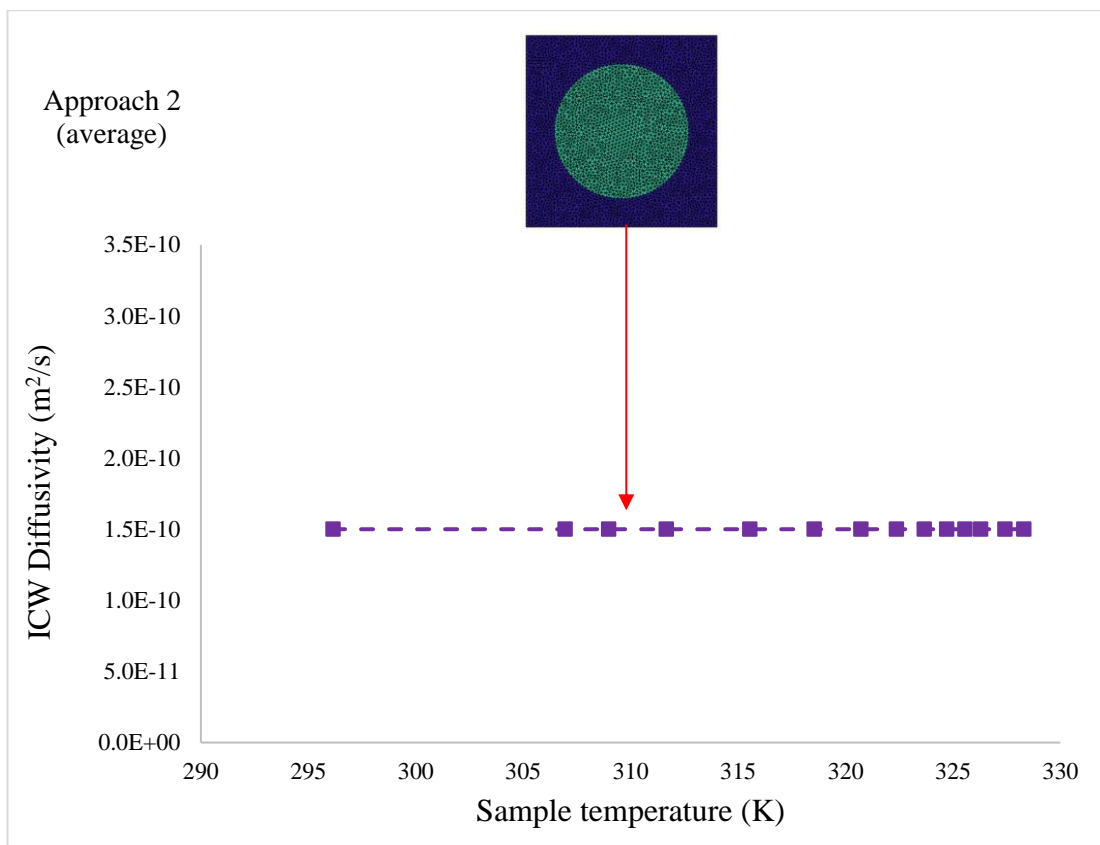


Figure 4.7. Diffusivity (m^2/s) of intracellular water for approach 2 (average). The temporal evolution of the microscale domain can be seen along the top of the figure, purple denotes ICW and green denotes FW.

Approach 3 assumes that the fluctuating experimental results can be approximated through assuming a linear decrease in the ICW content at the microscale. Approach 3 utilizes the temperature dependent (Arrhenius relationship) macroscale

diffusivity. Assuming a linear decrease in ICW content (representing cellular deformation/ rupturing) is consistent with Halder et al. (2011). The results for this approach can be seen in Figure 4.8. The diffusivity initially increases similar to base case. This is due to the nature of the macroscale Arrhenius temperature dependent diffusivity. In the early stages of drying, the effective macroscale diffusivity significantly increases, whereas the ICW content only slightly decreases and the diffusivity of FW remains fairly constant. Therefore, the increase in reflected in the ICW diffusivity. After the initial increase, the ICW diffusivity progressively decreases to achieve the effective macroscale diffusivity Arrhenius relationship. The approach resulted in an ICW diffusivity range of 1.81×10^{-10} to $1.12 \times 10^{-11} \text{ m}^2/\text{s}$.

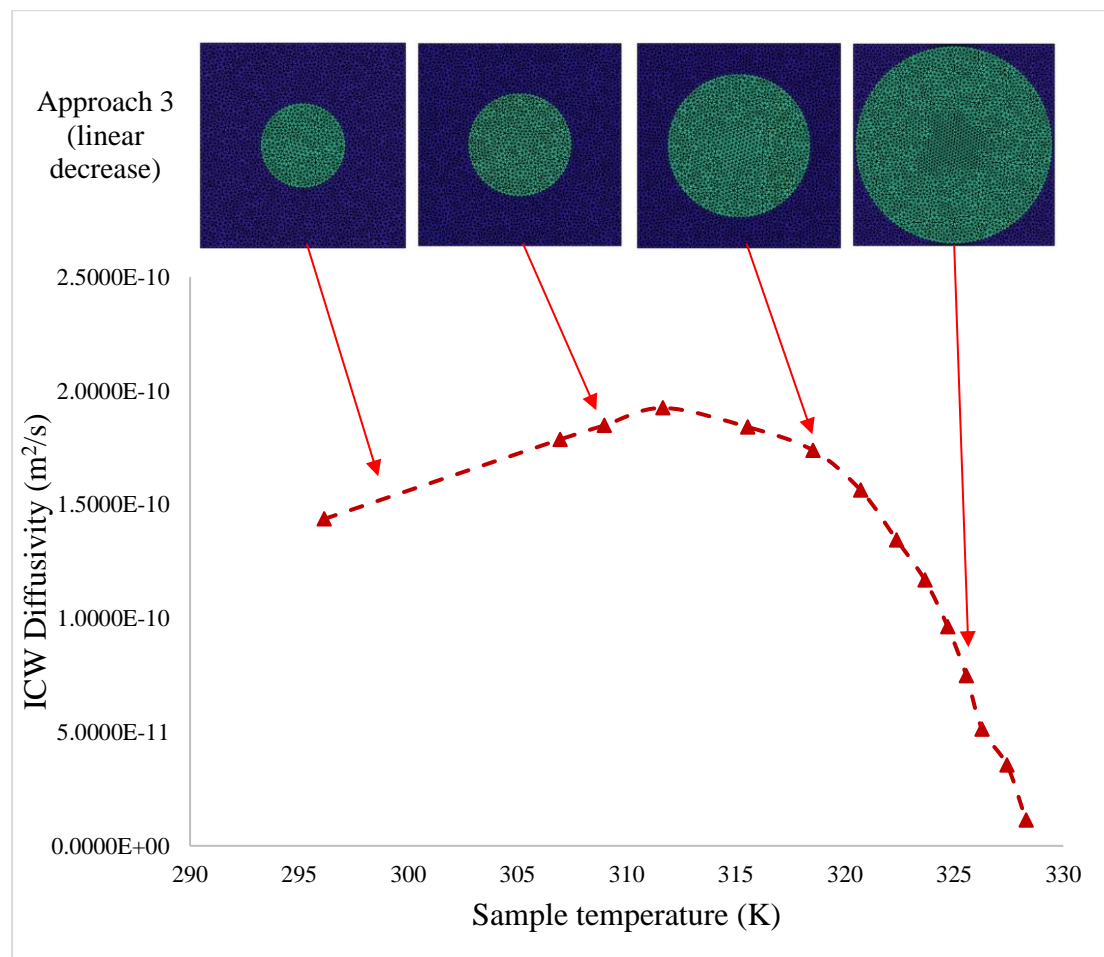


Figure 4.8. Diffusivity (m^2/s) of intracellular water for approach 3 (linear decrease). The temporal evolution of the microscale domain can be seen along the top of the figure, purple denotes ICW and green denotes FW.

Approach 4 considers diffusivity in individual stages and utilizes the temperature dependent (Arrhenius relationship) macroscale diffusivity. The stages are defined on the cellular deformation which occurs throughout the drying process. For convective drying at 60 °C, three stages were considered: stage 1 cell membrane are intact, stage 2 progressive cell rupturing occurs and stage 3 ultimate cell rupturing. This approach results in separate diffusivities and microscale domains for each stage, Figure 4.9. The microscale domains were constructed through utilizing the same experimental data as the base approach to create averages for each stage.

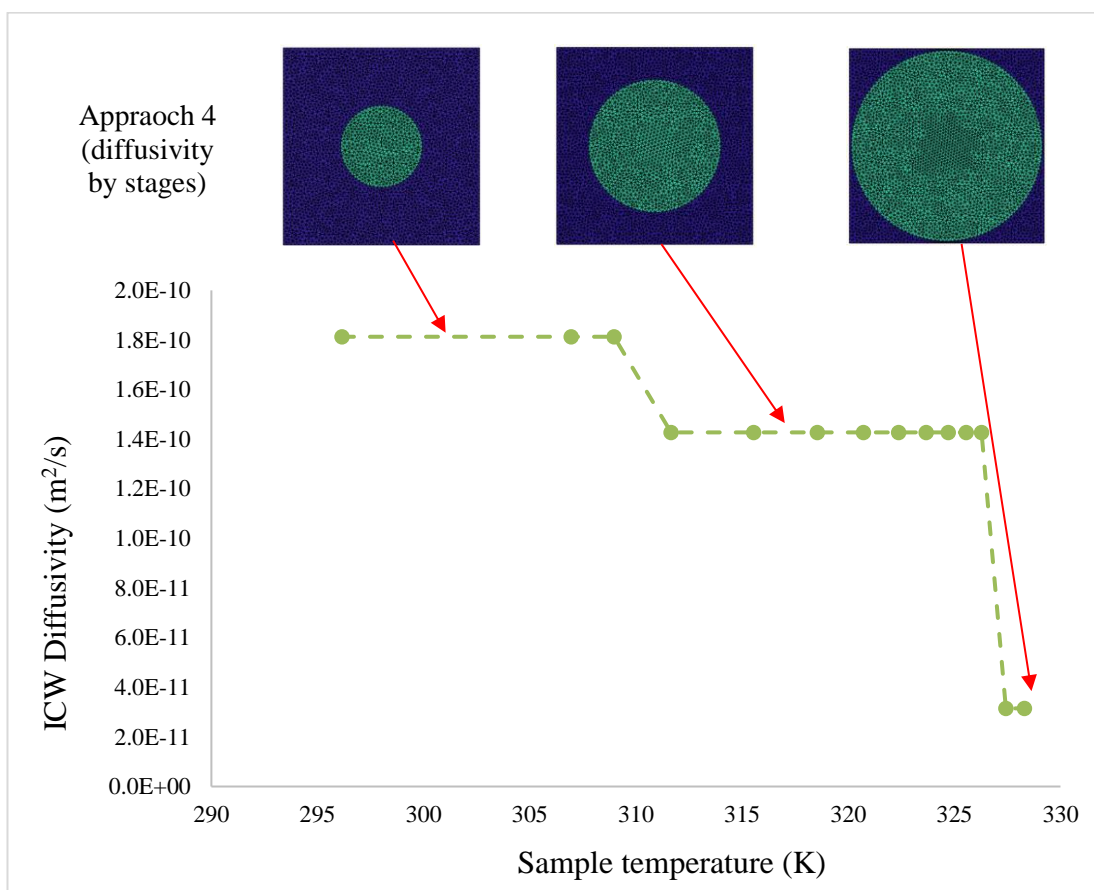


Figure 4.9. Diffusivity (m^2/s) of intracellular water for approach 4 (diffusivity by stages). The temporal evolution of the microscale domain can be seen along the top of the figure, purple denotes ICW and green denotes FW.

4.8.3 Comparison of temporal approaches

Approach 2 (average), approach 3 (linear decrease) and approach 4 (diffusivity by stages) all approximate the cellular deformation of approach 1 (base case) through

different assumptions. Considering the average or diffusivity by stages requires comprehensive knowledge of the microstructural evolution which generally results in high experimental cost. These approaches do describe the temporal heterogeneity, however multiscale models excel in optimization scenarios where modeling is utilized to calculate the optimal drying conditions and dryer design taking advantage of generalized properties. As comprehensive knowledge of the microstructure evolution is required, considering the average or diffusivity by stages would limit the model's advantages in these situations, restricting the applications of any property constructed. Additionally, approach 4 (diffusivity by stages) is an interesting concept but shows no significant advantage in this application. The approach could show potential at higher drying temperatures where significant changes to a materials microstructure occur within a particular stage, i.e. case hardening.

Approach 3 (linear decrease) is interesting. The approach requires some microstructural knowledge (i.e. the initial and final ICW content) however significantly less microstructural knowledge compared to the other approaches. Additionally, literature already exists for the initial ICW content for a variety of fruits and vegetables, which minimizes the experimental cost (Halder et al., 2011; Khan et al., 2016). Approach 3 also demonstrated the most practicality. The approach was able to capture the initial increase in ICW diffusivity which occurred within the base case, before progressively decreasing to achieve the Arrhenius relationship. Therefore, approach 3 (linear decrease) was selected for the property development.

4.9 DIFFUSIVITY ESTIMATION FOR ICW

Approach 3 (linear decrease) was utilized for the ICW diffusivity relationship development. The property was developed in terms of sample temperature (T_s) and intracellular water content (WC_{ICW}). The finalized function was,

$$D_{ICW} = \exp \left[\begin{matrix} -110.32 + 0.55536T_s + 0.095148WC_{ICW} \\ -0.00090738T_s^2 - 0.0007235WC_{ICW}^2 \end{matrix} \right]. \quad (4.19)$$

A visualization of the ICW diffusivity function can be found in Figure 4.10. Within this contour plot, the ICW diffusivity for any given sample temperature and ICW content can be seen within the given range. All coefficients have P-values under

0.05 and thus were considered significant. The function has a R^2 of 0.999, though, it should be noted the property is developed off the assumption (linear decrease) with a small data set. Some interesting observations can be made by investigating and comparing this function to published literature. The ICW content trend for apple tissue has been reported for convective drying at 45, 60 and 70 °C (Khan et al., 2018). The work reported that at low drying temperatures (45°C) the ICW content remains fairly constant (88%-79%) whereas at medium to high temperatures (above 50°C) the ICW fluctuates before dropping off in the latter stages of drying. Additionally, other authors have also demonstrated this trend for other food materials (Halder et al., 2011). The current study investigates drying at 60°C. To further investigate the proposed function, a case study for drying apples at 45°C can be considered. For this case, if the expected sample temperature and constant WC_{ICW} are input within the proposed function the ICW diffusivity would be between 1.41×10^{-10} to $1.8 \times 10^{-10} \text{ m}^2/\text{s}$. Once homogenization is performed, the effective macroscale diffusivity would be 1.99×10^{-10} to $2.569 \times 10^{-10} \text{ m}^2/\text{s}$ which agrees with literature (Beigi, 2016; Kara & Doymaz, 2015).

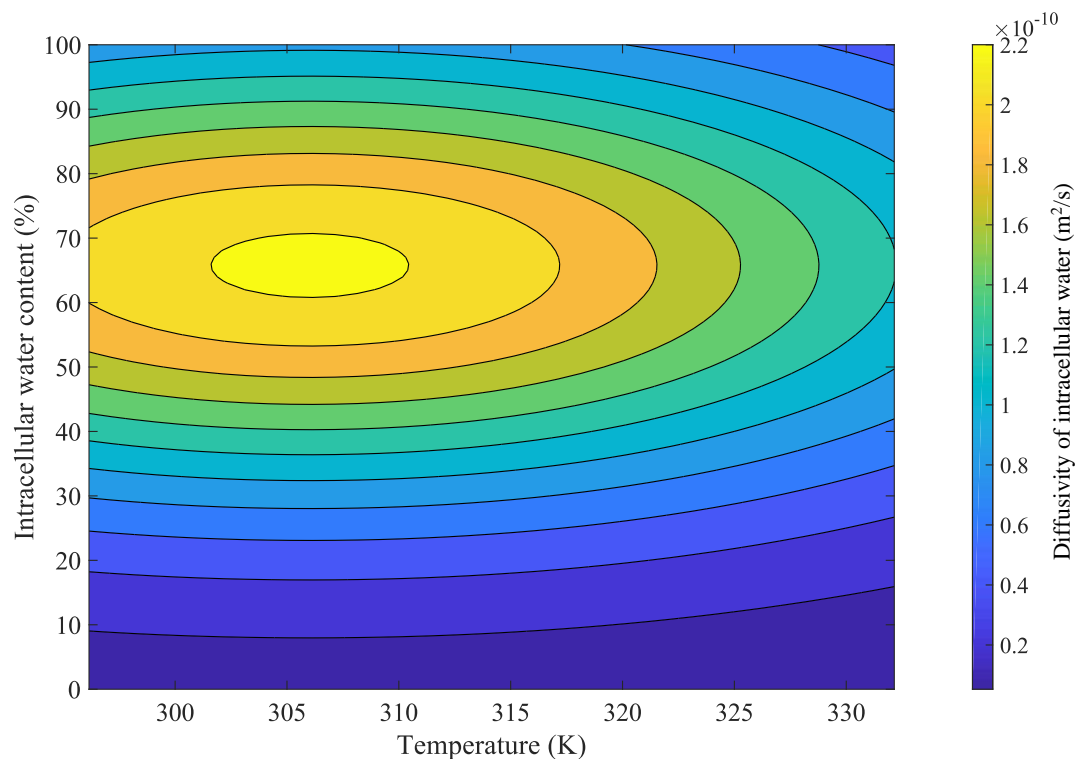


Figure 4.10. Proposed D_{ICW} (m^2/s) function [Equation (4.19)] in terms of sample temperature (K) and intracellular water content (%).

Though the proposed function [Equation (4.19)] is constructed for apple, the ICW content (WC_{ICW}) and its trend are different for each food material during drying. This opens the possibility to apply the function to other food materials. Literature has reported the initial ICW content for various fruits and vegetables i.e. apricot, pear, potato and eggplant (Halder et al., 2011; Khan et al., 2016), however much more work is still required. Therefore, the robustness of the proposed equation and its applicability to other food materials must be investigated in future works with a larger dataset. The proposed function does have the possibility of transitioning towards a generalized diffusivity for food material during drying. Note that the residuals for the proposed function can be found in Appendix A.

4.9.1 Discussion and outlook

The developed relationship for ICW diffusivity considers two subdomains at the microscale, ICW and FW. This allows the water heterogeneity to be considered while maintaining a reasonable computational cost. The magnitude of the effective diffusivity uncovered within the inverse analysis is on the mid to lower end of the expected range, $10^{-9}\text{--}10^{-11}\text{ m}^2/\text{s}$ (Panagiotou et al., 2004; Saravacos & Maroulis, 2001), for food material. This is important to remember when evaluating the proposed equation for property prediction. The existing macroscale effective diffusivity data within literature should be treated cautiously. Many of the published values are larger than the reported coefficients for self-diffusion and/or diffusion of species in the solvent with no porous structure (Lentzou et al., 2019). Also, many published works consider a perfect geometry with no deformation, often causing the predictive model and experimental data to significantly deviate in the latter stages of drying (Tzempelikos et al., 2015). The effective macroscale moisture diffusivity could be 0.1–50% smaller than free diffusion as the food matrices are porous media (Khaled & Vafai, 2003). Deformation is an important factor to consider, whether it's to model the physical process (Mayor & Sereno, 2004) or to incorporate its effects within the appropriate properties. This research incorporated its effects through the inverse study and heterogeneity consideration. Also, alternatively a basic method of incorporating some shrinkage is to consider the average radius within Fick's equation rather than the initial radius. The developed relationship for ICW diffusivity encompasses the effects

of the vacuole, tonoplast membrane, cytoplasm, cell membrane and cell wall within the ICW diffusivity. This is because only two subdomains are considered at the microscale. This lumping could have a negative effect on the proposed functions applicability to other food materials. Theoretical models nowadays have become more complex and more physics-based which allows the generalization of properties to become a real possibility in the near future.

4.10 CONCLUSION

The development of the property relationship for ICW is a step towards a more mechanistic approach to diffusivity. The inverse analysis and temporal heterogeneity investigation allowed the real temporal cellular morphology to be investigated and appropriate assumptions to be compared. The property relationship was developed in terms of two variables, material temperature and intracellular water content. This opens the possibility of using the function for other food materials, however the proposed function is yet to be validated for food material other than apple. Additionally, though the ICW diffusivity relationship was constructed for approach 3 (linear decrease), the temporal heterogeneity investigation provides insight into different options available to consider the temporal heterogeneity of the material. The other approaches investigated can be used in different scenarios where they are suitable. For example, the average ICW diffusivity can be used to cut down on computational cost when knowledge of the microstructural evolution is well known and considering diffusivity by stage can be used when the effect of cell rupturing is of key interest. The proposed function for ICW diffusivity will allow future models to consider a more realistic description of the physics during food drying.

Acknowledgements

This study was funded by the Department of Education and Training (AUS) through a Research Training Program (Stipend) Domestic (RTP) scholarship.

REFERENCES

- Auriault, J.-L., Boutin, C., & Geindreau, C. (2010). *Homogenization of coupled phenomena in heterogeneous media* (Vol. 149): John Wiley & Sons.
- Beigi, M. (2016). Influence of drying air parameters on mass transfer characteristics of apple slices. *Heat and Mass Transfer*, 52(10), 2213-2221. <https://doi.org/10.1007/s00231-015-1735-8>
- Białobrzewski, I. (2006). Simulation of changes in the density of an apple slab during drying. *International Communications in Heat and Mass Transfer*, 33(7), 880-888. <https://doi.org/10.1016/j.icheatmasstransfer.2006.02.017>
- Carr, E. J., & Turner, I. W. (2014). Two-scale computational modelling of water flow in unsaturated soils containing irregular-shaped inclusions. *International Journal for Numerical Methods in Engineering*, 98, 157-173. <https://doi.org/10.1002/nme.4625>
- Cengel, Y. (2003). *Heat, Transfer Mass: A practical approach*: Mc-Graw Hill Education, Columbus, GA, USA.
- Cengel, Y. A., & Boles, M. A. (2002). Thermodynamics: an engineering approach. *Sea, 1000*, 8862.
- Dadmohammadi, Y., & Datta, A. K. (2019). Prediction of effective moisture diffusivity in plant tissue food materials over extended moisture range. *Drying Technology*, 1-15. <https://doi.org/10.1080/07373937.2019.1690500>
- Datta, A. K. (2007). Porous media approaches to studying simultaneous heat and mass transfer in food processes. II: Property data and representative results. *Journal of food engineering*, 80(1), 96-110. <https://doi.org/10.1016/j.jfoodeng.2006.05.012>
- Geuzaine, C., & Remacle, J. F. (2009). Gmsh: A 3-D finite element mesh generator with built-in pre-and post-processing facilities. *International journal for numerical methods in engineering*, 79(11), 1309-1331. <https://doi.org/10.1002/nme.2579>

- Golestani, R., Raisi, A., & Aroujalian, A. (2013). Mathematical modeling on air drying of apples considering shrinkage and variable diffusion coefficient. *Drying Technology*, 31, 40-51. <https://doi.org/10.1080/07373937.2012.714826>
- Halder, A., Datta, A. K., & Spanswick, R. M. (2011). Water transport in cellular tissues during thermal processing. *AIChE Journal*, 57(9), 2574-2588. <https://doi.org/10.1002/aic.12465>
- Ho, Q. T., Carmeliet, J., Datta, A. K., Defraeye, T., Delele, M. A., Herremans, E., . . . Nicolai, B. M. (2013). Multiscale modeling in food engineering. *Journal of Food Engineering*, 114, 279-291. <https://doi.org/10.1016/j.jfoodeng.2012.08.019>
- Joardder, M. U., Brown, R. J., Kumar, C., & Karim, M. (2015). Effect of cell wall properties on porosity and shrinkage of dried apple. *International Journal of Food Properties*, 18(10), 2327-2337. <https://doi.org/10.1080/10942912.2014.980945>
- Joardder, M. U., Karim, A., Kumar, C., & Brown, R. J. (2014). Determination of effective moisture diffusivity of banana using thermogravimetric analysis. *Procedia Engineering*, 90, 538-543. <https://doi.org/10.1016/j.proeng.2014.11.769>
- Kara, C., & Doymaz, İ. (2015). Effective moisture diffusivity determination and mathematical modelling of drying curves of apple pomace. *Heat and Mass transfer*, 51(7), 983-989. <https://doi.org/10.1007/s00231-014-1470-6>
- Khaled, A. R. A., & Vafai, K. (2003). The role of porous media in modeling flow and heat transfer in biological tissues. *International Journal of Heat and Mass Transfer*, 46(26), 4989-5003. [https://doi.org/10.1016/S0017-9310\(03\)00301-6](https://doi.org/10.1016/S0017-9310(03)00301-6)
- Khan, M. I. H., Farrell, T., Nagy, S. A., & Karim, M. A. (2018). Fundamental Understanding of Cellular Water Transport Process in Bio-Food Material during Drying. *Scientific Reports*, 8(1), 15191. <https://doi.org/10.1038/s41598-018-33159-7>

- Khan, M. I. H., & Karim, M. (2017). Cellular water distribution, transport, and its investigation methods for plant-based food material. *Food Research International*, 99, 1-14. <https://doi.org/10.1016/j.foodres.2017.06.037>
- Khan, M. I. H., Kumar, C., Joardder, M. U. H., & Karim, M. (2017). Determination of appropriate effective diffusivity for different food materials. *Drying Technology*, 35(3), 335-346. <https://doi.org/10.1080/07373937.2016.1170700>
- Khan, M. I. H., Nagy, S. A., & Karim, M. (2018). Transport of cellular water during drying: An understanding of cell rupturing mechanism in apple tissue. *Food Research International*, 105, 772-781. <https://doi.org/10.1016/j.foodres.2017.12.010>
- Khan, M. I. H., Wellard, R. M., Nagy, S. A., Joardder, M. U. H., & Karim, M. A. (2016). Investigation of bound and free water in plant-based food material using NMR T2 relaxometry. *Innovative Food Science & Emerging Technologies*, 38, 252-261. <https://doi.org/10.1016/j;ifset.2016.10.015>
- Kumar, C., Joardder, M. U. H., Farrell, T. W., & Karim, M. (2018). Investigation of intermittent microwave convective drying (IMCD) of food materials by a coupled 3D electromagnetics and multiphase model. *Drying Technology*, 36(6), 736-750. <https://doi.org/10.1080/07373937.2017.1354874>
- Kumar, C., Joardder, M. U. H., Farrell, T. W., & Karim, M. A. (2016). Multiphase porous media model for intermittent microwave convective drying (IMCD) of food. *International Journal of Thermal Sciences*, 104, 304-314. <https://doi.org/10.1016/j.ijthermalsci.2016.01.018>
- Kumar, C., Millar, G. J., & Karim, M. (2015). Effective diffusivity and evaporative cooling in convective drying of food material. *Drying Technology*, 33(2), 227-237. <https://doi.org/10.1080/07373937.2014.947512>
- Lentzou, D., Boudouvis, A. G., Karathanos, V. T., & Xanthopoulos, G. (2019). A moving boundary model for fruit isothermal drying and shrinkage: An optimization method for water diffusivity and peel resistance estimation. *Journal of Food Engineering*, 263, 299-310. <https://doi.org/10.1016/j.jfoodeng.2019.07.010>

- Mahiuddin, M., Khan, M. I. H., Kumar, C., Rahman, M. M., & Karim, M. (2018). Shrinkage of food materials during drying: Current status and challenges. *Comprehensive Reviews in Food Science and Food Safety*, 17(5), 1113-1126. <https://doi.org/10.1111/1541-4337.12375>
- Mavroudis, N. E., Gekas, V., & Sjöholm, I. (1998). Osmotic dehydration of apples—effects of agitation and raw material characteristics. *Journal of Food Engineering*, 35(2), 191-209. [https://doi.org/10.1016/S0260-8774\(98\)00015-6](https://doi.org/10.1016/S0260-8774(98)00015-6)
- Mayor, L., & Sereno, A. M. (2004). Modelling shrinkage during convective drying of food materials: a review. *Journal of Food Engineering*, 61(3), 373-386. [https://doi.org/10.1016/S0260-8774\(03\)00144-4](https://doi.org/10.1016/S0260-8774(03)00144-4)
- Pace, E. L. (1962). Scientific foundations of vacuum technique (Dushman, Saul). *Journal of Chemical Education*, 39(8), A606. <https://doi.org/10.1021/ed039pA606>
- Panagiotou, N., Krokida, M., Maroulis, Z., & Saravacos, G. (2004). Moisture diffusivity: literature data compilation for foodstuffs. *International Journal of Food Properties*, 7(2), 273-299. <https://doi.org/10.1081/JFP-120030038>
- Pavliotis, G. A., & Stuart, A. (2008). *Multiscale methods: averaging and homogenization*: Springer Science & Business Media.
- Perré, P. (2007). Multiscale aspects of heat and mass transfer during drying. *Transport in Porous Media*, 66, 59-76. <https://doi.org/10.1007/s11242-006-9022-2>
- Perré, P., Almeida, G., Ayoub, M., & Frank, X. (2016). New modelling approaches to predict wood properties from its cellular structure: image-based representation and meshless methods. *Annals of Forest Science*, 73(1), 147-162. <https://doi.org/10.1007/s13595-015-0519-0>
- Pham, N. D., Khan, M., & Karim, M. (2020). A mathematical model for predicting the transport process and quality changes during intermittent microwave convective drying. *Food Chemistry*, 126932. <https://doi.org/10.1016/j.foodchem.2020.126932>

Prawiranto, K., Defraeye, T., Derome, D., Verboven, P., Nicolai, B., & Carmeliet, J. (2018). New insights into the apple fruit dehydration process at the cellular scale by 3D continuum modeling. *Journal of Food Engineering*, 239, 52-63. <https://doi.org/10.1016/j.jfoodeng.2018.06.023>

Rahman, M. M., Gu, Y., & Karim, M. (2018). Development of realistic food microstructure considering the structural heterogeneity of cells and intercellular space. *Food Structure*, 15, 9-16. <https://doi.org/10.1016/j.foostr.2018.01.002>

Rahman, M. M., Joardder, M. U., & Karim, A. (2018). Non-destructive investigation of cellular level moisture distribution and morphological changes during drying of a plant-based food material. *Biosystems Engineering*, 169, 126-138. <https://doi.org/10.1016/j.biosystemseng.2018.02.007>

Rahman, M. M., Joardder, M. U. H., Khan, M. I. H., Nghia, D. P., & Karim, M. A. (2018). Multi-scale model of food drying: Current status and challenges. *Critical Reviews in Food Science and Nutrition*. <https://doi.org/10.1080/10408398.2016.1227299>

Ratti, C., Crapiste, G., & Rotstein, E. (1989). A new water sorption equilibrium expression for solid foods based on thermodynamic considerations. *Journal of Food Science*, 54(3), 738-742. <https://doi.org/10.1111/j.1365-2621.1989.tb04693.x>

Saravacos, G. D., & Maroulis, Z. B. (2001). *Transport properties of foods*: CRC Press.

Sibgatullin, T., De Jager, P., Vergeldt, F., Gerkema, E., Anisimov, A., & Van As, H. (2007). Combined analysis of diffusion and relaxation behavior of water in apple parenchyma cells. *Biophysics*, 52(2), 196-203. <https://doi.org/10.1134/S0006350907020091>

Tzempelikos, D. A., Mitrakos, D., Vouros, A. P., Bardakas, A. V., Filios, A. E., & Margaris, D. P. (2015). Numerical modeling of heat and mass transfer during convective drying of cylindrical quince slices. *Journal of Food Engineering*, 156, 10-21. <https://doi.org/10.1016/j.jfoodeng.2015.01.017>

- Vega-Mercado, H., Marcela Góngora-Nieto, M., & Barbosa-Cánovas, G. V. (2001). Advances in dehydration of foods. *Journal of Food Engineering*, 49(4), 271-289. [https://doi.org/10.1016/S0260-8774\(00\)00224-7](https://doi.org/10.1016/S0260-8774(00)00224-7)
- Wang, Z., Sun, J., Liao, X., Chen, F., Zhao, G., Wu, J., & Hu, X. (2007). Mathematical modeling on hot air drying of thin layer apple pomace. *Food Research International*, 40(1), 39-46. <https://doi.org/10.1016/j.foodres.2006.07.017>
- Welsh, Z., Simpson, M. J., Khan, M. I. H., & Karim, M. (2018). Multiscale Modeling for Food Drying: State of the Art. *Comprehensive Reviews in Food Science and Food Safety*, 17(5), 1293-1308. <https://doi.org/10.1111/1541-4337.12380>
- Welsh, Z. G., Khan, M. I. H., & Karim, M. (2021). Multiscale modeling for food drying: A homogenized diffusion approach. *Journal of Food Engineering*, 292, 110252. <https://doi.org/10.1016/j.jfoodeng.2020.110252>
- Weres, J., & Olek, W. (2005). Inverse Finite Element Analysis of Technological Processes of Heat and Mass Transport in Agricultural and Forest Products. *Drying Technology*, 23(8), 1737-1750. <https://doi.org/10.1081/DRT-200065191>
- Zogzas, N. P., Maroulis, Z. B., & Marinos-Kouris, D. (1996). Moisture Diffusivity Data Compilation in Foodstuffs. *Drying Technology*, 14(10), 2225-2253. <https://doi.org/10.1080/07373939608917205>

Chapter 5: Comprehensive multiscale model for drying plant-based food material

Welsh, Z., Simpson, M. J., Khan, M. I. H., & Karim, M. A. (2020). Generalized moisture diffusivity for food drying through multiscale modeling. (Prepared for submission)

Statement of Contribution of Co-Authors for Thesis by Published Paper

The following is the suggested format for the required declaration provided at the start of any thesis chapter which includes a co-authored publication.

The authors listed below have certified that:

1. they meet the criteria for authorship and that they have participated in the conception, execution, or interpretation, of at least that part of the publication in their field of expertise;
2. they take public responsibility for their part of the publication, except for the responsible author who accepts overall responsibility for the publication;
3. there are no other authors of the publication according to these criteria;
4. potential conflicts of interest have been disclosed to (a) granting bodies, (b) the editor or publisher of journals or other publications, and (c) the head of the responsible academic unit, and
5. they agree to the use of the publication in the student's thesis and its publication on the [QUT's ePrints site](#) consistent with any limitations set by publisher requirements.

In the case of this chapter:

Welsh, Z. G., Simpson, M. J., Khan, M. I. H., & Karim, M. A. (2020). Generalized moisture diffusivity for food drying. (Prepared for submission)

Contributor	Statement of contribution
Zachary G. Welsh	Generation of concept, conducted experiments, model concept, model construction and model analysis, manuscript preparation, drafting and critically reviewing the manuscript
QUT Verified Signature	
Date: 2/12/2020	
M. J. Simpson	Assisted in drafting, organising and critically revising the manuscript.
M. I. H. Khan	Assisted in experiments, manuscript drafting and critically revising the manuscript.
M. A. Karim	Supervision, concept refinement, manuscript revision, manuscript editing, author for correspondence and final approval

Principal Supervisor Confirmation

I have sighted email or other correspondence from all Co-authors confirming their certifying authorship. (If the Co-authors are not able to sign the form please forward their email or other correspondence confirming the certifying authorship to the GRC).


Name

QUT Verified Signature
Signature


Date

5.1 ABSTRACT

Drying plant-based food materials can be time consuming and energy intensive, making optimization of its processes essential. However, current mathematical models are plagued with condition-dependent diffusivities restricting their performance in developing optimal drying strategies. Multiscale modeling is one technique which can help transition towards a more physics-based approach, improving a model's predictive capabilities. This research constructs a multiscale food drying model utilizing a generalized moisture diffusivity to investigate its predictive capabilities. The study investigates two food materials (apple and potato) convective drying at two different temperatures (47°C and 64°C). Additionally, to be able to utilize the generalized diffusivity, cell rupturing must be considered. Therefore, a theoretical rupturing threshold was developed exploiting the equilibrium vapor pressure to recognize which transport mechanisms were occurring. The generalized diffusivity was able to distinguish between the two materials and was able to describe the experimental data accurately at both drying temperatures. The generalized property resulted in diffusivities with the range of 1.94×10^{-10} - $5.14 \times 10^{-10} \text{ m}^2/\text{s}$.

5.2 INTRODUCTION

Drying plant-based food materials, such as fruits and vegetables, involves simultaneous heat and mass transport with anisotropic deformation (Datta, 2007; Mahiuddin et al., 2018). Drying can be very time consuming and energy intensive (Chua et al., 2001; Kudra, 2004) making optimization of its processes, systems and configurations very important. Mathematical modelling is crucial in the development of optimal drying strategies, since a modelling and simulation-based approach facilitates the investigation of multiple design and control configurations for a wide range of process conditions (Defraeye, 2014). However, current mathematical food drying models are plagued with condition-dependent properties with limited predictive capabilities, restricting a model's performance in these optimization scenarios. Moving towards a more physics-based model will aid in improving a model's predictive capabilities while minimizing the empirical information required.

Multiscale modeling can help transition towards a more physics-based approach. Multiscale modeling is considered to be a series of sub-models which investigates the

behavior of a particular product, such as moisture, over multiple spatial scales, considering substantial physics for a reasonable computational cost (Rahman et al., 2018). One property which can greatly benefit from multiscale modeling is the diffusivity of moisture.

Considering condition-dependent moisture diffusivity has been very common in mathematical food drying models. This has been a forced preference, due to the lack of comprehensive knowledge of the transport phenomena occurring, complex deformation and heterogeneous structure of the material (Adrover et al., 2019; Welsh et al., 2018). Commonly, to model moisture migration, all transport mechanisms are lumped and Fickian diffusion is assumed. The effective diffusivity is then estimated through curve fitting techniques and the Arrhenius framework. These curve fitting techniques are high in experimental cost and often consider a perfect geometry with no deformation, causing the predictive model and experimental data to significantly deviate in the latter stage of drying (Tzempelikos et al., 2015). In reality, the moisture transport depends on many interacting processes and is strongly influenced by deformation. The migration of intracellular water (ICW) also plays a major role as it can cause dynamic modifications to the materials structure (uneven volume reductions and cell rupturing). Due to its influence, many researchers have attempted to incorporate deformation within their models (Mahiuddin et al., 2018; Prothon et al., 2003). Adrover et al. (2019) considered a moving boundary model for isothermal drying and shrinkage of food material. The work accounted for the volume reduction, borrowing literature from the swelling of polymer matrices, and considered constant diffusivity and diffusivity through volume reduction. Lentzou et al. (2019) also developed a moving boundary model to describe isothermal food drying and shrinkage. The work investigated figs and utilized an optimization method to estimate the water diffusivity and peel resistance. With recent advances in cellular experimental investigating techniques (Dadmohammadi et al., 2020; Khan et al., 2018), models have been transitioning towards more mechanistic approaches. Dadmohammadi and Datta (2019) introduced a new diffusivity function, using a more mechanistic approach. The approach treats the material as a porous media, using parameters such as relative permeability, porosity, tortuosity and constrictivity. However, the approach still only models the macroscale requiring unique phase dependent diffusivities for each material. Welsh et al. (2021) developed a food drying model considering multiscale

strategies. The work utilized average diffusivities with predetermined temperature dependent microscales, requiring extensive experimental data. However, to utilize the full predictive capabilities of multiscale modeling, the microscale should be dynamic and actively depend on what is occurring at a macroscale. Food material's unique deformation under an external heat source adds complexity to achieving this goal, especially the presence of cell rupturing.

With this in mind, we construct a multiscale food drying model to investigate its predictive capabilities. The work investigates two different food materials (apple and potato) convective drying at two different temperatures (47°C and 64°C). The model utilizes a single upscaled effective diffusivity for all food materials. Additionally, to be able to utilize the upscaled property, cell rupturing must be practically considered. Therefore, a cell rupturing investigation is conducted to develop a theoretical threshold in order to characterize which transport mechanisms are occurring. The results are validated and compared to experimental data.

5.3 MODEL DEVELOPMENT

5.3.1 Drying model

The core multiscale model was developed previously (Welsh et al., 2021) considering two spatial scales, a microscale and a macroscale, Figure 5.1. This study extends the model, introducing the novel rupture threshold while investigating the generalized diffusivity. The macroscale transport model was developed using an axisymmetric coordinate system, Figure 5.1 (a), based on the following assumptions: (1) internal convective flow and heat generation can be neglected, (2) drying air properties are constant, (3) axisymmetric heating occurs, (4) moisture is only evaporated from the surface and (5) thermal equilibrium exists between all phases.

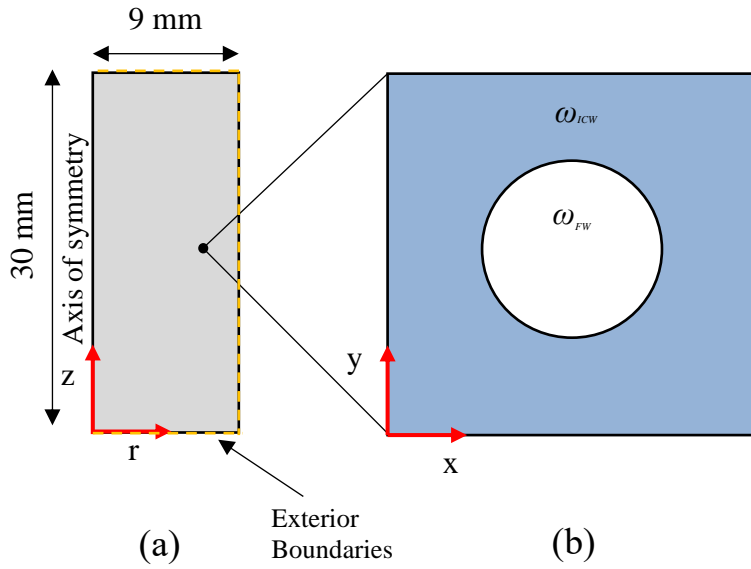


Figure 5.1. Domains (a) axisymmetric macroscale domain and (b) microscale domain.

Macroscale conservation equations

The macroscale conservation equations for mass and energy are based on Fick's law of diffusion and Fourier's law of heat transfer. These equations solve for the moisture concentration C (mol/m³) and temperature T (K) in terms of position and time. The respective equations are given by (Golestani et al., 2013),

$$\frac{\partial C}{\partial t} + \frac{1}{r} \frac{\partial}{\partial r} \left[-D_{H,eff} r \frac{\partial C}{\partial r} \right] + \frac{\partial}{\partial z} \left[-D_{H,eff} \frac{\partial C}{\partial z} \right] = 0 , \quad (5.1)$$

$$\rho c_p \frac{\partial T}{\partial t} + \frac{1}{r} \frac{\partial}{\partial r} \left[-k r \frac{\partial T}{\partial r} \right] + \frac{\partial}{\partial z} \left[-k \frac{\partial T}{\partial z} \right] = 0 , \quad (5.2)$$

where t is the time (s), ρ is the density of the food tissue (kg/m³), c_p is the specific heat of the food tissue (J/(kg·K)), k is the thermal conductivity of the food material (W/(m·K)) and $D_{H,eff}$ is the upscaled effective moisture diffusivity (m²/s). The effective moisture diffusivity depends on the temperature at any given point within the sample and WC_{ICW} , the ICW content (%).

Microscale mass conservation

To achieve the multiscale model, a microscale was introduced at each point in the macroscale representing the heterogeneous structure of the food material. This

assumption is valid when the scale parameter trends to zero, implying the homogeneities vanish, leading to a homogeneous material (Pavliotis & Stuart, 2008; Welsh et al., 2021). This is essential when deriving a model via homogenization, commonly referred to as the separation of scales (Auriault et al., 2010; Carr & Turner, 2014). The microscale considered two sub domains, ICW denoted as ω_{ICW} and intercellular water [free water (FW)] denote as ω_{FW} , Figure 5.1 (b). The macroscale mass transport, Equation (5.1), is coupled to the microscale mass transport equation defined as,

$$\frac{\partial c}{\partial t} + \frac{\partial}{\partial x} \left(-D \frac{\partial c}{\partial x} \right) + \frac{\partial}{\partial y} \left(-D \frac{\partial c}{\partial y} \right) = 0 , \quad (5.3)$$

where c is the microscale concentration (mol/m^3) and D is the cellular diffusivity (m^2/s) equaling D_{ICW} if $x, y \in \omega_{ICW}$ and D_{FW} if $x, y \in \omega_{FW}$.

5.3.2 Boundary conditions

The boundary conditions for the mass flux and heat transfer at the exterior surface was given by,

$$\mathbf{n} \cdot \left[-D_{H,eff} \nabla C \right] = h_m \frac{(p_{v eq} - p_{v air})}{RT} , \quad (5.4)$$

$$\mathbf{n} \cdot \left[-k \nabla T \right] = h_T (T - T_{air}) - h_m \frac{(p_{v eq} - p_{v air})}{RT} \lambda M_w , \quad (5.5)$$

where h_m is the mass transfer coefficient (m/s), h_T is the heat transfer coefficient ($\text{W}/(\text{m}^2 \cdot \text{K})$), $p_{v eq}$ is the equilibrium vapor pressure, $p_{v air}$ is the vapor air pressure of ambient air (Pa), \mathbf{n} is the unit vector normal to the boundary, R is the universal gas constant ($\text{J}/(\text{mol} \cdot \text{K})$), T_{air} is the drying air temperature (K), M_w molar mass of water (g/mol) and λ is the latent heat of evaporation (J/kg). The equilibrium vapor pressure for each food material can be derived from the respective sorption isotherm. Therefore, the equilibrium vapor pressure for apple ($p_{v eq,apl}$) and potato ($p_{v eq,pot}$) are (Ratti et al., 1989),

$$p_{v eq,apl} = p_{v sat}(T) \exp(-0.182M_{db}^{-0.696} + 0.232e^{-43.949M_{db}} M_{db}^{0.0411} \ln[p_{v sat}(T)]) , \quad (5.6)$$

$$p_{v eq,pot} = p_{v sat}(T) \exp(-0.0267M_{db}^{-1.656} + 0.0107e^{-1.287M_{db}} M_{db}^{1.513} \ln[p_{v sat}(T)]) . \quad (5.7)$$

A visual representation of Equation (5.6) and Equation (5.7) can be seen in Figure 5.2 (a) and (b) respectively. The saturated vapor pressure is given by (Vega-Mercado et al., 2001),

$$p_{v,sat} = \exp \left[-\frac{5800.2206}{T} + 1.3915 - 0.0486T + \left(0.4176 \times 10^{-4}T^2 - 0.1445 \times 10^{-7}T^3 + 6.546 \ln(T) \right) \right]. \quad (5.8)$$

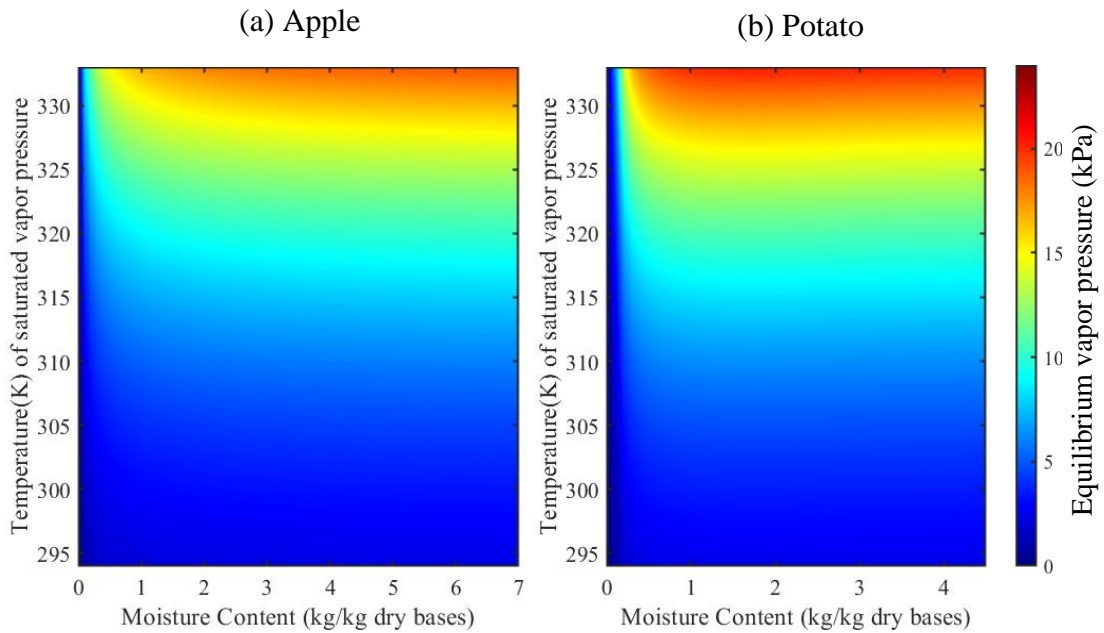


Figure 5.2. Visual representation of the equilibrium vapor pressure (kPa) of (a) apple and (a) potato, Equation (5.6) and Equation (5.7) respectively.

The last boundary condition is the symmetric condition applied at $r=0$, defined as

$$\mathbf{n} \cdot [-D_{H,eff} \nabla C] = 0, \quad (5.9)$$

$$\mathbf{n} \cdot [-k \nabla T] = 0. \quad (5.10)$$

Food material properties

The thermophysical properties for each material are located within Table 5.1. These properties are a function of either moisture content, wet (M_{wb}) or dry (M_{db}) bases, and/or sample temperature.

Table 5.1. Material Properties

Parameter	Value (unit)	Reference
Apple		
Density, ρ_{apl}	837 (kg/m ³)	Mavroudis et al. (1998)
Specific heat, $c_{p,apl}$	1000(1.4+3.22 M_{wb}) (J/(kg·K))	Białobrzewski (2006)
Thermal conductivity, k_{apl}	0.49-0.443exp(-0.206 M_{wb}) (W/(m·K))	Mattea et al. (1986)
Initial moisture content, M_0	6.8 (kg/kg dry bases)	This study
Initial wet bases moisture content, $M_{0,wb}$	0.86 (kg/kg wet bases)	This study
Initial ICW content, $WC_{apl,0}$	87.8%	Khan et al. (2016)
Potato		
Density, ρ_{pot}	1055 (kg/m ³)	Khan et al. (2017)
Specific heat, $c_{p,pot}$	4184(0.406+0.00146 T +0.203 M_{db} -0.249 M_{db}^2) (J/(kg·K))	Tripathy and Kumar (2009)
Thermal conductivity, k_{pot}	0.5963- $\left(\frac{0.1931}{M_{db}}\right)+\left(\frac{0.0301}{M_{db}^2}\right)$ (W/(m·K))	Mattea, et al. (1986)
Initial moisture content, $M_{0,wb}$	4.4 (kg/kg dry bases)	This study
Initial wet bases moisture content, $M_{0,wb}$	0.81 (kg/kg wet bases)	This study
Initial ICW content, $WC_{pot,0}$	81.3%	Khan et al. (2016)

Homogenized effectivity diffusivity

The 2D homogenized effective diffusivity is denoted by (Welsh et al., 2021),

$$D_{H,eff} = \begin{bmatrix} \frac{1}{\omega} \int_{\omega} D(x, y) \left(\frac{\partial u_1}{\partial x} + 1 \right) d\omega & \frac{1}{\omega} \int_{\omega} D(x, y) \frac{\partial u_2}{\partial x} d\omega \\ \frac{1}{\omega} \int_{\omega} D(x, y) \frac{\partial u_1}{\partial y} d\omega & \frac{1}{\omega} \int_{\omega} D(x, y) \left(\frac{\partial u_2}{\partial y} + 1 \right) d\omega \end{bmatrix}, \quad (5.11)$$

where ω is the area of the macroscale domain, u_1 and u_2 are the corrective factors and the solution of the periodic cell problem:

$$\nabla \cdot (D \nabla(u_j + \mathbf{e}_j)) = 0, \quad j = 1, 2, \quad (5.12)$$

where

$$\mathbf{e}_1 = \begin{bmatrix} 1 \\ 0 \end{bmatrix}, \quad \mathbf{e}_2 = \begin{bmatrix} 0 \\ 1 \end{bmatrix}. \quad (5.13)$$

$$u_j \text{ is } \omega\text{-periodic}, \quad (5.14)$$

$$\frac{1}{\omega} \int_A u_j d\omega = 0. \quad (5.15)$$

The solution of Equation (5.12), the corrective factors, is unique only up to an additive constant (Auriault et al., 2010), requiring Equation (5.15), a zero mean constraint, to achieve a single unique solution. However, any of these unique solutions are suitable as the effective homogenized diffusivity only requires the gradient of u_j (Carr & Turner, 2014).

5.3.3 Cellular structure representation within the microscale domain

The cellular structure of apple consists of a few key components: protoplast (composed of vacuole, tonoplast membrane and cytoplasm), the cell membrane, cell wall and intercellular space (Prawiranto et al., 2018). These cellular components dynamically deform due to the various transport mechanisms occurring. Additionally, drying at different temperatures can cause different cellular deformation, adding complexities to representing the temporal heterogeneity of water (Khan et al., 2018). This work considers two sub-domains within the microscale, ICW denoted as ω_{ICW} and FW denote as ω_{FW} . This groups the effects of the protoplast, cell membrane and

cell wall within the ICW domain. This lumping saves on computational cost but could have a negative effect on the accuracy of the model. The intercellular spaces were grouped and represented as a circle, Figure 5.1 (b). This circle was assumed to be located at the center of the microscale domain, requiring minimal microstructural knowledge but forcing the homogenized diffusivity to be isotropic. The ratio between sub-domains within the microscale is the key factor to represent the materials heterogeneity (Welsh et al., 2021).

5.3.4 Cellular diffusivity properties for ICW and FW

To complete the homogenization, the diffusivity of each cellular sub-domain is required. Welsh et al. (2020) recently conducted a multiscale temporal investigation on the cellular diffusivity of apple tissue during drying. The work developed a function for the diffusivity of ICW incorporating cell rupturing within the property. The function is (Welsh et al., 2020):

$$D_{ICW} = \exp \left[\begin{array}{l} -110.32 + 0.55536T_s + 0.095148WC_{ICW} \\ -0.00090738T_s^2 - 0.0007235WC_{ICW}^2 \end{array} \right], \quad (5.16)$$

where T_s is the sample temperature (K) and WC_{ICW} is the intracellular water content (%). The function has only been validated for apple tissue, though its validity for other food material will be investigated within this work. The diffusivity of FW is (Pace, 1962):

$$D_{FW} = 2.26 \times 10^{-5} \left[\frac{T}{273.15} \right]^{1.81}. \quad (5.17)$$

5.4 EVOLUTION OF INTRACELLULAR WATER- RUPTURING THRESHOLD

In order to use Equation (5.16) ICW and its evolution during drying had to be considered within the model. ICW has the ability to transport three main ways: cell to cell, cell to pore or through a cell membrane rupture (Khan & Karim, 2017). Commonly only cell to cell and cell to pore transport is considered within theoretical models, even though cell rupturing can significantly influence the transport process, associated deformation and the quality of a dried product (Dinçer & Zamfirescu, 2016;

Khan et al., 2018). Deformation and cell collapse can be caused indirectly by gradients of temperature, difference in vapor pressure, or in osmotic pressure between the product and the surrounding environment (Prothon et al., 2003). The ICW diffusivity function [Equation (5.16)] incorporates all three transport mechanisms, therefore, cell rupturing must be incorporated within the evolution of ICW. The model must be able to recognize if, when and the rate at which cell rupturing has occurred. It is well established cell rupturing occurs due to a loss in turgor pressure. Additionally, turgor pressure is linked and has an impact on the sorption isotherm of the protoplast within the material (Prawiranto et al., 2018). Turgor pressure (MPa) is

$$\psi_p = \psi_c - \psi_s, \quad (5.18)$$

where ψ_c is the osmotic potential (MPa) and ψ_s is the water potential (MPa) at the cytoplasma side of the cell membrane. This approach has been utilizing within dehydration models in relation to the water activity. These works simulate water transport (Fanta et al., 2013) and deformation (Aregawi et al., 2014) at the microscale, however cell rupturing is not incorporated. Within the field of food drying, cell rupturing is commonly described in association with temperature. The cell membrane remains intact until the sample temperature reaches about 50 °C (Halder et al., 2011). Due to the convective heating profile, the surface reaches 50 °C first and the cell adjacent to the surface lose their rigidity and tend to become droopy (near rupturing limit) (Khan & Karim, 2017). The cells loss turgor pressure and tend to fail due to the impose thermal stress due to the continuous penetration of heat energy (Khan & Karim, 2017). This has been demonstrated for various food materials (low and highly porous) (Khan et al., 2018; Khan & Karim, 2017; Khan et al., 2017a).

With this in mind, the current work utilizes the macroscale equilibrium vapor pressure to determine if and when cell rupturing occurs. An investigation will be conducted to develop a theoretical equilibrium vapor pressure threshold utilizing the average of the domain. The equilibrium vapor pressure is a product dependent relationship constructed through the material sorption isotherm (Ratti et al., 1989). The property is moisture and temperature dependent and as the material dries, p_{veq} at the surface experiences an initial increase, before decreasing (pressure drop). As the material heats up a large pressure difference can be generated within the material depending on the drying temperature. This phenomenon will be exploited to

characterize which transport mechanisms are occurring within the material. The investigation will consider convective drying at 50 °C, utilizing the known cell membrane temperature limit to uncover the maximum equilibrium vapor pressure at this temperature. This maximum will become the theoretical threshold. A visual representation of the threshold can be seen in Figure 5.3. When the threshold is not reached, cell rupturing will not occur and WC_{ICW} will remain constant at its initial value, Figure 5.3 (a). When p_{veq} exceeds the threshold, cell rupturing will occur and WC_{ICW} will linearly decrease, Figure 5.3 (b). This corresponds to the assumption within (Welsh et al., 2020). The rate at which WC_{ICW} decrease is formulated from Khan et al. (2018) and Khan et al., (2017b) for apple and potato respectively. This results in ICW content functions of $-0.0033 \times t + 87.8$ for apple and $-0.003 \times t + 81.3$ for potato when cell rupturing occurred.

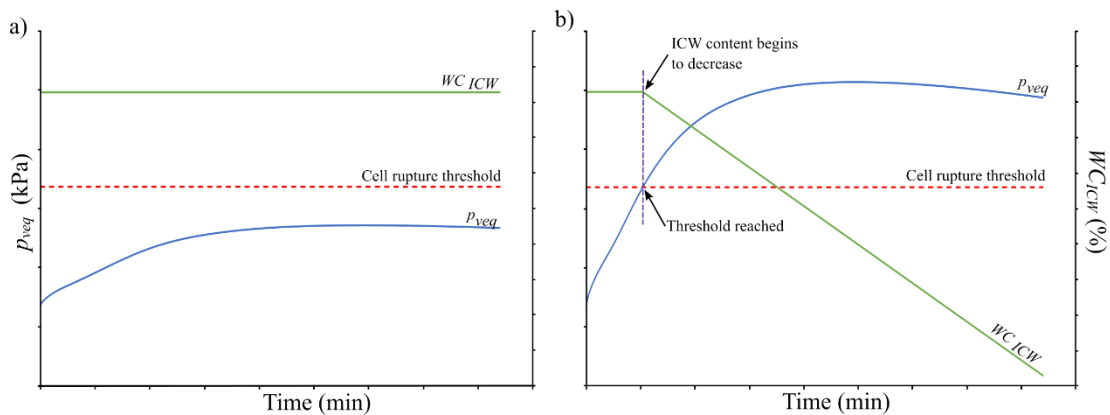


Figure 5.3. Visual representation of proposed theoretical cell rupturing threshold, a) threshold is not reached and cell rupturing does not occur, b) threshold is reached and cell rupturing occurs.

5.4.1 Remaining Properties

The remaining input parameters can be seen in Table 3.2.

Table 5.2. Input parameters

Parameter	Value (unit)	Reference
Density of water, ρ_w	995 (kg/m ³)	Cengel (2003)
Initial sample temperature, T_0	295 (K)	This study
Latent heat of evaporation, λ	2358600 (J/kg)	Cengel (2003)
Universal gas constant, R	8.314 (J/(mol·K))	Cengel and Boles (2002)
Molar mass of water, M_w	0.018016 (kg/mol)	Cengel and Boles (2002)
Partial vapor pressure, $p_{v\ air}$	1250 (Pa)	This study
Heat transfer coefficient, h_T	13.2 (W/(m ² ·K))	Assumed, (Khan et al., 2020)

5.4.2 Mass transfer coefficient

The mass transfer coefficient is also a condition-dependent parameter. It is strongly influenced by the airflow distribution and deformation the product experiences (Defraeye & Radu, 2018). Khan et al. (2020) investigated spatial dependent heat and mass transfer coefficients demonstrating their influence on the drying kinetics. The work concluded a larger overpredict can occur if the spatial distribution of airflow is not considered. Therefore, to minimize the mass transfer coefficient influence on the results it will be solved through an inverse problem. This allowed the study to focus on investigating the generalized diffusivity. For the inverse problem, the mass transfer coefficient (h_m) is unknown and predicted based on the minimization between the simulated and experimental moisture drying curves. A Levenberg-Marquardt optimization algorithm coupled with the finite element method was applied with the objective functions as

$$OF(h_m) = \int \left[\overline{M}_{db,exp}(t) - \overline{M}_{db,num}(t, h_m) \right]^2 dt, \quad (5.19)$$

where $\overline{M}_{db,exp}$ is the average dry bases moisture content from the experimental investigation and $\overline{M}_{db,num}$ is the average dry bases moisture content from the simulation.

5.4.3 Computational strategy

The modeling procedure is shown in Figure 5.4. The upscaled effective diffusivity was solved in MATLAB 2018a coupled with Gmsh (Geuzaine & Remacle, 2009) to construct the microscale domains. Once $D_{H,eff}$ was solved, the cell rupturing investigation was conducted. Both the cell rupturing investigation and the macroscale heat and mass transport model were solved in COMSOL Multiphysics 5.3a. Lastly, a sensitivity investigation was conducted on some key parameters with uncertainty.

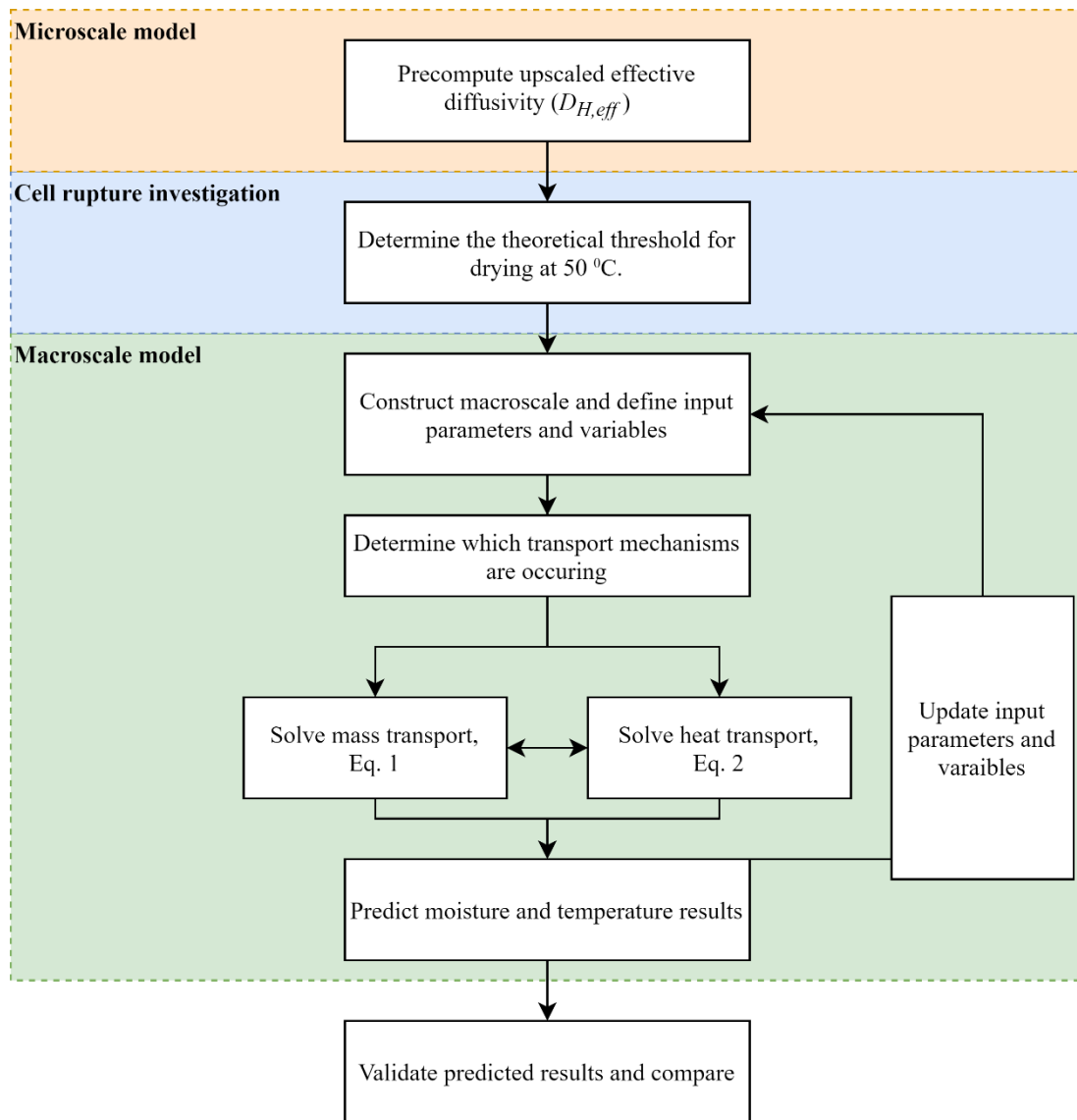


Figure 5.4. Computational methodology.

5.4.4 Experimental investigation

Two different food materials are investigated within this work, Granny Smith apples and Brushed potatoes. They were purchased from a local supermarket at commercial maturity. The samples were prepared based on the standard sample

preparation procedure (Asabe & Home). Each product was washed and cut into cylindrical slices (mesocarp or pulp portions) using a fruit sample preparation tool [a stainless-steel Cork Borer (JH-1225)]. The initial dimensions of the samples were 30 mm in length and 18 mm in diameter. Typically, convective food drying is conducted at temperatures between 40 to 80 °C. Therefore, the drying experiments were performed at mean temperatures of 47 °C and 64 °C with an air velocity of 1 m/s. These temperatures were selected as examples as two different types of cellular deformation (minimal cellular deformation and significant deformation). The driers inlet and outlet were perpendicular to one another creating uneven velocity distribution. Two sets of experiment data were required to validate the model: the average moisture content and average surface temperature of the sample. To record the moisture content, each sample was weighed individually in regular intervals throughout the drying process, every 10 mins for the first hour then every 30 minutes till completion. This was done utilizing a digital electronic balance with a capacity of 50 g and an accuracy of ±0.001g. The measurements were completed within 10 seconds during the drying process. To record the sample surface temperature, a thermal image camera was utilized (FLIR-E6390). The experimental procedure was replicated three times. Therefore, a total of 12 samples were dried, 6 apple samples and 6 potato samples.

5.5 RESULTS

The results are presented in four main parts: the upscaled effective diffusivity, drying at low temperatures (47 °C), drying at medium temperatures (64 °C) and a sensitivity investigation. Drying at low temperatures results in no cell rupturing whereas significant cell rupturing occurs when drying at medium temperatures. This allows the predictive capabilities of the generalized diffusivity to be investigated in depth. The equilibrium vapor pressure investigation is presented within section 5.5.3. All error bars displayed within the results show plus-minus one standard deviation of the mean experimental data. All averages shown within the results were calculated using Equation C.1 within Appendix C.

5.5.1 Upscaled effective diffusivity

Homogenization was performed for all combinations of sample temperature (T_s) and intracellular water content (WC_{ICW}) to construct the generalized effective diffusivity function. This created the following function,

$$D_{H,eff} = \exp \left[\begin{array}{l} -106.6 + 0.5548T_s + 0.029502WC_{ICW} \\ -0.00090648T_s^2 - 0.00041019WC_{ICW}^2 \end{array} \right]. \quad (5.20)$$

A visual representation of the upscaled effective macroscale diffusivity can be seen in Figure 5.5. Most food materials have an initial ICW content between 76 to 92 % (represent by the red boundaries in Figure 5.5). Within this region, there is a gradient in both ICW content and temperature. As the ICW content decreases, the effective diffusivity increases. There is because there is a higher percentage of FW within the sample and as FW is easily transported. As temperature increases within this region, the diffusivity initially increases before tapering off at higher temperatures. However, the effective diffusivity does remain fairly constant if cell rupturing doesn't occur. Once cell rupturing occurs (region below the bottom red boundary), the diffusivity significantly increases. When there is minimal ICW left in the material the diffusivity decreases.

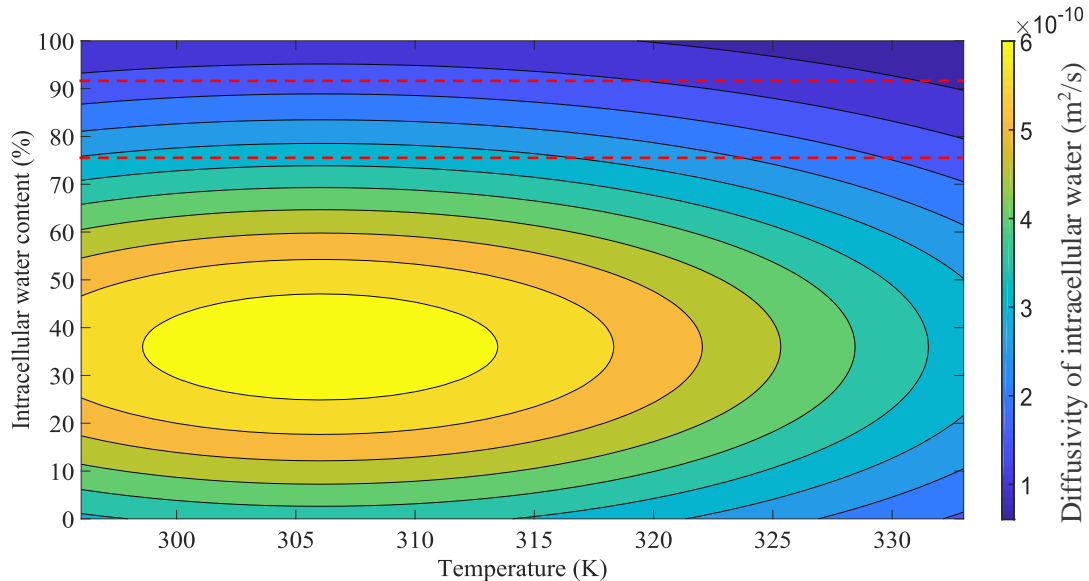


Figure 5.5. Visual representation of the effective diffusivity (m^2/s) function ($D_{H,eff}$) .

5.5.2 Drying at low temperatures - no cell rupturing occurs

Mass transfer coefficient

The mass transfer coefficient (h_m) was solved through an inverse problem for drying apple at low temperatures. This approach resulted in a lower than expected average mass transfer coefficient of 0.00381 m/s. This value was used for the remainder of the study. During food drying, the mass transfer coefficient depends on the velocity field (spatially dependent) and macroscale deformation (temporal dependent). Literature demonstrates models tend to overpredict experimental data when not considering a spatially dependent mass transfer coefficient (Khan et al., 2020) and can underpredict experimental data when considering a spatially dependent h_m without macroscale deformation (Defraeye & Radu, 2018). The presented model does not consider a varying velocity field or the macroscale deformation, rather compensating for their effects through the inverse calculation of the mass transfer coefficient.

Drying kinetics

The presented multiscale model accurately predicts drying at lower temperatures achieving a low mean relative error (MRE) of 1.52% for apple and 3.18% for potato, Figure 5.6. The generalized diffusivity was successful in distinguishing between the two materials through considering their ICW content. Apples and potatoes have different initial ICW contents, 87.8% and 81.3 % respectively. This resulted in a difference in their effective diffusivities, Figure 5.7. These values can be compared to literature cautiously, due to the condition-dependent nature of previously published diffusivity data. The magnitudes of the generalized diffusivity can be compared to 1.594×10^{-10} m²/s for Granny smith apples at 40 °C (Simpson et al., 2015) and $3.6 \times 10^{-10} - 4.3 \times 10^{-10}$ m²/s for potato at 40°C (Hassini et al., 2007).

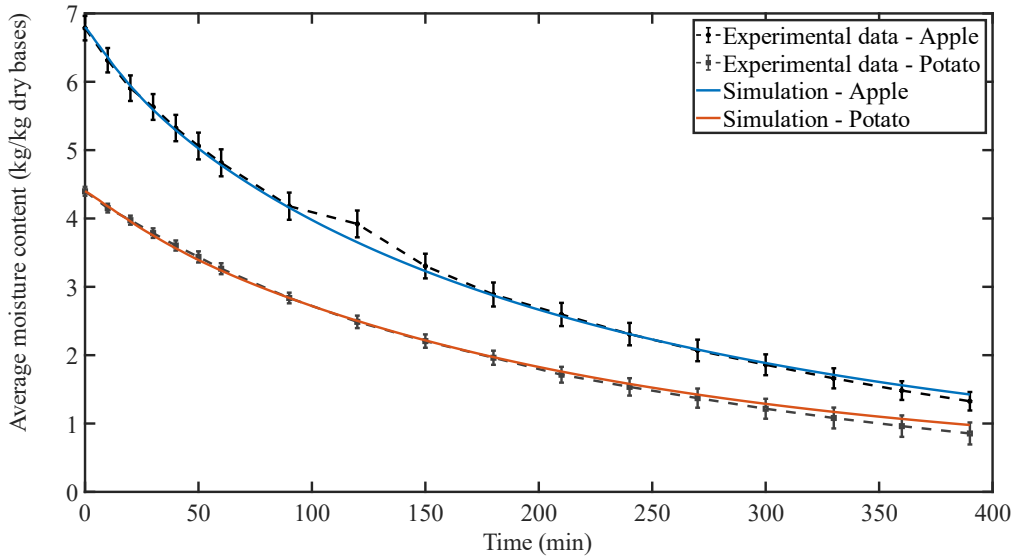


Figure 5.6. Average moisture content (kg/kg dry bases) for drying at 47 °C. Error bars represent plus-minus one standard deviation of the triplicate experimental data.

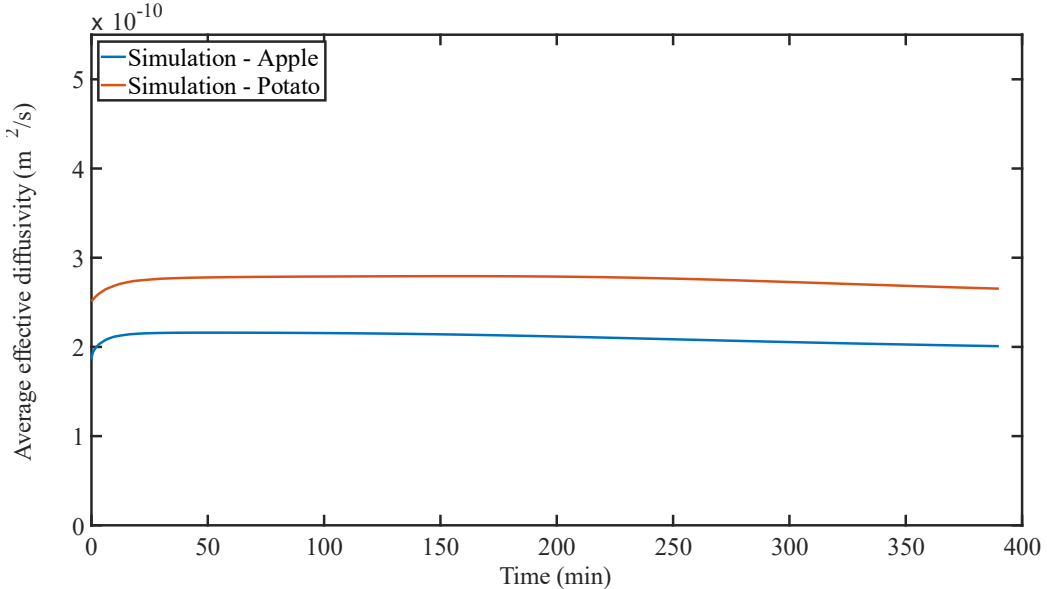


Figure 5.7. Average macroscale diffusivity (m^2/s) for drying at 47 °C.

Temperature profile

The presented model accurately predicts the average temperature profile when drying at lower temperatures, Figure 5.8. The model achieved low MREs of 0.46% for apple and 0.65% for potato. However, the model does significant overpredict the temperature profile in the early stages of drying. This also caused a sharp initial increase in diffusivity, Figure 5.7. This overprediction is consistent with models in literature which consider a constant/average heat transfer coefficient (Defraeye & Radu, 2018; Khan et al., 2020; Welsh et al., 2021). To improve the temperature profile,

the heat transfer coefficient could be considered in terms of a velocity field (spatially dependent) (Khan et al., 2020) and/or in terms of the deforming sample (Gulati & Datta, 2015). However, this would increase the computational cost of the model. Additionally, applying multiscale modelling to the thermal conductivity of the material could help further minimize this overprediction.

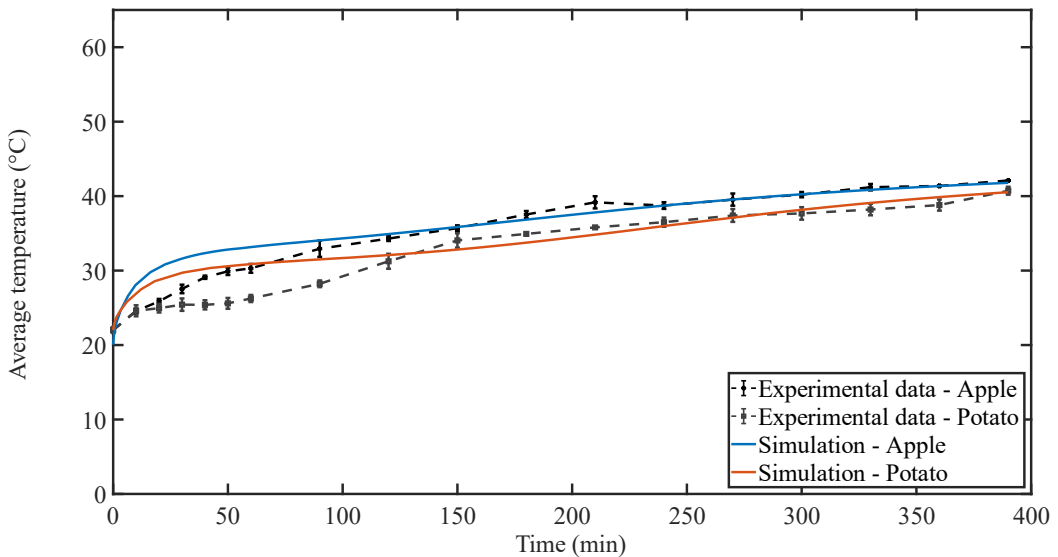


Figure 5.8. Average Temperature (°C) for drying at 47 °C. Error bars represent plus-minus one standard deviation of the triplicate experimental data.

5.5.3 Drying at medium temperatures - significant cell rupturing occurs

Before the generalized diffusivity could be applied to drying at medium temperatures, the equilibrium vapor pressure threshold investigation was conducted.

Rupture threshold development

The results of the equilibrium vapor pressure threshold investigation can be seen in Figure 5.9. The investigation solves the computational model considered the upscaled diffusivity, Equation (5.20), while drying at 50 °C. Additionally, it was assumed cell rupturing had not occurred, therefore WC_{ICW} remained constant at their initial percentages. This resulted in a unique threshold for each food material, 7080 Pa for apple and 8004 Pa for potato. The spatial distribution of each material at their associated threshold can also be seen in Figure 5.9 (a) and Figure 5.9 (b) for apple and potato respectively.

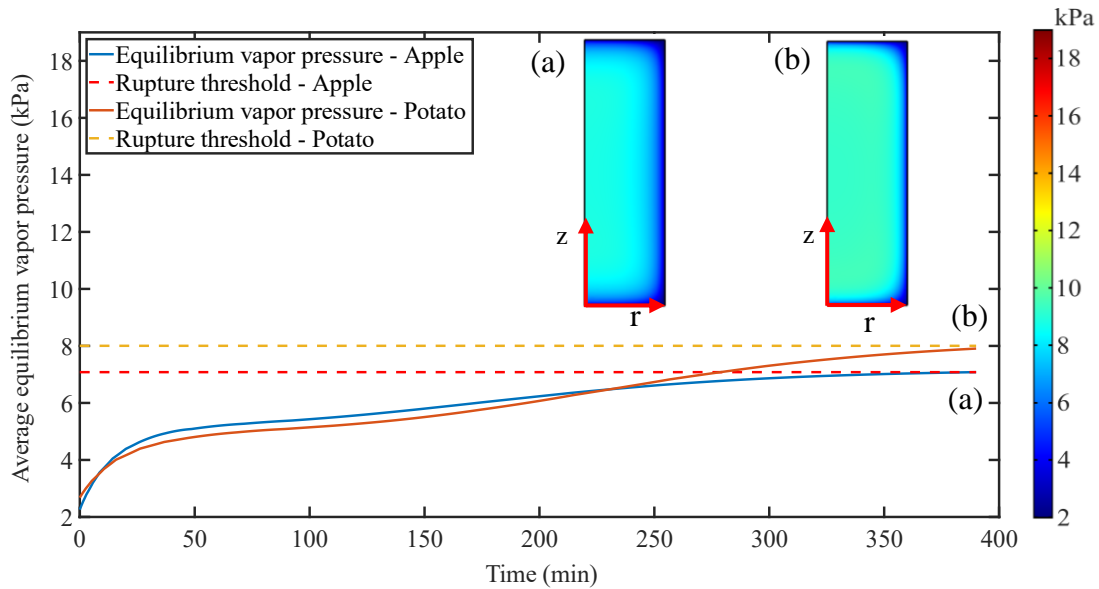


Figure 5.9. Rupturing threshold investigation using the average equilibrium vapor pressure (kPa), (a) spatial distribution of apple at threshold and (b) spatial distribution of potato at threshold.

Drying Kinetics

The presented model accurately predicts the drying kinetics at medium temperatures, Figure 5.10. The model achieved MREs of 4.8% for apple and 7.8% for potato, slightly worse MREs than drying at lower temperatures. The greatest deviation between the experiment data and simulations can be seen in the latter stages of drying, especially for potato. Though, the model remains within the error bars. The resulting effective diffusivities can be seen in Figure 5.11. Once the rupture threshold is reached, the diffusivity experiences a sudden jump. This is a limitation of the assumed trend of ICW when cell rupturing occurs; trend is precomputed rather than computed on the fly. The unique rupture thresholds cause cell rupturing to commence at different points in time for both materials, mimicking the real world (Khan et al., 2018; Khan et al., 2017b). The effective diffusivity results can be compared to $0.713 \times 10^{-11} - 7.66 \times 10^{-10}$ m²/s for Red Delicious apples at a temperature range of 35-55°C (Beigi, 2016) and $5.42 \times 10^{-10} - 1.92 \times 10^{-9}$ m²/s for drying potato at 40-70 °C (Hassini et al., 2007).

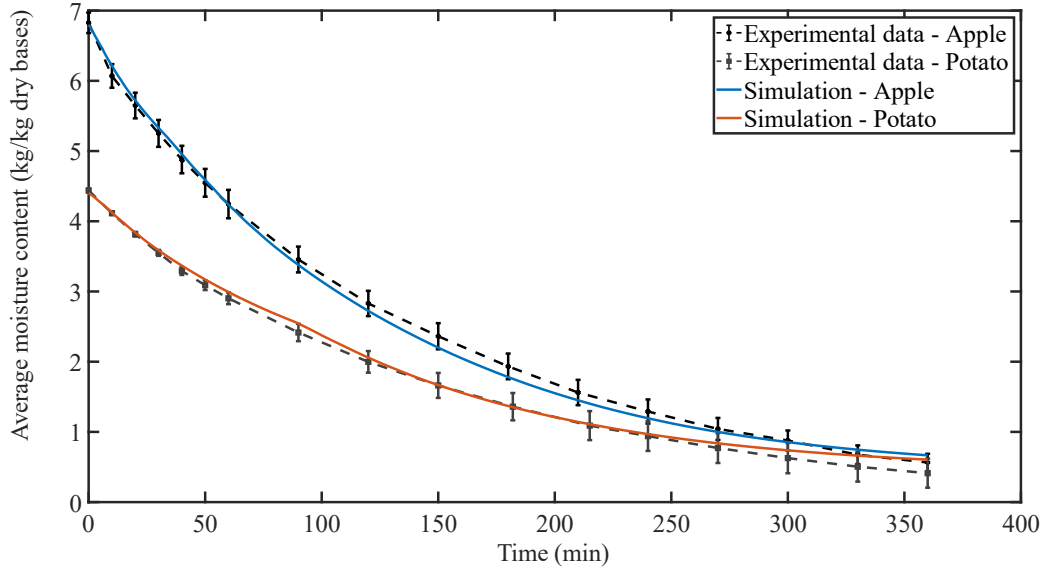


Figure 5.10. Average moisture content (kg/kg dry bases) for drying at 64 °C. Error bars represent plus-minus one standard deviation of the triplicate experimental data.

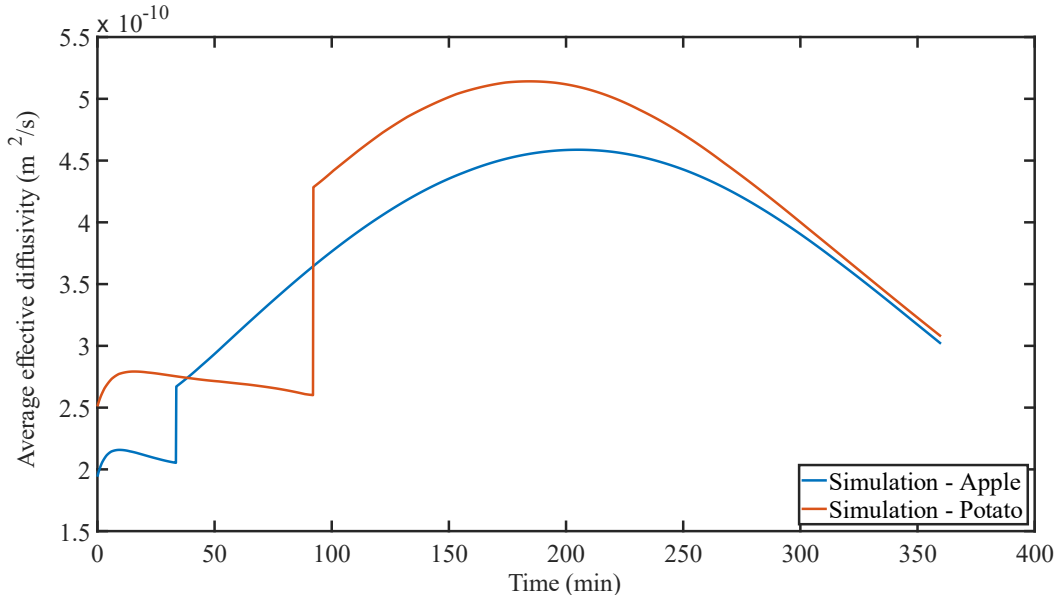


Figure 5.11. Average macroscale diffusivity (m^2/s) for drying at 64 °C.

Temperature profile

The presented model predicted the average temperature reasonably well achieving a low MRE of 0.89% for apple and 0.67% for potato, Figure 5.12. These MREs are similar to drying at lower temperatures. The same overprediction exists in the early stages of drying. Looking closely at Figure 5.12, potato doesn't experience a smooth transition when the rupture threshold is reached (at 92 min), but stabilizes as drying continues. Apple on the other hand does experience a smooth transition once the threshold is reached.

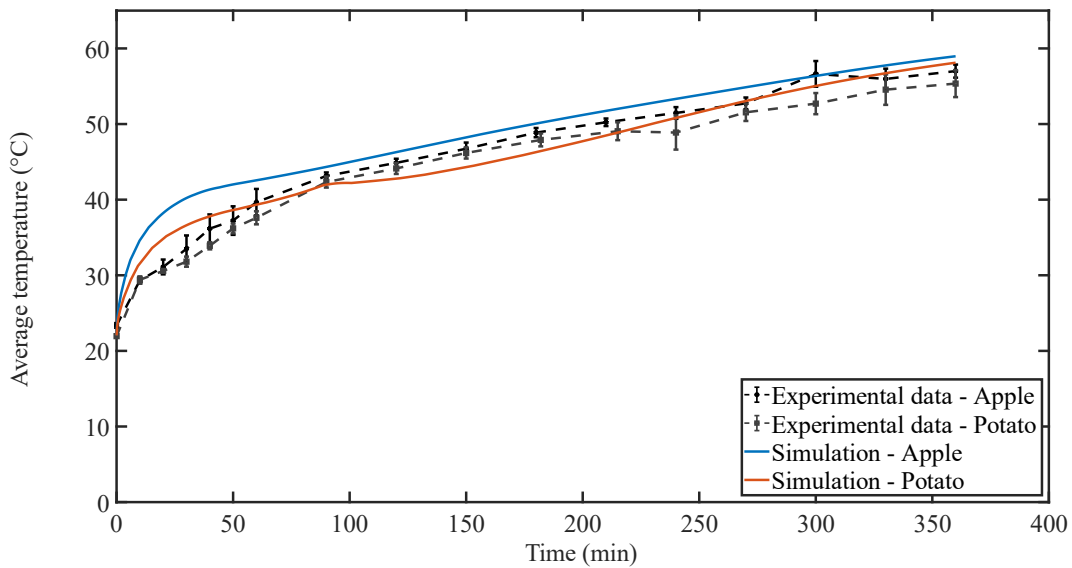


Figure 5.12. Average temperature ($^{\circ}\text{C}$) for drying at $64\text{ }^{\circ}\text{C}$. Error bars represent plus-minus one standard deviation of the triplicate experimental data.

Equilibrium vapor pressure when drying at medium temperatures

The average equilibrium vapor pressure in relation to the ICW content can be seen in Figure 5.13 and Figure 5.14 for apple and potato respectively. When the rupture threshold is reached, minimal pressure gradient exists within the sample. The distribution is very similar to the distribution uncovered within the threshold development. This can be seen when comparing Figure 5.9 (a) and (b) to Figure 5.13 (a) and Figure 5.14 (a). Once the threshold is reached, a significant pressure gradient. This trend exists for both materials.

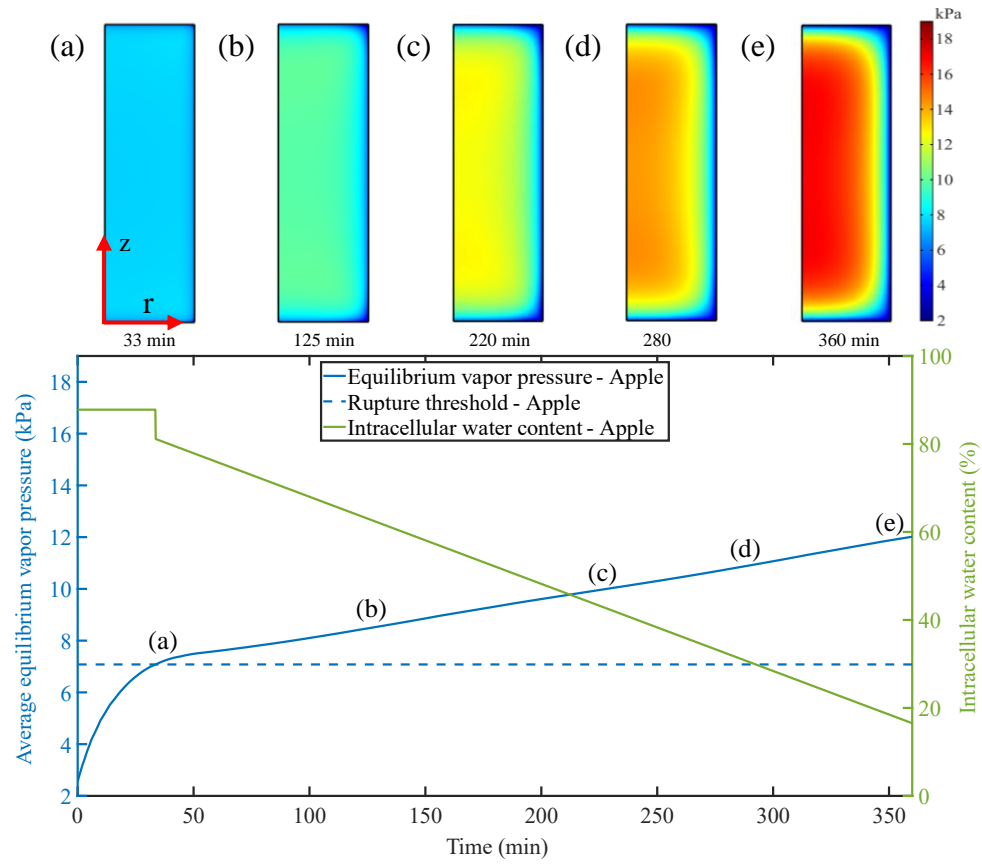


Figure 5.13. The average equilibrium vapor pressure (kPa) and ICW content (%) of apple drying at 64 °C. Spatial distribution of the equilibrium vapor pressure at (a) 33 mins (when threshold is reached), (b) 125 mins, (c) 220 mins, (d) 280 mins and (e) 360 mins.

The ICW content with respect to time can be seen for each material in Figure 5.13 and Figure 5.14. Each material remains at its initial percentage until the threshold is reached. Once the rupture threshold is reached the ICW content linearly decreases. The rate at which ICW linearly decreases was precomputed based on the initial and final ICW percentages within published literature (Khan et al., 2018; Khan et al., 2017b). This precomputation creates the sharp drop in ICW content when the threshold is reached for each material. Potato reaches its threshold later in drying therefore the drop is greater, causing the uneven transition discussed within the temperature profile (Figure 5.12).

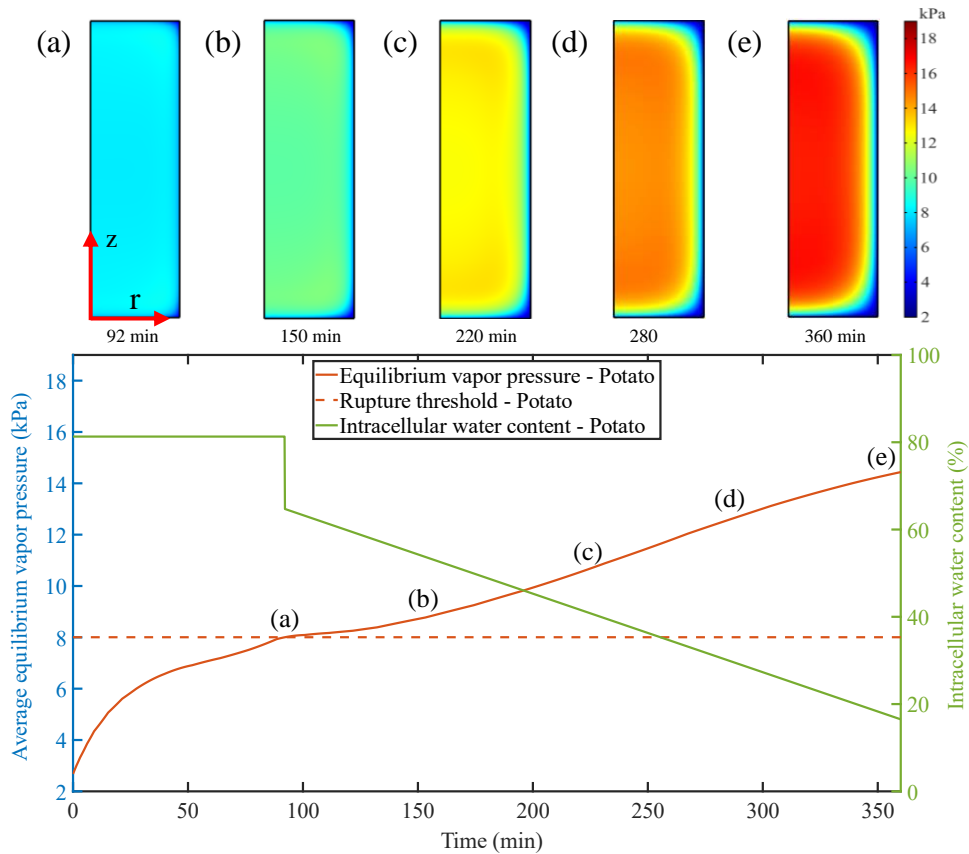


Figure 5.14. The average equilibrium vapor pressure (kPa) and ICW content (%) of potato drying at 64 °C. Spatial distribution of the equilibrium vapor pressure at (a) 92 mins (when threshold is reached), (b) 125 mins, (c) 220 mins, (d) 280 mins and (e) 360 mins.

5.5.4 Sensitivity investigation

The constructed multiscale model requires a large number of input parameters, Table 5.1 and Table 5.2. Some of these key parameters contain uncertainty or variability due to their availability in literature and the nature of fruits and vegetables. Therefore, it is important to conduct a sensitivity investigation to have greater confidence in the presented model. For example, the density of apple tissue can vary from the inner and outer parenchyma by about 12% (Mavroudis et al., 1998). To evaluate the sensitivity of the predicted model, the material density and the heat transfer coefficient were investigated by varying the utilised values by $\pm 10\%$ while drying at low temperatures. These parameters were investigated in relation to the average moisture content (kg/kg dry bases) and average temperature (°C).

The presented model's sensitivity to density can be seen in Figure 5.15. The average moisture content is not sensitive to the change in density, Figure 5.15 (a). However, the changes in density do influence the temperature profile in the later stages of drying. For both materials, plus 10% underpredicts the average temperature, whereas minus 10% causes a small overprediction, Figure 5.15 (b). The change in density did not improve the model's ability to predict the temperature profile in the early stages of drying.

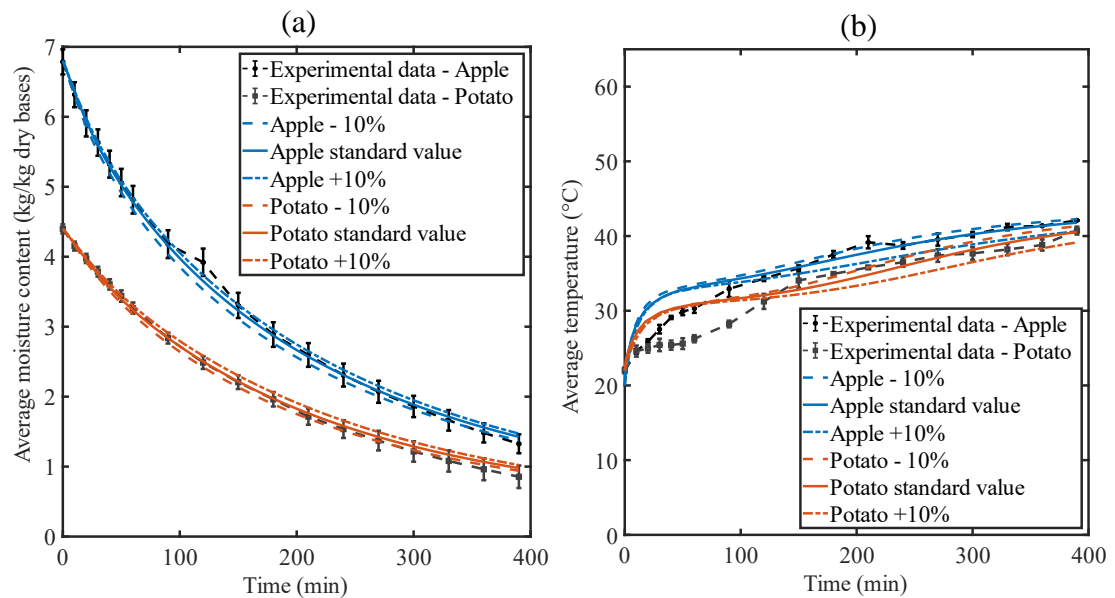


Figure 5.15. Sensitivity investigation for the material density $\pm 10\%$, a) average moisture content (kg/kg dry bases), b) average temperature ($^{\circ}\text{C}$).

The presented model's sensitivity to the heat transfer coefficient can be seen in Figure 5.16. The moisture content was not significantly influenced by the change in heat transfer coefficient, Figure 5.16 (a), however as expected, the temperature profile was sensitive to the heat transfer coefficient. For both materials, plus 10% caused a small overprediction in the temperature profile, whereas minus 10% caused a substantial underprediction, Figure 5.16 (b). Therefore, underpredicting the heat transfer coefficient has a larger influence on the presented model.

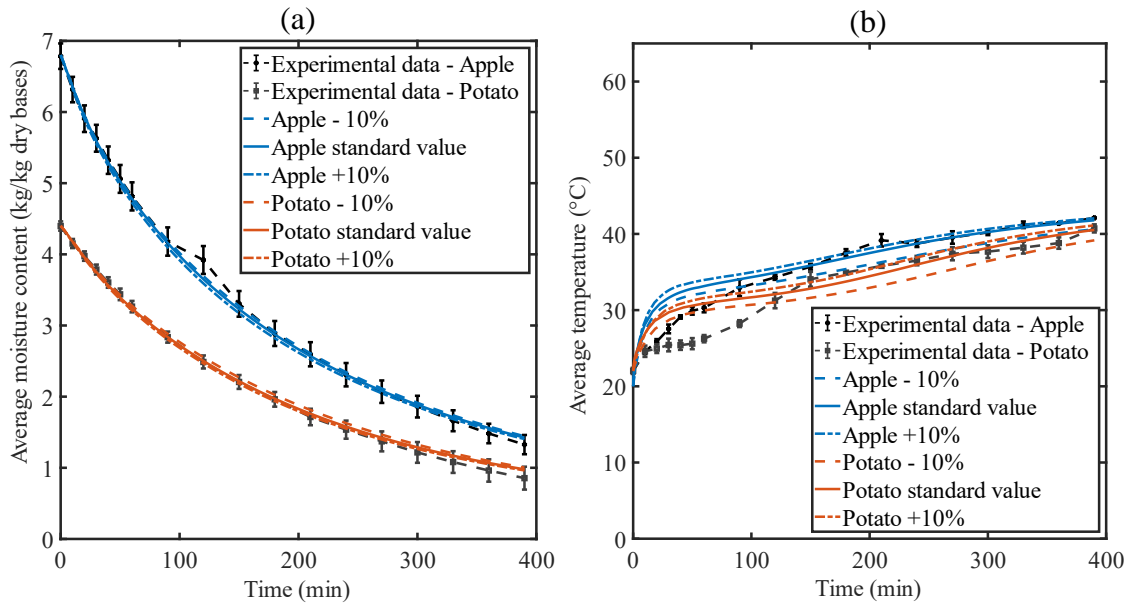


Figure 5.16. Sensitivity investigation for the heat transfer coefficient $\pm 10\%$, a) average moisture content (kg/kg dry bases), b) average temperature ($^{\circ}\text{C}$).

5.6 DISCUSSION

The generalized diffusivity successfully describes drying at low and medium temperatures for both materials. The effective diffusivity function was able to distinguish the materials through their ICW content rather than their porosity. The generalized diffusivity is in terms of temperature and ICW content, allowing the property to be applicable for multiple materials (apple and potato) drying at multiple temperatures (with different microstructural deformation). The theoretical cell rupturing threshold allowed the property to appropriately adapt to the different drying conditions. At low temperatures the threshold is not reached, and the effective diffusivity remains fairly constant, Figure 5.7. This suggests an average diffusion coefficient is sufficient when drying at lower temperatures. Defraeye and Verboven (2017) also concluded that a constant diffusivity coefficient is sufficient for engineering problems drying at low temperatures ($20\text{ }^{\circ}\text{C}$). At medium temperatures the threshold is reached, causing the effective diffusivity to spike and peak in the middle stages of drying, Figure 5.11. This is somewhat contradictory to published literature where generally the effectivity diffusivity gradually decreases with moisture (Dadmohammadi & Datta, 2019; Hassini et al., 2007). Though these studies do not consider cell rupturing. It is well established FW is effortlessly transported during drying (Welsh et al., 2018). Therefore, if we assume once a cell is ruptured the ICW

water rushes out of the cell and becomes FW, logically there should be a spike/large increase in the effective diffusivity of the material. Toward the latter stages of drying the effective diffusivity drops off, matching the published trends in literature, Figure 5.11. Though it is unclear if the magnitude of the drop is correct. The presented model does begin to deviate in the latter stages of drying. In fact, the model deviates in the latter stages for both materials at both drying temperatures, most predominate is potato drying at 64 °C. The model simplifies some aspects of food material such as considering the material as single phase, no macroscale deformation and considering an average mass transfer coefficient. This was done to keep a reasonable computational cost and to focus on the generalized diffusivity. Vapor transport can play a large role in the final stages of drying. Some consideration of the macroscale deformation, a multiphase material and/or transfer coefficients which are spatially dependent and/or influenced by deformation will improve the model's prediction in the latter stages.

There were two key assumption made in order to achieve the novel generalized property. These were centrally focused around the ICW and its trend during drying. The first major assumption was to assume the ICW content remains constant at its initial percentage when cell rupturing does not occur. When drying at lower temperatures (where cell rupturing does not occur) the average ICW content over the drying time is slightly below its initial percentage (roughly 5% below, inferred from (Welsh et al., 2021)). This is due to the evolution of the material, microscale deformation and porosity. Considering this marginal difference would require comprehensive knowledge of the microstructural evolution (extensive experimental investigation) and increase the computational cost. Therefore, the assumption was made to keep the ICW content constant at its initial percentage. The rate at which ICW linearly decreased when cell rupturing occurs was the second key assumption. The rate was deduced from published literature (Khan et al., 2018; Khan et al., 2017b) and considered in terms of drying time. This is not ideal and is a limitation of the presented model. More work is required to develop an improved function describing the trend of ICW content once the cell rupturing threshold is reached. Recent advancements in experimental investigating techniques will aid in developing these functions (Dadmoammadi, et al., 2020; Khan, Farrell, et al., 2018; Khan, Patel, Mahiuddin, & Karim, 2021).

5.7 CONCLUSION

The generalized diffusivity successfully described drying at low and medium temperatures for both materials (apple and potato). A novel theoretical equilibrium vapor pressure threshold was introduced, allowing the model to recognize if and when cell rupturing had occurred. This resulted in unique rupture thresholds for each material. Being able to recognize if cell rupturing has occurred greatly improved the predictive capabilities of the diffusivity. Additionally, this will allow future researchers to conduct in depth optimization investigations. The generalized property resulted in effective diffusivities of 1.94×10^{-10} - 4.59×10^{-10} m²/s for apple and 2.51×10^{-10} - 5.14×10^{-10} m²/s for potato. The presented model only moderately predicted the experimental temperature profile. The model could be refined by introducing more general heat and mass transfer coefficients that depend on position and time as a result of material deformation. However, this will increase the computational cost of the mathematical model. The generalized diffusivity will aid in mathematical food drying models reaching their full potential.

5.8 ACKNOWLEDGEMENTS

This study was funded by the Department of Education and Training (AUS) through a Research Training Program (Stipend) Domestic (RTP) scholarship. The third author acknowledges the supports from the Advance Queensland Fellowship Project (AQF) (the grant ID: 02073-2015-30358/15).

REFERENCES

- Adrover, A., Brasiello, A., & Ponso, G. (2019). A moving boundary model for food isothermal drying and shrinkage: General setting. *Journal of Food Engineering*, 244, 178-191. <https://doi.org/10.1016/j.jfoodeng.2018.09.018>
- Aregawi, W. A., Abera, M. K., Fanta, S. W., Verboven, P., & Nicolai, B. (2014). Prediction of water loss and viscoelastic deformation of apple tissue using a multiscale model. *Journal of Physics: Condensed Matter*, 26, 464111. <https://doi.org/10.1088/0953-8984/26/46/464111>
- Asabe, J., & Home, A. American society of agricultural and biological engineers.
- Auriault, J.-L., Boutin, C., & Geindreau, C. (2010). *Homogenization of coupled phenomena in heterogenous media* (Vol. 149): John Wiley & Sons.
- Beigi, M. (2016). Influence of drying air parameters on mass transfer characteristics of apple slices. *Heat and Mass Transfer*, 52(10), 2213-2221. <https://doi.org/10.1007/s00231-015-1735-8>
- Białobrzewski, I. (2006). Simulation of changes in the density of an apple slab during drying. *International Communications in Heat and Mass Transfer*, 33(7), 880-888. <https://doi.org/10.1016/j.icheatmasstransfer.2006.02.017>
- Carr, E. J., & Turner, I. W. (2014). Two-scale computational modelling of water flow in unsaturated soils containing irregular-shaped inclusions. *International Journal for Numerical Methods in Engineering*, 98, 157-173. <https://doi.org/10.1002/nme.4625>
- Cengel, Y. (2003). *Heat, Transfer Mass: A practical approach*: Mc-Graw Hill Education, Columbus, GA, USA.
- Cengel, Y. A., & Boles, M. A. (2002). Thermodynamics: an engineering approach. *Sea, 1000*, 8862.
- Chua, K. J., Mujumdar, A. S., Hawlader, M. N. A., Chou, S. K., & Ho, J. C. (2001). Convective drying of agricultural products. Effect of continuous and stepwise change in drying air temperature. *Drying Technology*, 19(8), 1949-1960. <https://doi.org/10.1081/DRT-100107282>

- Dadmohammadi, Y., & Datta, A. K. (2019). Prediction of effective moisture diffusivity in plant tissue food materials over extended moisture range. *Drying Technology*, 1-15. <https://doi.org/10.1080/07373937.2019.1690500>
- Dadmohammadi, Y., Kantzas, A., Yu, X., & Datta, A. K. (2020). Estimating permeability and porosity of plant tissues: Evolution from raw to the processed states of potato. *Journal of Food Engineering*, 277, 109912. <https://doi.org/10.1016/j.jfoodeng.2020.109912>
- Datta, A. K. (2007). Porous media approaches to studying simultaneous heat and mass transfer in food processes. I: Problem formulations. *Journal of Food Engineering*, 80(1), 80-95. <https://doi.org/10.1016/j.jfoodeng.2006.05.013>
- Defraeye, T. (2014). Advanced computational modelling for drying processes – A review. *Applied Energy*, 131, 323-344. <https://doi.org/10.1016/j.apenergy.2014.06.027>
- Defraeye, T., & Radu, A. (2018). Insights in convective drying of fruit by coupled modeling of fruit drying, deformation, quality evolution and convective exchange with the airflow. *Applied Thermal Engineering*, 129, 1026-1038. <https://doi.org/10.1016/j.applthermaleng.2017.10.082>
- Defraeye, T., & Verboven, P. (2017). Convective drying of fruit: Role and impact of moisture transport properties in modelling. *Journal of Food Engineering*, 193, 95-107. <http://dx.doi.org/10.1016/j.jfoodeng.2016.08.013>
- Dincer, I., & Zamfirescu, C. (2016). *Drying phenomena: theory and applications*: John Wiley & Sons.
- Fanta, S. W., Abera, M. K., Ho, Q. T., Verboven, P., Carmeliet, J., & Nicolai, B. M. (2013). Microscale modeling of water transport in fruit tissue. *Journal of Food Engineering*, 118, 229-237. <https://doi.org/10.1016/j.jfoodeng.2013.04.003>
- Geuzaine, C., & Remacle, J. F. (2009). Gmsh: A 3-D finite element mesh generator with built-in pre-and post-processing facilities. *International journal for numerical methods in engineering*, 79(11), 1309-1331. <https://doi.org/10.1002/nme.2579>

- Golestani, R., Raisi, A., & Aroujalian, A. (2013). Mathematical modeling on air drying of apples considering shrinkage and variable diffusion coefficient. *Drying Technology*, 31, 40-51. <https://doi.org/10.1080/07373937.2012.714826>
- Gulati, T., & Datta, A. K. (2015). Mechanistic understanding of case-hardening and texture development during drying of food materials. *Journal of Food Engineering*, 166, 119-138. <https://doi.org/10.1016/j.jfoodeng.2015.05.031>
- Halder, A., Datta, A. K., & Spanswick, R. M. (2011). Water transport in cellular tissues during thermal processing. *AICHE Journal*, 57(9), 2574-2588. <https://doi.org/10.1002/aic.12465>
- Hassini, L., Azzouz, S., Peczalski, R., & Belghith, A. (2007). Estimation of potato moisture diffusivity from convective drying kinetics with correction for shrinkage. *Journal of Food Engineering*, 79(1), 47-56. <https://doi.org/10.1016/j.jfoodeng.2006.01.025>
- Khan, M. I. H., Farrell, T., Nagy, S. A., & Karim, M. A. (2018). Fundamental Understanding of Cellular Water Transport Process in Bio-Food Material during Drying. *Scientific Reports*, 8(1), 15191. <https://doi.org/10.1038/s41598-018-33159-7>
- Khan, M. I. H., & Karim, M. A. (2017). Cellular water distribution, transport, and its investigation methods for plant-based food material. *Food Research International*, 99(Part 1), 1-14. <https://doi.org/10.1016/j.foodres.2017.06.037>
- Khan, M. I. H., Kumar, C., Joardder, M. U. H., & Karim, M. A. (2017). Determination of appropriate effective diffusivity for different food materials. *Drying Technology*, 35, 335-346. <https://doi.org/10.1080/07373937.2016.1170700>
- Khan, M. I. H., Nagy, S. A., & Karim, M. A. (2018). Transport of cellular water during drying: An understanding of cell rupturing mechanism in apple tissue. *Food Research International*, 105, 772-781. <https://doi.org/10.1016/j.foodres.2017.12.010>
- Khan, M. I. H., Patel, N., Mahiuddin, M., & Karim, M. A. (2021). Characterisation of mechanical properties of food materials during drying using nanoindentation. *Journal of Food Engineering*, 291, 110306. <https://doi.org/10.1016/j.jfoodeng.2020.110306>

Khan, M. I. H., Wellard, R. M., Nagy, S. A., Joardder, M. U. H., & Karim, M. A. (2016). Investigation of bound and free water in plant-based food material using NMR T2 relaxometry. *Innovative Food Science & Emerging Technologies*, 38, 252-261. <https://doi.org/10.1016/j.ifset.2016.10.015>

Khan, M. I. H., Wellard, R. M., Nagy, S. A., Joardder, M. U. H., & Karim, M. A. (2017a). Experimental investigation of bound and free water transport process during drying of hygroscopic food material. *International Journal of Thermal Sciences*, 117(Supplement C), 266-273. <https://doi.org/10.1016/j.ijthermalsci.2017.04.006>

Khan, M. I. H., Wellard, R. M., Nagy, S. A., Joardder, M. U. H., & Karim, M. A. (2017b). Experimental investigation of bound and free water transport process during drying of hygroscopic food material. *International Journal of Thermal Sciences*, 117, 266-273. <https://doi.org/10.1016/j.ijthermalsci.2017.04.006>

Khan, M. Imran H., Welsh, Z., Gu, Y., Karim, M. A., & Bhandari, B. (2020). Modelling of simultaneous heat and mass transfer considering the spatial distribution of air velocity during intermittent microwave convective drying. *International Journal of Heat and Mass Transfer*, 153, 119668. <https://doi.org/10.1016/j.ijheatmasstransfer.2020.119668>

Kudra, T. (2004). Energy Aspects in Drying. *Drying Technology*, 22(5), 917-932. <https://doi.org/10.1081/DRT-120038572>

Lentzou, D., Boudouvis, A. G., Karathanos, V. T., & Xanthopoulos, G. (2019). A moving boundary model for fruit isothermal drying and shrinkage: An optimization method for water diffusivity and peel resistance estimation. *Journal of Food Engineering*, 263, 299-310. <https://doi.org/10.1016/j.jfoodeng.2019.07.010>

Mahiuddin, M., Khan, M. I. H., Kumar, C., Rahman, M. M., & Karim, M. A. (2018). Shrinkage of food materials during drying: Current status and challenges. *Comprehensive Reviews in Food Science and Food Safety*, 17 (5), 1113-1126. <https://doi.org/10.1111/1541-4337.12375>

- Mattea, M., Urbicain, M. J., & Rotstein, E. (1986). Prediction of Thermal Conductivity of Vegetable Foods by the Effective Medium Theory. *Journal of Food Science*, 51(1), 113-115. <https://doi.org/10.1111/j.1365-2621.1986.tb10848.x>
- Mavroudis, N. E., Gekas, V., & Sjöholm, I. (1998). Osmotic dehydration of apples—effects of agitation and raw material characteristics. *Journal of Food Engineering*, 35(2), 191-209. [https://doi.org/10.1016/S0260-8774\(98\)00015-6](https://doi.org/10.1016/S0260-8774(98)00015-6)
- Pace, E. L. (1962). Scientific foundations of vacuum technique (Dushman, Saul). *Journal of Chemical Education*, 39(8), A606. <https://doi.org/10.1021/ed039pA606>
- Pavliotis, G. A., & Stuart, A. (2008). *Multiscale methods: averaging and homogenization*: Springer Science & Business Media.
- Prawiranto, K., Defraeye, T., Derome, D., Verboven, P., Nicolai, B., & Carmeliet, J. (2018). New insights into the apple fruit dehydration process at the cellular scale by 3D continuum modeling. *Journal of Food Engineering*, 239, 52-63. <https://doi.org/10.1016/j.jfoodeng.2018.06.023>
- Prothon, F., Ahrné, L., & Sjöholm, I. (2003). Mechanisms and Prevention of Plant Tissue Collapse during Dehydration: A Critical Review. *Critical Reviews in Food Science and Nutrition*, 43(4), 447-479. <https://doi.org/10.1080/10408690390826581>
- Rahman, M. M., Joardder, M. U. H., Khan, M. I. H., Nghia, D. P., & Karim, M. A. (2018). Multi-scale model of food drying: Current status and challenges. *Critical Reviews in Food Science and Nutrition*. <https://doi.org/10.1080/10408398.2016.1227299>
- Ratti, C., Crapiste, G., & Rotstein, E. (1989). A new water sorption equilibrium expression for solid foods based on thermodynamic considerations. *Journal of Food Science*, 54(3), 738-742. <https://doi.org/10.1111/j.1365-2621.1989.tb04693.x>
- Simpson, R., Ramírez, C., Birchmeier, V., Almonacid, A., Moreno, J., Nuñez, H., & Jaques, A. (2015). Diffusion mechanisms during the osmotic dehydration of

Granny Smith apples subjected to a moderate electric field. *Journal of Food Engineering*, 166, 204-211. <https://doi.org/10.1016/j.jfoodeng.2015.05.027>

Tripathy, P. P., & Kumar, S. (2009). Modeling of heat transfer and energy analysis of potato slices and cylinders during solar drying. *Applied Thermal Engineering*, 29(5), 884-891. <https://doi.org/10.1016/j.applthermaleng.2008.04.018>

Tzempelikos, D. A., Mitrakos, D., Vouros, A. P., Bardakas, A. V., Filios, A. E., & Margaris, D. P. (2015). Numerical modeling of heat and mass transfer during convective drying of cylindrical quince slices. *Journal of Food Engineering*, 156, 10-21. <https://doi.org/10.1016/j.jfoodeng.2015.01.017>

Vega-Mercado, H., Marcela Góngora-Nieto, M., & Barbosa-Cánovas, G. V. (2001). Advances in dehydration of foods. *Journal of Food Engineering*, 49(4), 271-289. [https://doi.org/10.1016/S0260-8774\(00\)00224-7](https://doi.org/10.1016/S0260-8774(00)00224-7)

Welsh, Z., Khan, M. I. H., Simpson, M. J., & Karim, M. (2020). A multiscale approach to estimate the cellular diffusivity during food drying. *Food Research International*, (Under review).

Welsh, Z., Simpson, M. J., Khan, M. I. H., & Karim, M. (2018). Multiscale Modeling for Food Drying: State of the Art. *Comprehensive Reviews in Food Science and Food Safety*, 17(5), 1293-1308. <https://doi.org/10.1111/1541-4337.12380>

Welsh, Z. G., Khan, M. I. H., & Karim, M. (2021). Multiscale modeling for food drying: A homogenized diffusion approach. *Journal of Food Engineering*, 292, 110252. <https://doi.org/10.1016/j.jfoodeng.2020.110252>

Chapter 6: Conclusions

This chapter provides a summary of the research, specific conclusions, the contributions and significance of the research, limitations of the study and future work.

6.1 CONCLUSIONS

This research applied multiscale modelling to develop a moisture diffusivity with improved predictive capabilities for drying plant-based food material. The approach investigated the cellular water heterogeneity, in terms of space and time, to construct a generalised moisture diffusivity. The generalised diffusivity was capable of distinguishing between materials, while accurately describing the drying kinetics at various drying temperatures. The specific objectives of the study were:

1. Develop a multiscale homogenisation model capable of incorporating the spatial cellular water heterogeneity of food material during drying.
2. Utilise the constructed multiscale model to investigate the temporal water heterogeneity of food material during drying.
3. Develop a comprehensive multiscale model with a generalised moisture diffusivity to investigate its predictive capabilities for drying plant-based food material.

Chapter 2 presented a comprehensive literature review on multiscale modelling for the application of drying plant-based food materials. During drying, food material experiences unique deformation under an external heat source, restricting the applicability of published multiscale literature. The review investigated past multiscale literature, multiscale frameworks, solution techniques for space and time, challenges for the topic and future directions. The chapter concluded that one-way and two-way coupled models hold potential for establishing multiscale modelling within the field. However, concerns were raised for one-way coupled models, as their scaling (upscaling/downscaling) operation is precomputed. Therefore, if drying causes the microstructure of the material to change drastically, one-way coupled models may not be capable of capturing these changes. Therefore, a concurrent approach or an approach which dynamically depends of the microscale may be more applicable.

Chapter 3 introduced the core multiscale model of the thesis and focused on considering the spatial water heterogeneity in food material during drying. The work constructed a single-phase axisymmetric model simulating the simultaneous heat and mass transport of apple tissue drying at three different temperatures (45, 60 and 70 °C). Additionally, the multiscale approach was compared to existing techniques for moisture diffusivity. The chapter found that the material's heterogeneous microstructure was able to be approximated by considering two cellular subdomains, intracellular spaces and intercellular spaces. This groups the effects of the protoplast, cell membrane and cell wall within the intracellular subdomain. Additionally, by having unique microscale domains at each drying temperature (varying the heterogeneity), the model was able to accurately describe the drying kinetics. However, this required comprehensive knowledge of the microstructural evolution at each drying temperature. The model also only moderately predicted drying at higher temperatures, unable to adapt to the dynamic cellular heterogeneity and additional processes occurring at these temperatures (i.e. case hardening).

Chapter 4 conducted a temporal investigation on the constructed multiscale model, investigating the temporal heterogeneity to deduce the diffusivity of ICW. An inverse study was used and the real cellular phase morphology with appropriate assumptions to represent its dynamic heterogeneity were investigated. Three approaches were considered to approximate the dynamic heterogeneity of ICW: considering an average, considering a linear decrease and considering diffusivity in stages. It was found, when significant cell rupturing occurs, the dynamic heterogeneity can be approximately by assuming a linear decrease in ICW content. Therefore, a relationship for the diffusivity of ICW in terms of two variables, sample temperature and ICW content, was created. The constructed relationship is applicable to various food materials through considering their ICW content.

Chapter 5 combined the findings of Chapter 3 and 4 to develop a comprehensive multiscale model with a generalised moisture diffusivity for drying plant-based food material. The model investigated two materials (apple and potato) drying at two different drying temperatures (low and medium). The ICW diffusivity relationship, constructed in Chapter 4, was utilised to develop a single upscaled effective diffusivity for both materials. The upscaled property was in terms of sample temperature and ICW content, therefore dynamically depending on the microstructural evolution. In order to

utilise the upscaled property, a novel rupture threshold was developed and presented. The threshold exploited the equilibrium vapor pressure to characterise which transport mechanisms were occurring. This resulted in a unique rupture threshold for each material. The generalised diffusivity demonstrated improved predictive capabilities, being able to successfully describe the drying kinetics of multiple materials (apple and potato) drying at multiple temperatures (low and medium).

This thesis achieved its aims and objectives and as a result constructed a generalised moisture diffusivity with improved predictive capabilities. The findings of this study will allow mathematical food drying models to reach their full potential, transitioning away from condition-dependent properties, while improving a model's predictive capabilities.

The following specific conclusions can be drawn from the study:

- The multiscale mathematical model and generalised diffusivity accurately considered the spatial and temporal water heterogeneity within food material during drying. Additionally, the multiscale model considers cell rupturing.
- When the microstructural evolution is well known, through an extensive experimental investigation, the average cellular heterogeneity can be considered. This is especially applicable when drying below 50°C where minimal cell rupturing occurs.
- When significant deformation (cell rupturing) occurs, the dynamic cellular water heterogeneity can be approximated by assuming a linear decrease in the ICW content of the material.
- When the microstructural evolution is not well defined, the comprehensive multiscale model can be applied.
- Cell rupturing can be considered through the novel rupture threshold exploiting the equilibrium vapor pressure to characterise which transport mechanisms are occurring.

6.2 CONTRIBUTION TO KNOWLEDGE AND SIGNIFICANCE OF THIS RESEARCH

The specific contributions and significance of this research are listed below:

- A novel multiscale model for drying plant-based food material is presented. The model will allow future mathematical models to transition towards more physics-based models, improving their accuracy and predictive capabilities while minimising their dependency on condition-dependent properties.
- The generalised moisture diffusivity will allow future researchers to conduct large scale optimisation investigations to optimise drying processes, systems and configurations for minimal experimental cost. Specifically, utilising the generalised property can significantly reduce the experimental cost when designing a drier to dry multiple materials, requiring only one material to be investigated experimentally. This will aid in the development of optimum drying systems with improved food quality.
- The multiscale model can be used by industry to accurately predict the drying time, drying kinetics and the energy requirements of a particular drier's design, aiding in the development of optimal drying systems. The generalised property and multiscale model would be particularly useful when designing commercial scale driers, taking advantage of the generalised property.
- The novel rupturing threshold allows models to characterise which transport mechanisms and associated cellular deformation is occurring. During convective drying, the rupturing and deformation of cells have many negative consequences on the final quality of food material, leading to taste, colour and nutritional deterioration (Maskan, 2001). Therefore, being able to predict cell rupturing computationally will allow new investigations to be conducted with the intent of minimising shrinkage while improving quality. Additionally, the multiscale model provides a platform to consider anisotropic cellular deformation, allowing more accurate shrinkage models to be developed in the future.
- The multiscale approach can be applied to other properties, i.e. thermal conductivity, to further advance mathematical models.

- The constructed ICW diffusivity relationship will aid in the development of in-depth microscale models, providing new insight into what occurs at a cellular scale when drying food material.

6.3 RESEARCH LIMITATIONS AND FUTURE WORK

Within this study there are some limitations which can be overcome in future works. These are:

- **The energy conservation equation used throughout this research does not consider the heat flux due to internal moisture migration.** The simplified energy conservation equation used assumes due to the low drying rate food material experiences during convective drying the heat flux due to internal moisture migration can be neglected (Defraeye & Verboven, 2017). However, at higher temperatures this assumption can become less valid. Therefore, in future works the energy balance can be extended to consider these additional terms.
- **The developed multiscale approach did not consider macroscale deformation and the effects of heat and mass transfer coefficients varying in space and time.** The multiscale model could be extended to include these phenomena. Additionally, the macroscale deformation could be coupled with the microstructural evolution to incorporate anisotropic deformation. This would further improve the model's predictive capabilities but also increase its computational cost, requiring additional governing equations to complete the model (i.e. a turbulence model and solid mechanics with a moving mesh). The author did aid in conducting a separate investigation (Khan et al., 2020) looking into the effects of a velocity field on the heat and mass transfer coefficients of apple tissue during drying (investigating the effects of space).
- **When considering two cellular subdomains, the multiscale approach was only moderately accurate when drying at higher temperatures.** Additional processes occur when drying at higher temperature, i.e. case hardening. Future studies can work to extend the multiscale model to incorporate these phenomena using published macroscale multiphase non-equilibrium models as a foundation (Gulati & Datta, 2015).

- **The developed ICW diffusivity relationship groups the effects of the protoplast, cell membrane and cell wall within the intracellular subdomain.** This grouping is efficient and saves on computational cost when the macroscale results are the focus of the mathematical model. However, this grouping may not always be appropriate and could restrict the applicability of the multiscale approach. Further microscale experimental investigations and mathematical models need to be developed to provide new insight into the microscale transport and the properties of these cellular environments during drying. New developments in experimental techniques will aid in this research (Dadmohammadi et al., 2020; Khan et al., 2021).
- **The generalised diffusivity is precomputed using the multiscale approach.** The approach can be extended to produce a concurrent multiscale model. In Chapter 5, the generalised diffusivity actively depends on the microstructural evolution using the ICW trend and rupture threshold. The approach could be refined to construct a concurrent model, removing the ICW trend assumptions, using the microstructural evolutions directly.
- **The representation of microstructure facilitates isotropic homogenised diffusivity.** Throughout this work, all intercellular spaces were grouped and represented as a circle within the microscale domains. This is efficient and effective, requiring minimal microstructural knowledge. However, the circle is assumed to be located at the centre of the domain, forcing the homogenised diffusivity to be isotropic. The model could be extended to consider anisotropic diffusivity by considering an off-centred circle or the real microstructure of the material. However, this will also require a concurrent model to accurately predict its evolution with time. Additionally, considering the real cellular structure and its microstructural evolution could allow anisotropic deformation to be considered.
- **The generalised diffusivity only investigated two materials, apple and potato.** In chapter 5, the developed generalised diffusivity was investigated with two materials under two different drying conditions (drying at low and medium temperatures). This allowed its predictive capabilities to be investigated in depth for various forms of cellular deformation. Apples and potatoes are the most common food materials investigated with theoretical model for drying, and as a result limited knowledge exist for constructing mathematical models for other food

materials. In the future, the diffusivity could be utilised to investigate more food materials. However, to achieve this goal, significant research is required within the field to uncover others materials microstructural evolution and establish their accurate thermal properties (i.e. effective specific heat or thermal conductivity).

6.4 FINAL REMARKS

Within this thesis, multiscale modelling was applied to develop a generalised moisture diffusivity for food material during drying. The constructed model considered two spatial scales, a microscale and a macroscale, to incorporate the materials heterogeneity in terms of space and time. Additionally, to improve the predictive capabilities of the generalised property, cell rupturing was considered through a novel rupture threshold. The threshold was unique for each material. The constructed generalised moisture diffusivity demonstrated great predictive capabilities, being able to distinguish between materials through considering their ICW content. The novel model will aid in the development of optimum drying systems with improved food quality, facilitating in depth investigations to optimise drying processes, systems and configurations for minimal experimental cost.

REFERENCES

- Dadmohammadi, Y., Kantzas, A., Yu, X., & Datta, A. K. (2020). Estimating permeability and porosity of plant tissues: Evolution from raw to the processed states of potato. *Journal of Food Engineering*, 277, 109912. <https://doi.org/10.1016/j.jfoodeng.2020.109912>
- Defraeye, T., & Verboven, P. (2017). Convective drying of fruit: Role and impact of moisture transport properties in modelling. *Journal of Food Engineering*, 193, 95-107. <https://doi.org/http://dx.doi.org/10.1016/j.jfoodeng.2016.08.013>
- Gulati, T., & Datta, A. K. (2015). Mechanistic understanding of case-hardening and texture development during drying of food materials. *Journal of Food Engineering*, 166, 119-138. <https://doi.org/10.1016/j.jfoodeng.2015.05.031>
- Khan, M. I. H., Patel, N., Mahiuddin, M., & Karim, M. A. (2021). Characterisation of mechanical properties of food materials during drying using nanoindentation. *Journal of Food Engineering*, 291, 110306. <https://doi.org/10.1016/j.jfoodeng.2020.110306>
- Khan, M. Imran H., Welsh, Z., Gu, Y., Karim, M. A., & Bhandari, B. (2020). Modelling of simultaneous heat and mass transfer considering the spatial distribution of air velocity during intermittent microwave convective drying. *International Journal of Heat and Mass Transfer*, 153, 119668. <https://doi.org/10.1016/j.ijheatmasstransfer.2020.119668>
- Maskan, M. (2001). Kinetics of colour change of kiwifruits during hot air and microwave drying. *Journal of Food Engineering*, 48(2), 169-175. [https://doi.org/https://doi.org/10.1016/S0260-8774\(00\)00154-0](https://doi.org/https://doi.org/10.1016/S0260-8774(00)00154-0)

Appendices

APPENDIX A

a.) Heat and mass transfer coefficients

Temperature has minimal effect on the properties of air, with assumption (2) the air properties were considered at 60°C. The resulting heat and mass transfer coefficients can be found in Table A.1.

Table A.1. Summary of heat and mass calculations

Parameter	Value	Reference
Air velocity, v	0.7 m/s	This study
Characteristic length, L_c	0.03 m	This study
Density of air, ρ_{air}	1.051077 kg/m ³	Interpolated (Incropora, et al., 2011)
Specific heat of air, $c_{p\ air}$	1008.326 kJ/(kg·K)	Interpolated (Incropora et al., 2011)
Viscosity of air, μ_{air}	2.00512×10^{-5} kg/(m·s)	Interpolated (Incropora et al., 2011)
Kinematic viscosity of air, ν_{air}	1.92249×10^{-5} m ² /s	Interpolated (Incropora et al., 2011)
Thermal conductivity of air, k_{air}	0.028753 W/(m·K)	Interpolated (Incropora et al., 2011)
Prandtl number, Pr	0.702359	Interpolated (Incropora et al., 2011)
Binary mass diffusivity, D_{AB}	2.6×10^{-5} m ² /s	(Incropora et al., 2011)

Reynold's Number, Re_{L_c}	$\frac{\rho_{air} v L_c}{\mu} = 1100.813$	This study
Schmidt Number, Sc	$\frac{v}{D_{AB}} = 0.739$	This study
Nusselt number, Nu_{L_c}	$0.683 Re_{L_c}^{0.466} \text{Pr}^{1/3}$ $= 15.875$	This study
Sherwood number, Sh_{L_c}	$0.683 Re_{L_c}^{0.466} Sc^{1/3}$ $= 16.1494$	This study
Heat transfer coefficient, h_T	$\frac{k_{air} Nu_{L_c}}{L_c}$ $= 15.215 \text{ W / (m}^2 \cdot \text{K)}$	This study
Mass transfer coefficient, h_m	$\frac{D_{AB} Sh_{L_c}}{L_c} = 0.01 \text{ m / s}$	This study

b) *Calculating the average moisture content and temperature*

The average moisture content and temperature was calculated within COMSOL through the standard numerical integration method (quadrature) with an integration order of 4. This can be described as,

$$\frac{1}{\omega} \int f(x) d\omega \approx \frac{1}{\omega} \sum_i f(x_i) w_i \quad (\text{A.1})$$

where f is the variable (either moisture or temperature), x_i is the location of the integration points and w_i is the corresponding weight factors.

APPENDIX B

a.) Heat and mass transfer coefficients

All air properties were considered at 60°C. The resulting heat and mass transfer coefficients can be found in Table B.2.

Table B.2. Summary of heat and mass calculations

Parameter	Value	Reference
Air velocity, v	0.7 m/s	This study
Characteristic length, L_c	0.018 m	This study
Density of air, ρ_{air}	1.051077 kg/m ³	Interpolated (Incropera, et al., 2011)
Specific heat of air, $c_p \text{ air}$	1008.326 kJ/(kg·K)	Interpolated (Incropera, et al., 2011)
Viscosity of air, μ_{air}	2.00512×10^{-5} kg/(m·s)	Interpolated (Incropera, et al., 2011)
Kinematic viscosity of air, ν_{air}	1.92249×10^{-5} m ² /s	Interpolated (Incropera, et al., 2011)
Thermal conductivity of air, k_{air}	0.028753 W/(m·K)	Interpolated (Incropera, et al., 2011)
Prandtl number, Pr	0.702359	Interpolated (Incropera, et al., 2011)
Binary mass diffusivity, D_{AB}	2.6×10^{-5} m ² /s	(Incropera, et al., 2011)
Reynold's Number, Re_{L_c}	660.4875	This study
Schmidt Number, Sc	0.739	This study
Nusselt number, Nu_{L_c}	12.51	This study
Sherwood number, Sh_{L_c}	12.72842	This study
Heat transfer coefficient, h_T	19.98 W/(m ² ·K)	This study
Mass transfer coefficient, h_m	0.018 m/s	This study

b.) Statistics of property development

The residual plot of the developed property function can be seen in Figure B.1.

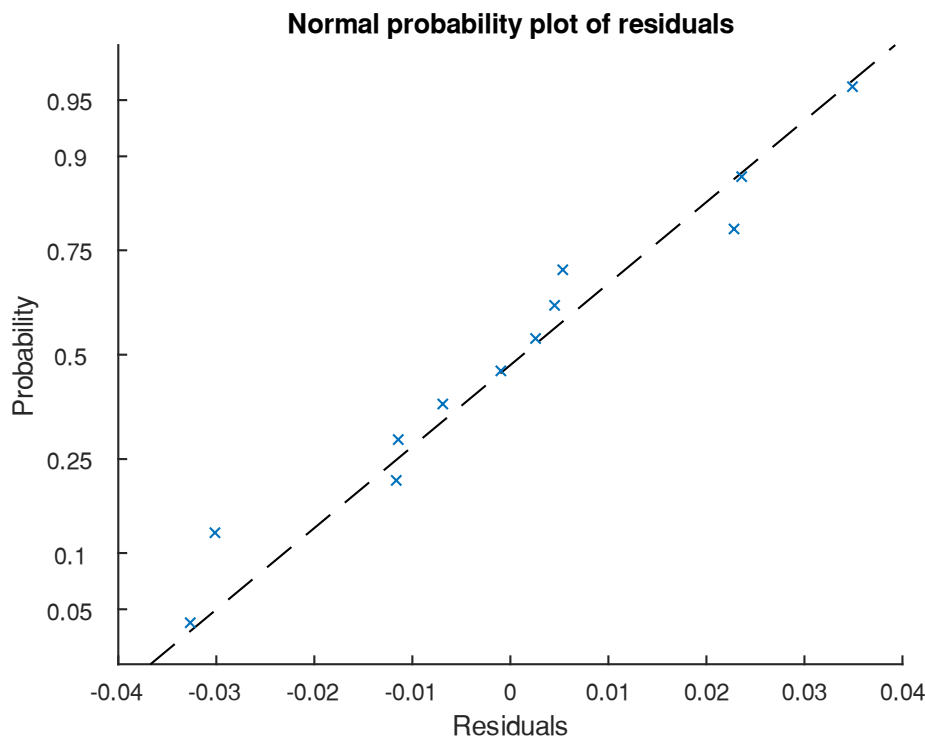


Figure B.1. Residual plot of the property developed for the diffusivity of ICW.

c.) **Converting concentrations to wet and dry bases.**

The wet and dry moisture contents were considered as,

$$M_{wb} = \frac{C M_w}{\rho} \quad (\text{B.1})$$

$$M_{db} = \frac{M_{wb}}{1 - M_{wb}} \quad (\text{B.2})$$

where M_{wb} is the wet bases moisture content (kg/kg wet bases), M_{db} is the dry bases moisture content (kg/kg dry basis), C is the instantaneous moisture concentration (mol/m^3), ρ is the density of apple tissue (kg/m^3) and M_w molar mass of water (kg/mol).

REFERENCES

Incropera, F. P., Bergman, T. L., Lavine, A. S., & Dewitt, D. P. (2011). *Fundamentals of heat and mass transfer* (Vol. 7th). Hoboken, N.J: John Wiley.

APPENDIX C

The average moisture content, temperature, equilibrium vapor pressure and diffusivity was calculated within COMSOL through the standard numerical integration method (quadrature) with an integration order of 4. This can be described as,

$$\frac{1}{\omega} \int f(x) d\omega \approx \frac{1}{\omega} \sum_i f(x_i) w_i \quad (\text{C.1})$$

where f is the variable (either moisture, temperature, equilibrium vapor pressure or diffusivity), x_i is the location of the integration points and w_i is the corresponding weight factors.

APPENDIX D

a) Boundary Condition investigation

During the examination process of this dissertation questions were raised about the boundary conditions used and therefore a boundary condition investigation was conducted. The boundary conditions for convective drying food material are represented in a few ways in literature. The heat and mass transfer boundary conditions used within this work were,

$$\mathbf{n} \cdot [-D\nabla C] = h_m \frac{(p_{v eq} - p_{v air})}{RT}, \quad (\text{D.1})$$

$$\mathbf{n} \cdot [-k \nabla T] = h_T (T - T_{air}) - h_m \frac{(p_{v eq} - p_{v air})}{RT} \lambda M_w, \quad (\text{D.2})$$

where C is the macroscale moisture concentration (mol/m^3), T is the material's temperature (K), k is the thermal conductivity of the food material ($\text{W}/(\text{m}\cdot\text{K})$), D is the cellular diffusivity (m^2/s), h_m is the mass transfer coefficient (m/s), h_T is the heat transfer coefficient ($\text{W}/(\text{m}^2\cdot\text{K})$), $p_{v eq}$ is the equilibrium vapor pressure, $p_{v air}$ is the vapor air pressure of ambient air (Pa), \mathbf{n} is the unit vector normal to the boundary, R is the universal gas constant ($\text{J}/(\text{mol}\cdot\text{K})$), T_{air} is the drying air temperature (K), M_w molar mass of water (g/mol) and λ is the latent heat of evaporation (J/kg). Within these boundary conditions $p_{v eq}$ is calculated from the material's sorption isotherm and $p_{v air}$ is calculated from considering the relative humidity and temperature of the external drying air [Full explanation on precomputing $p_{v air}$ can be found in Khan, et al. [1]]. This representation of the boundary conditions is common in literature [1, 2]. Examiner 2 proposed the following boundary conditions,

$$\mathbf{n} \cdot [-D\nabla C] = \frac{h_m}{R} \left(\frac{p_{v eq}}{T_s} - \frac{p_{v air}}{T_{air}} \right), \quad (\text{D.3})$$

$$\mathbf{n} \cdot [-k \nabla T] = h_T (T - T_{air}) - \frac{h_m}{R} \left(\frac{p_{v eq}}{T_s} - \frac{p_{v air}}{T_{air}} \right) \lambda M_w, \quad (\text{D.4})$$

where the drying air temperature is also considered directly within the pressure difference of the boundary conditions. As $p_{v air}$ is precomputed considering the relative humidity and temperature of the drying air, no significant difference was observed between the variations (candidates and examiners) of the boundary conditions,

demonstrated in Figure D.2. To perform the comparison in Figure D.2, the model constructed in Chapter 5 was utilised for convective drying apple tissue at 47 °C.

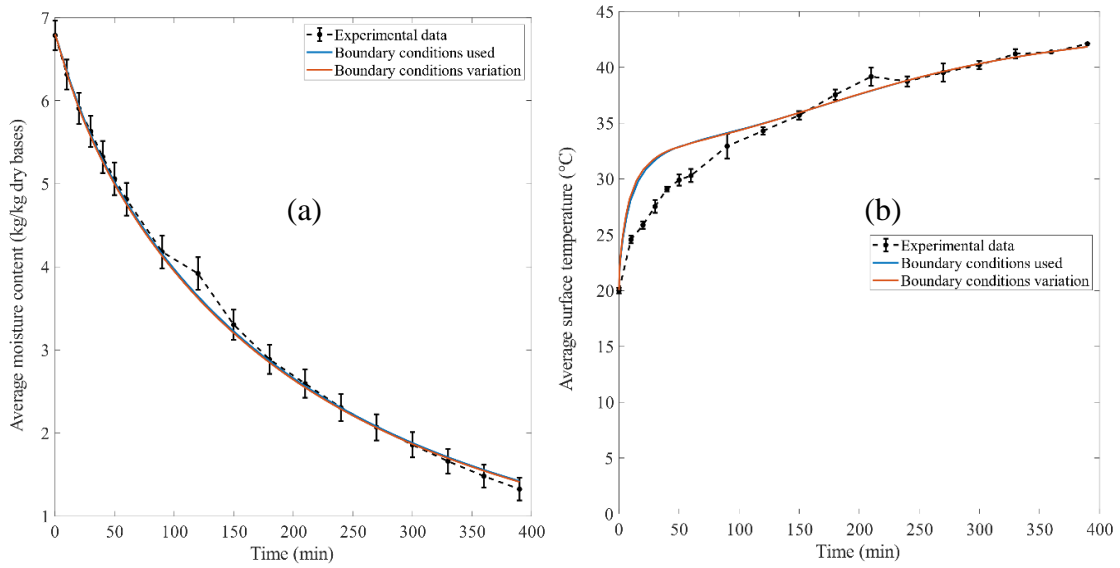


Figure D.2. Boundary condition comparison utilising the heat and mass transfer drying model constructed in Chapter 5 for convective drying apple tissue at 47°C, a) average moisture content (kg/kg dry bases), b) average surface temperature (°C).

References

- [1] M. Imran H. Khan, Z. Welsh, Y. Gu, M. A. Karim, and B. Bhandari, "Modelling of simultaneous heat and mass transfer considering the spatial distribution of air velocity during intermittent microwave convective drying," *International Journal of Heat and Mass Transfer*, vol. 153, p. 119668, 2020/06/01/ 2020.
- [2] C. Kumar, M. U. H. Joardder, T. W. Farrell, and M. A. Karim, "Multiphase porous media model for intermittent microwave convective drying (IMCD) of food," *International Journal of Thermal Sciences*, vol. 104, pp. 304-314, 6// 2016.